

(200)
T67N
No. 750

Transmitted to the Geological Survey.

TEI-750

GEOLOGY AND MINERALOGY

U. S. DEPARTMENT OF THE INTERIOR

**GEOLOGIC INVESTIGATIONS OF
RADIOACTIVE DEPOSITS**

**Semiannual Progress Report for June 1
to November 30, 1958**

**This report is preliminary and has not been edited or
reviewed for conformity with U. S. Geological Survey
standards and nomenclature.**

December 1958

**U. S. Geological Survey,
Washington, D. C.**

Prepared by

**Geological Survey for the
UNITED STATES ATOMIC ENERGY COMMISSION
Technical Information Service**



44558

LEGAL NOTICE

This report was prepared as an account of Government sponsored work. Neither the United States, nor the Commission, nor any person acting on behalf of the Commission:

A. Makes any warranty or representation, expressed or implied, with respect to the accuracy, completeness, or usefulness of the information contained in this report, or that the use of any information, apparatus, method, or process disclosed in this report may not infringe privately owned rights; or

B. Assumes any liabilities with respect to the use of, or for damages resulting from the use of any information, apparatus, method, or process disclosed in this report.

As used in the above, "person acting on behalf of the Commission" includes any employee or contractor of the Commission, or employee of such contractor, to the extent that such employee or contractor of the Commission, or employee of such contractor prepares, disseminates, or provides access to, any information pursuant to his employment or contract with the Commission, or his employment with such contractor.

This report has been reproduced directly from the best available copy.

Printed in USA. Price \$3.00. Available from the Office of Technical Services, Department of Commerce, Washington 25, D. C.

TEI-750

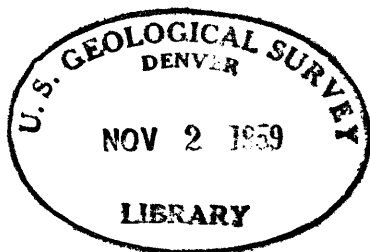
UNITED STATES DEPARTMENT OF THE INTERIOR
GEOLOGICAL SURVEY

GEOLOGIC INVESTIGATIONS OF RADIOACTIVE DEPOSITS

SEMIANNUAL PROGRESS REPORT*

June 1 to November 30, 1958

December 1958



44558

*This report concerns work done on behalf of the Divisions of Raw Materials and Research of the U. S. Atomic Energy Commission.

CONTENTS

	Page
Foreword	9
Geologic mapping	13
Colorado Plateau region	13
Lisbon Valley area, Utah-Colorado, by G. W. Weir and W. P. Puffett	14
Stratigraphy	14
Structure	19
Mineral deposits	21
Uranium and vanadium	21
Copper deposits	24
Western San Juan Mountains, Colorado	26
Laguna area, New Mexico, by R. H. Moench and J. S. Schlee	26
Grants, New Mexico, by R. E. Thaden	26
Ore controls	27
Geologic maps of the Colorado Plateau, by D. G. Wyant, W. A. Fischer, R. B. O'Sullivan, Helen Beikman, and P. L. Williams	31
Central region	32
Black Hills, South Dakota-Wyoming	32
Angostura Reservoir quadrangle, South Dakota, by Jon J. Connor	32
Pre-Inyan Kara stratigraphy	32
Inyan Kara stratigraphy	33
Post-Inyan Kara stratigraphy	35
Structure	37
Solution and brecciation of the Minnelusa formation, by C. G. Bowles and D. E. Walcott	37
Gas Hills, Wyoming	44
Eastern region	44
Mauch Chunk, Pennsylvania	44
Geologic topical studies	45
Colorado Plateau region	45
General stratigraphic studies, by L. C. Craig	45
Triassic studies	46
Lithologic studies, by R. A. Cadigan	46
San Rafael (Entrada) studies, by D. D. Dickey and J. C. Wright	59
Ambrosia Lake area, New Mexico	65
Central region	65
Inyan Kara group, Black Hills, Wyoming, by W. J. Mapel and C. L. Pillmore	65
Regional synthesis, Montana and the Dakotas	69
Alaska	69
Reconnaissance for uranium in Alaska	69

	Page
Geophysical Investigations	71
Colorado Plateau region	71
Regional geophysical studies, by H. R. Joesting, P. Edward Byerly, and J. E. Case	71
Central region	78
Texas Coastal Plain geophysical and geologic studies, by J. A. MacKallor, D. H. Eargle, and R. M. Moxham	78
Tortilla Hill area	81
Stratigraphy	81
Structure	84
Ore deposits and controls	84
General investigations	87
Physical properties of ore and host rock	87
Geophysical studies in uranium geology, by R. M. Hazlewood	88
Electronics laboratory, by W. W. Vaughn	88
Gamma-ray logging	89
Correlation of airborne radioactivity data with areal geology, by R. B. Guillou	90
Geochemical investigations	91
Distribution of elements	91
Radioactivity investigations	92
Radiogenic daughter products, by F. E. Senftle	92
Research programs	93
Physical behavior of radon, by A. B. Tanner	93
Distribution of uranium in igneous complexes	95
Uranium in some volcanic rocks, by David Gottfried	95
Evaluation of the lead-alpha (Larsen) method for determining the age of igneous rocks, by David Gottfried, H. W. Jaffe, and F. E. Senftle	101
Uranium and thorium in the Laramide intrusives of the Colorado Front Range, by George Phair	103
Uranium and thorium content of three early Paleozoic plutonic series in New Hampshire, by J. B. Lyons and Esper S. Larsen 3rd	108
Synthesis and solution chemistry of uranium	113
Studies of a reduced mineral from Ningyo-Toge mine, Japan, by T. Muto, R. Meyrowitz, and A. M. Pommer	113
Mineral synthesis, by A. M. Pommer and J. C. Chandler	113
Solution chemistry of uranium, by A. M. Pommer and I. A. Breger	114
Association of uranium with coalified logs, by I. A. Breger	114
Uranium in impregnated sandstones, by I. A. Breger and J. C. Chandler	115

	Page
Stable isotope analysis, by Irving Friedman and Betsy Levin . . .	116
Nuclear geology, by F. E. Senftle	116
Nuclear irradiation, by C. M. Bunker	120
Geochronology, by L. R. Stieff	122
Isotope geology of lead, by R. S. Cannon, Jr.	125
Natural radioactivity of the atmosphere, by H. B. Evans	128
Thermoluminescence, by F. E. Senftle	133
Geochemistry of thorium	134
Thorium determinations on rocks of the Boulder Creek batholith, by George Phair and David Gottfried	134
Modification of procedure for determining thorium in the low parts per million range, by F. S. Grimaldi and Lilly Jenkins	135
Investigations of thorium in veins, Gunnison County, Colorado, by J. C. Olson and D. C. Hedlund	136
Geologic thermometry of radioactive materials, by D. B. Stewart .	138
The system $\text{CaCO}_3\text{-SrCO}_3$	139
The system albite-silica-eucryptite-water	141
The system ZnS-FeS-MnS-CdS	145
Other studies	145
Crystallography of uranium and associated metals, by Howard T. Evans	147
Infrared and ultraviolet radiation studies, by R. M. Moxham . . .	149

ILLUSTRATIONS

	Page
Figure 1. Index map of Utah and Colorado showing location of Lisbon Valley area	15
2. Generalized geologic map of Lisbon Valley area showing location of Mt. Peale 4 SE quadrangle	15
3. Simplified geologic map of Mr. Peale 4 SE quadrangle	16
4. Explanation of symbols used on fig. 3	17
5. Simplified structural map of Mt. Peale 4 SE quadrangle	20
6. Map of Mt. Peale 4 SE quadrangle showing locations of mines and prospects	22
7. Index map showing order of, and progress in, compilation of 2 ^o sheets of Colorado Plateau geologic map	30
8. Generalized structure contour map of Angostura Reservoir quadrangle	36
9. Map of southern Black Hills showing Minnelusa formation outcrop, collapses, and locations of stratigraphic sections and water samples	38
10. Correlation of the Upper Minnelusa formation in the southern Black Hills	40
11. Breccia pipes in the Minnelusa formation, Custer County, South Dakota	41
12. Graphs showing percentage rock composition, grain size, and sorting in sedimentary rocks in the Paria Amphitheatre area, Garfield County, Utah	47
13. Dip-direction of crossbeds in basal part of Curtis formation, Emery and Sevier Counties, Utah	61
14. Cross-bedding consistency, basal beds of Curtis formation, Emery County, Utah	62
15. Generalized restored section showing correlation of rim-forming sandstone in Fall River formation, Black Hills, Wyoming	66
16. Map showing average direction of crossbeds in Lakota formation, Black Hills, Wyoming	67
17. Diagrams showing dip directions of crossbeds in Lakota formation, Wyoming	68
18. Regional geophysical surveys in central Colorado Plateau	72
19. Index map of central Texas coastal plain	79
20. Structure and thickness of Stones Switch sandstone, Karnes County area, Texas	80
21. Cross-sections showing relationship between silicification and land surface	83
22. Map showing radon concentrations in ground water, Tooele County, Utah	94

Figure 23.	Distribution of uranium in the volcanic rocks of the Modoc area, northern California	97
24.	Distribution of uranium in the volcanic rocks of the Strawberry Mountains, Oregon	97
25.	Distribution of uranium in some rocks of the Hinsdale formation and Potosi volcanic series	98
26.	Distribution of uranium in volcanic rocks of the Valles Mountains, New Mexico	99
27.	Magnetic susceptibilities of the three crystallographic forms of TiO_2	118
28.	Response of density logger in simulated formations. Curves show effects of various shielding configurations and spectral response	121
29.	Plan view of lithology traversed showing air sample and gamma-ray profiles along traverse line, Emigration Canyon ..	129
30.	Plan view of lithology traversed showing air sample and gamma-ray profiles along traverse line near Park City, Utah	131
31.	Plan view of traverse lines across uranium mine (A) and gamma-ray count and air sample count for traverse DAE (B) and traverse BAC (C).	132
32.	Thermal expansion of $SrCO_3$	140

TABLES

	Page
Table 1. Exposed rocks in the Mt. Peale 4 SE quadrangle, Utah-Colorado	18
2. Chemical analyses of spring water presumably issuing from the Minnelusa formation	43
3. Results of point count composition analyses of 29 samples of Jurassic rocks of San Rafael group, Farfield County, Utah	49
4. Measurements of dip-direction, crossbeds in basal part of Curtis formation	64
5. Regional gravity field work completed, May-September 1958	73
6. Summary of regional gravity surveys on Colorado Plateau through September 1958	76
7. Stratigraphy of Jackson group	82
8. Uranium content of volcanic rocks from New Jersey and Iceland	100
9. Uranium and thorium contents of rocks from the Highland- croft plutonic series	109
10. Uranium and thorium contents of the major rock types of the Oliverian plutonic series	110
11. Uranium and thorium contents of the major rock types of the New Hampshire plutonic series	111
12. Magnetic susceptibilities	119

FOREWORD

The Geological Survey began its investigations of radioactive deposits on behalf of the Division of Raw Materials of the Atomic Energy Commission in 1947. For about eight years after that time the program was directed toward the rapid discovery of suitable uranium deposits; little effort was devoted to long-range geologic studies. In 1952 a program of long-range laboratory research on uranium and other radioactive materials, under the sponsorship of the Division of Research of the AEC, was started; and in 1955 the rapid increase in the Nation's production of uranium made it possible to reorient the Raw Materials program toward long-range fundamental studies of the geologic processes that govern the formation of uranium deposits. These studies involve systematic geologic mapping and research, supported by appropriate geophysical and geochemical studies, designed to develop information on the Nation's actual and potential reserves and resources of radioactive raw materials, and on the size, shape, mineralogy, and geologic setting of different types of deposits.

On July 1, 1958 funds formerly appropriated to the Division of Raw Materials were transferred to the Survey's direct appropriation for continuation of long-range studies of the geology of uranium. Support by the Division of Research is also being decreased gradually over a period of several years, and part of that program is now being carried on under the Survey's direct appropriation. As a result of these changes, the Survey's uranium program is now integrated more closely than previously had been possible with its investigations of other mineral resources.

A most important objective of the Survey's program in the field of radioactive materials is the dissemination of information by the publication, as expeditiously as possible, of the results of its investigations. These results are published as Geological Survey Professional Papers, Bulletins or Bulletin chapters, Circulars, or maps, and as papers in scientific journals. During the six months covered by this report publications stemming from the program include eight Bulletins or Bulletin chapters, 13 maps, and 20 papers in scientific journals. During the same period three reports were placed on open file and one report was sent to the Technical Information Service Extension of AEC for reissue and distribution to the public. In addition, scientists working on the uranium program presented 10 papers at scientific meetings.

Since June 1954, when easing of security restrictions made possible the publication of much data that previously had been classified, four Professional Papers, 83 Bulletins or Bulletin chapters, 53 Circulars, and 375 maps stemming from the uranium program have been published by the Survey, and 186 papers by scientists working on the program have been published in scientific journals. During the same period 84 reports have been placed on open file, and 24 reports have been sent to the Technical Information Service Extension for reissue and distribution.

Survey scientists contributed 18 papers to the Second International Conference on the Peaceful Uses of Atomic Energy, held in Geneva, Switzerland, September 1-13, 1958. Two of these papers, which were presented orally, were:

Page, L. R., Some new mineralogical, geochemical, and geologic aids in uranium exploration.

Stead, F. W., Advances in radioactivity, radiochemical, and isotopic methods of prospecting.

Sixteen papers were published in the Proceedings of the Conference,
as follows:

Butler, A. P., Jr., Geologic appraisal of uranium resources of the United States.

Cannon, R. S., Jr., Stieff, L. R., and Stern, T. W., Radiogenic lead in non-radioactive materials, a clue in the search for uranium (see Isotope geology of lead, p. 122, and Geochronology, p. 125, this volume).

Dooley, J. R., Jr., The radioluxagraph, a fast, simple type of autoradiograph.

Fron del, Clifford, Descriptive mineralogy of uranium and thorium.

Hilpert, L. S., and Moench, R. E., The uranium deposits of the southern part of the San Juan Basin, New Mexico.

Larsen, E. S., Jr., Gottfried, David, and Malloy, Marjorie, Distribution of uranium in the volcanic rocks of the San Juan Mountains, southeastern Colorado (see Distribution of uranium in igneous complexes, p. 95, this volume).

MacKevett, E. M., Jr., Geology of the Ross-Adams uranium-thorium mine, Alaska (see Reconnaissance for uranium and thorium in Alaska, p. 69, this volume).

Moxham, R. M., Geologic evaluation of airborne radioactivity survey data (see Texas Coastal Plain geophysical and geologic studies, p. 78, this volume).

Norton, J. J., Griffiths, W. R., and Wilmarth, V. R., Geology and resources of beryllium in the United States.

Pierce, A. P., Mytton, J. W., and Barnett, P. R., Geochemistry of uranium in organic substances in petroliferous rocks.

Rosholt, J. N., Radioactive disequilibrium studies as an aid to understanding the natural migration of uranium and its decay products.

Shawe, D. R., Archbold, N. L., and Simmons, G. C., Geology and vanadium-uranium deposits of the Slick Rock district, San Miguel and Dolores Counties, Colorado.

Tanner, A. B., Increasing the efficiency of exploration drilling for uranium by measurements of radon in drill holes (see Physical behavior of radon, p. 93, this volume).

Scott, R. C. and Barker, F. B., Radium and Uranium in Ground Water of the United States.

Vaughn, W. W., Rhoden, V. C., and Wilson, E. E., Developments in radiation detection equipment for geology (see Electronics Laboratory, p. 38, this volume).

Vine, J. D., Swanson, V. E., and Bell, J. G., The role of humic acids in the geochemistry of uranium.

The Semiannual Reports, "Geologic Investigations of Radioactive Deposits," of which this volume is one, were prepared originally as administrative reports to the AEC. Beginning, however, with TEI-330, issued in June 1953, each Semiannual Report has been reissued and made available to the public by the Technical Information Service Extension of the AEC. Because the Atomic Energy Commission has a vital interest in, and a large responsibility for, the Nation's uranium programs, the Survey plans to continue the Semiannual Report series, even though most of its uranium program is not now sponsored by the AEC. The AEC will continue to make these reports available to the public through its Technical Information Service Extension. By this means both the AEC and the public will be kept informed of the more important developments in the program, prior to formal publication of results.

Most of the programs reported in this volume were started under the sponsorship of the Division of Raw Materials but are now being carried on under the Survey's own funds. One project, on the Geology and geochemistry of thorium, now carried under the direct appropriation, was formerly supported by the Division of Research. Projects started after July 1, 1958 in the field of radioactive deposits are reported in the same manner as the older projects.

This Semiannual Report is somewhat smaller than most of its predecessors, reflecting the decrease in the size of the Survey's uranium program over the past few years.

GEOLOGIC MAPPING

Colorado Plateau region

Geologic mapping as part of uranium investigations in the Colorado Plateau were started in 1947, and up to the present time more than twenty uranium-bearing areas within the Plateau region have been mapped. For the past several years the amount of field work has been progressively reduced, emphasis being placed on completion of programs previously started, and on preparation of final reports for publication in the Survey's Professional Paper or Bulletin series, or as Survey maps. In order to make results of the investigations available as expeditiously as possible, the progress of each project has been reported in Semiannual Reports to AEC, and, as work in particular areas has been completed, summary reports which are essentially expanded abstracts of the final report have been included in the Semiannual Report. Projects so reported in the previous Report, TEI-740, are:

Ute Mountains, Colorado: pages 21-29.

Moab-Inter-river-area, Utah: pages 36-47.

Orange Cliffs, Utah: pages 47-57; see also TEI-690, p. 107-112.

San Rafael Swell, Utah: pages 57-71.

Projects on which field and/or office work was in progress during the past six months are reported in the following pages.

Lisbon Valley area, Utah - Colorado
by
G. W. Weir and W. P. Puffett

The Lisbon Valley area includes about 700 square miles in southeastern Utah and southwestern Colorado (fig. 1). A simplified geologic map of the area is shown in figure 2. During the report period the geology of the Mt. Peale 4 SE quadrangle (fig. 2) was mapped and compiled. A simplified geologic map of the quadrangle is shown in figures 3 and 4.

Stratigraphy

The rocks exposed in the Mt. Peale 4 SE quadrangle are briefly described in table 1. The oldest formation is the Wingate sandstone of Late Triassic age; the youngest consolidated formation is the Mancos shale of Late Cretaceous age.

The Wingate sandstone and Kayenta formation are restricted to outcrops near a fault at the base of Three Step Hill in the northwest corner of the quadrangle. The Navajo sandstone crops out only at this locality and in McIntyre Canyon near the east edge of the quadrangle. Outcrops of the San Rafael group are confined to the rims of Three Step Hill and McIntyre Canyon. Of the youngest rocks the Mancos shale is exposed only in a downfaulted block in Lower Lisbon Valley. Thus, the bedrock for more than 90 percent of the quadrangle consists of only three formations: the Morrison, Burro Canyon, and Dakota. Quaternary landslide and wind- and water-deposited silt and fine sand cover much of the quadrangle.

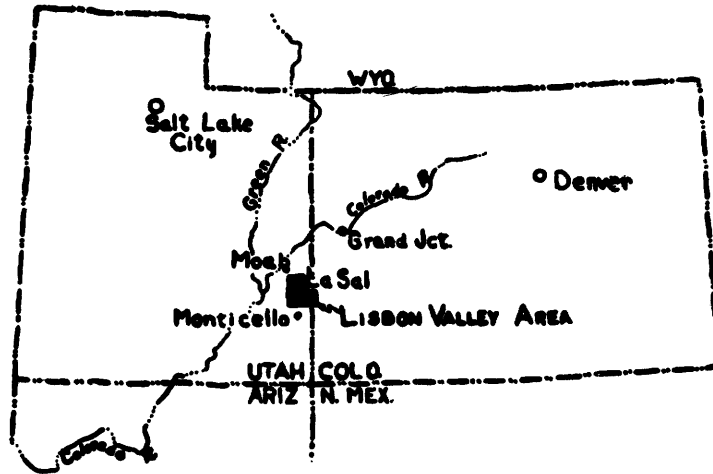


Fig. 1.--Index map of Utah, Colorado, and parts of adjacent states showing location of Lisbon Valley area, Utah-Colorado.

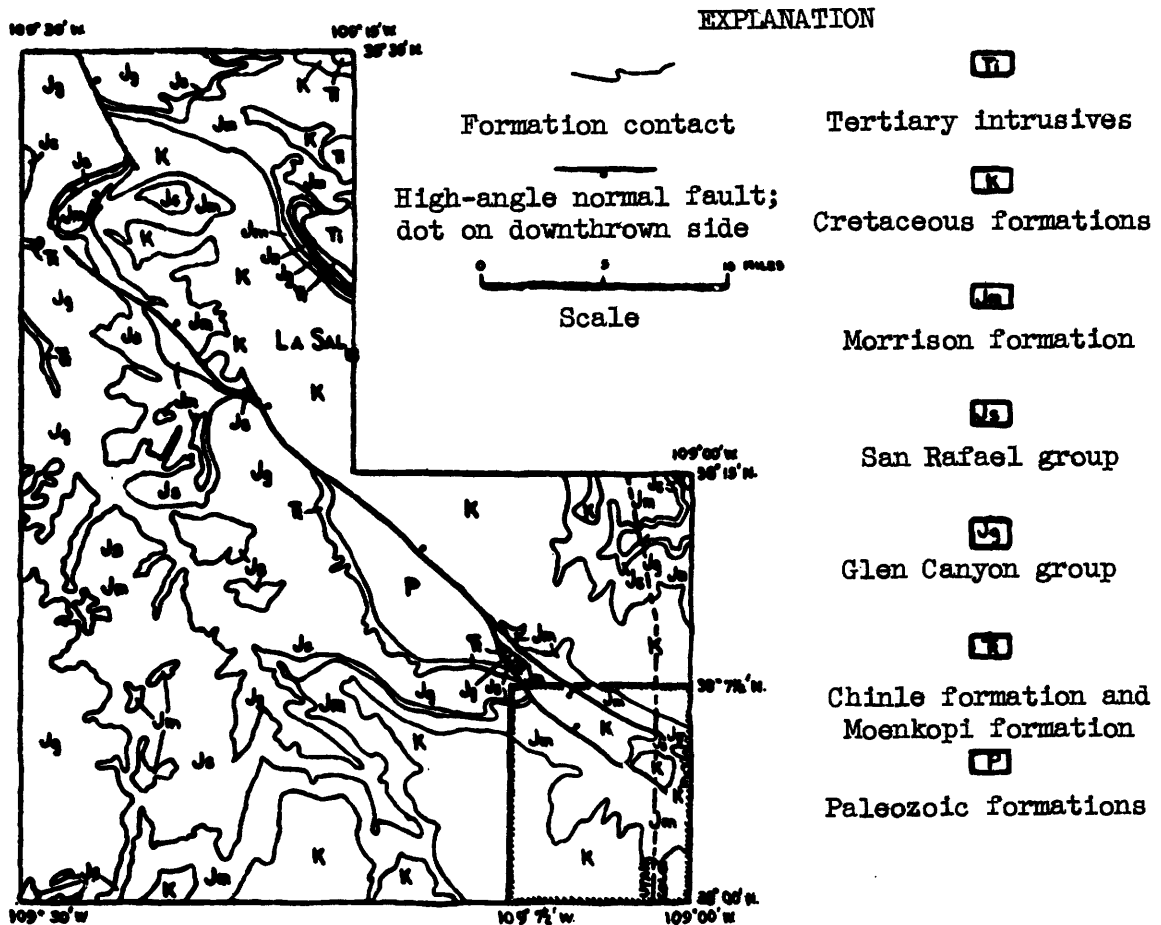
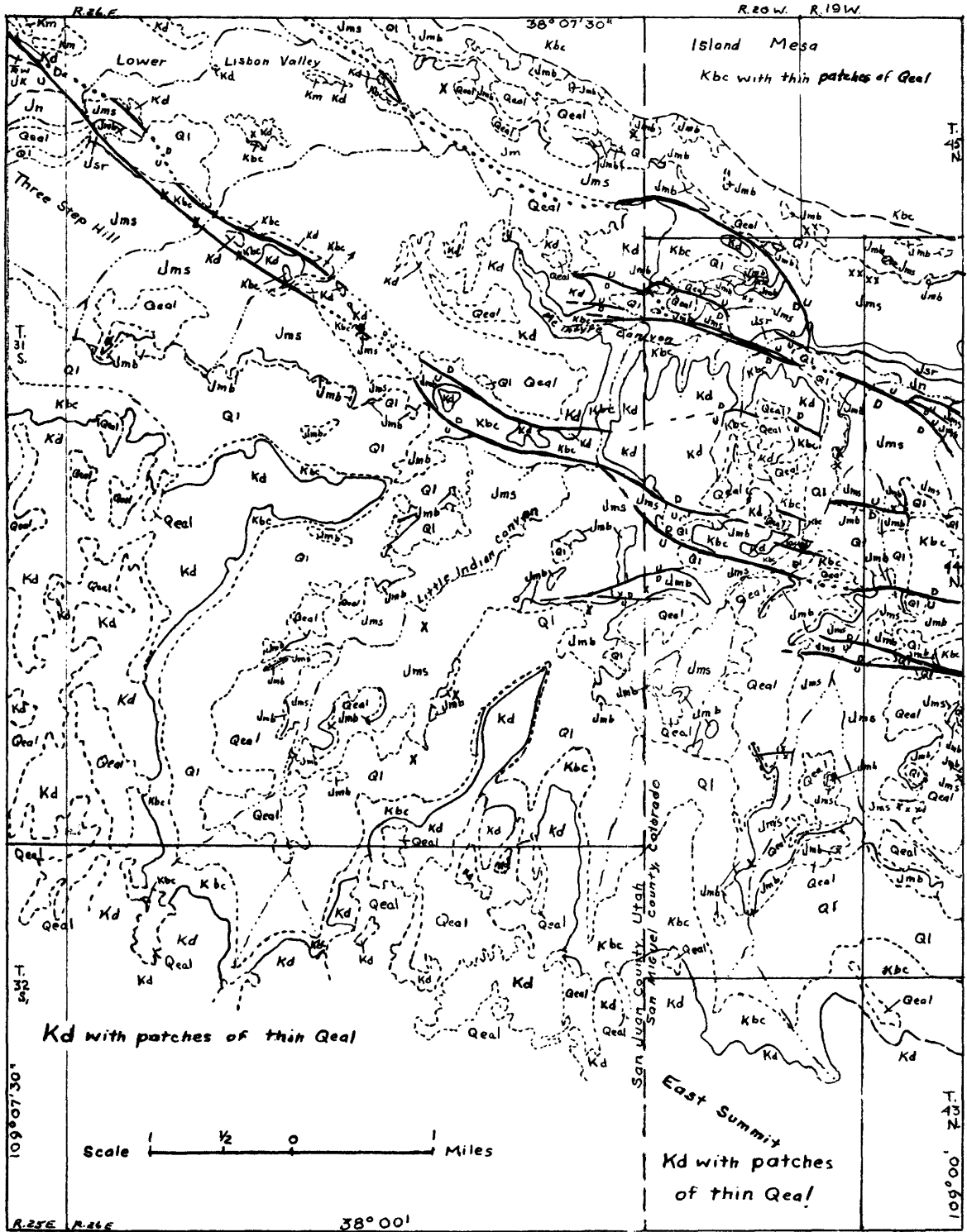


Fig. 2.--Generalized geologic map of the Lisbon Valley area showing location of the Mt. Peale 4 SE quadrangle, Utah-Colo. (hachured).



Geology by G.W. Weir and W.P. Puffett, 1938

Figure 3. Simplified geologic map of Mt. Peale 4 SE quadrangle

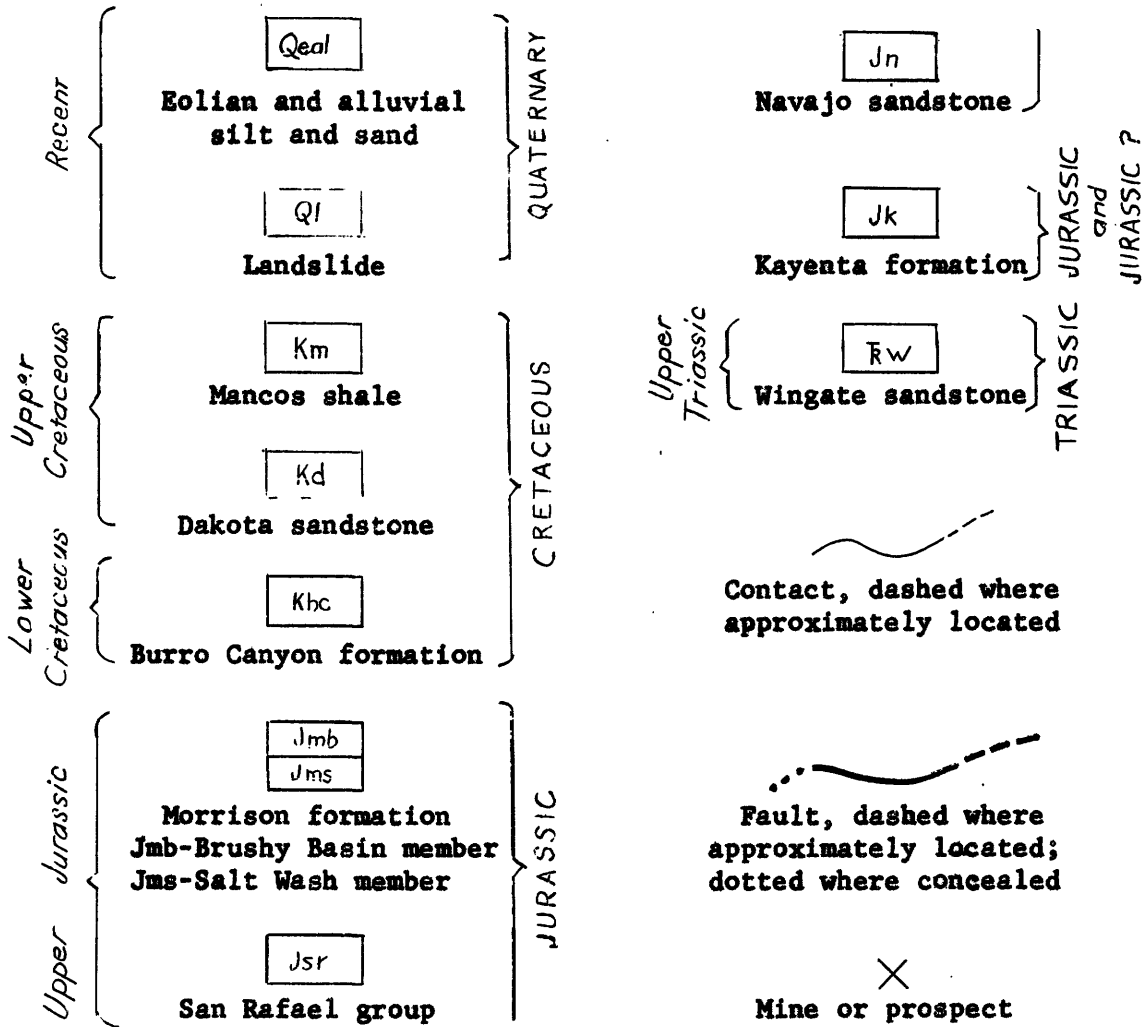


Figure 4. Explanation of symbols used on simplified geologic map of Mt. Peale 4 SE quadrangle (fig. 3).

SYSTEM	SERIES	FORMATION	THICKNESS (Feet)	CHARACTER and Map Symbol (Fig. 3)	
Quaternary		Surficial deposits	0 - 50 (?)	Dark red to light grayish-brown eolian and alluvial silt and sand covering mesa tops and filling valleys (Qeal). Landslide consisting mainly of the Burro Canyon formation and the Brushy Basin member of the Morrison formation (Ql).	
Cretaceous	Upper	Mancos shale	200 (?)	Dark gray shale with common <u>Gryphaea</u> near base; top eroded (Km).	
		Dakota sandstone	150	Light to dark brown medium-grained sandstone and conglomerate with common plant fossils; caps cliffs (Kd).	
	Lower	Burro Canyon formation	200 - 250	Light brown to gray medium-grained sandstone and conglomerate, gray sandy limestone and chert; forms cliff (Kbc).	
Jurassic	Upper	Morrison fm. San Rafael group	Brushy Basin member	420	Chiefly red and green bentonitic mudstone; dark brown pebble conglomerate and sandstone fairly persistent at base; forms steep slope (Jmb).
			Salt Wash member	350	Light brown to reddish brown fine- to medium-grained sandstone interbedded with red mudstone; forms ledges and benches (Jms).
			Summerville formation	60 - 90	Dark red mudstone with thin beds of light brown fine-grained sandstone (Jsr).
			Entrada sandstone	160	Massive buff horizontally and cross-stratified fine-grained sandstone; forms smooth rounded cliff (Jsr).
			Carmel formation	20 - 40	Red silty sandstone; forms rounded ledge (Jsr).
		Navajo sandstone	180 - 200	Very light gray to buff cross-stratified fine-grained sandstone; forms cliff (Jn).	
Juras- sic ?		Kayenta formation	220	Red and gray sandstone interbedded with red siltstone; forms irregular cliff (Jk).	
Triassic		Wingate sandstone	260	Grayish orange fine-grained sandstone, mostly cross-stratified; base not exposed (Fw). Conformably overlies Chinle formation (not exposed) about 400 feet thick, composed of red mudstone and sandstone with thin gray sandstone at base.	

Table 1. Exposed rocks of the Mt. Peale 4 SE quadrangle, Utah-Colorado

Structure

The Lisbon Valley area lies within the Paradox fold and fault belt, a tectonic region dominated by northwest-trending folds and faults (Kelley, 1955). Figure 5 is a simplified structure contour map of the Mt. Peale 4 SE quadrangle. The contours are drawn on the exposed and projected base of the Morrison formation.

The Mt. Peale 4 SE quadrangle lies in a structural col between the Lisbon Valley anticline to the northwest and the Dolores anticline to the southwest (Cater, 1955). These anticlines are underlain by thickened rolls of salt of Paleozoic age; the Mt. Peale 4 SE quadrangle probably is an area from which salt was withdrawn during the growth of the neighboring salt anticlines. The relative withdrawal of salt resulted in a series of northwest- to west-trending normal faults in the north half of the quadrangle. Displacements are downward toward Lower Lisbon Valley and McIntyre Canyon so that a graben is formed in the north part of the quadrangle. The greatest throw is along a fault in the northwest corner of the quadrangle where the Dakota sandstone has been dropped against the Wingate sandstone, a throw of about 2,000 feet. The faults tend to die out near the state line from both the northwest and southeast. A few miles to the northwest, the faults coalesce into the Lisbon Valley fault, one of the major faults of the Paradox fold and fault belt. The faults in Colorado are less continuous, more nearly west trending, and belong to a group of small faults cutting the northeast flank of the Dolores anticline in the Horse Range Mesa quadrangle, Colorado (Cater, 1955).

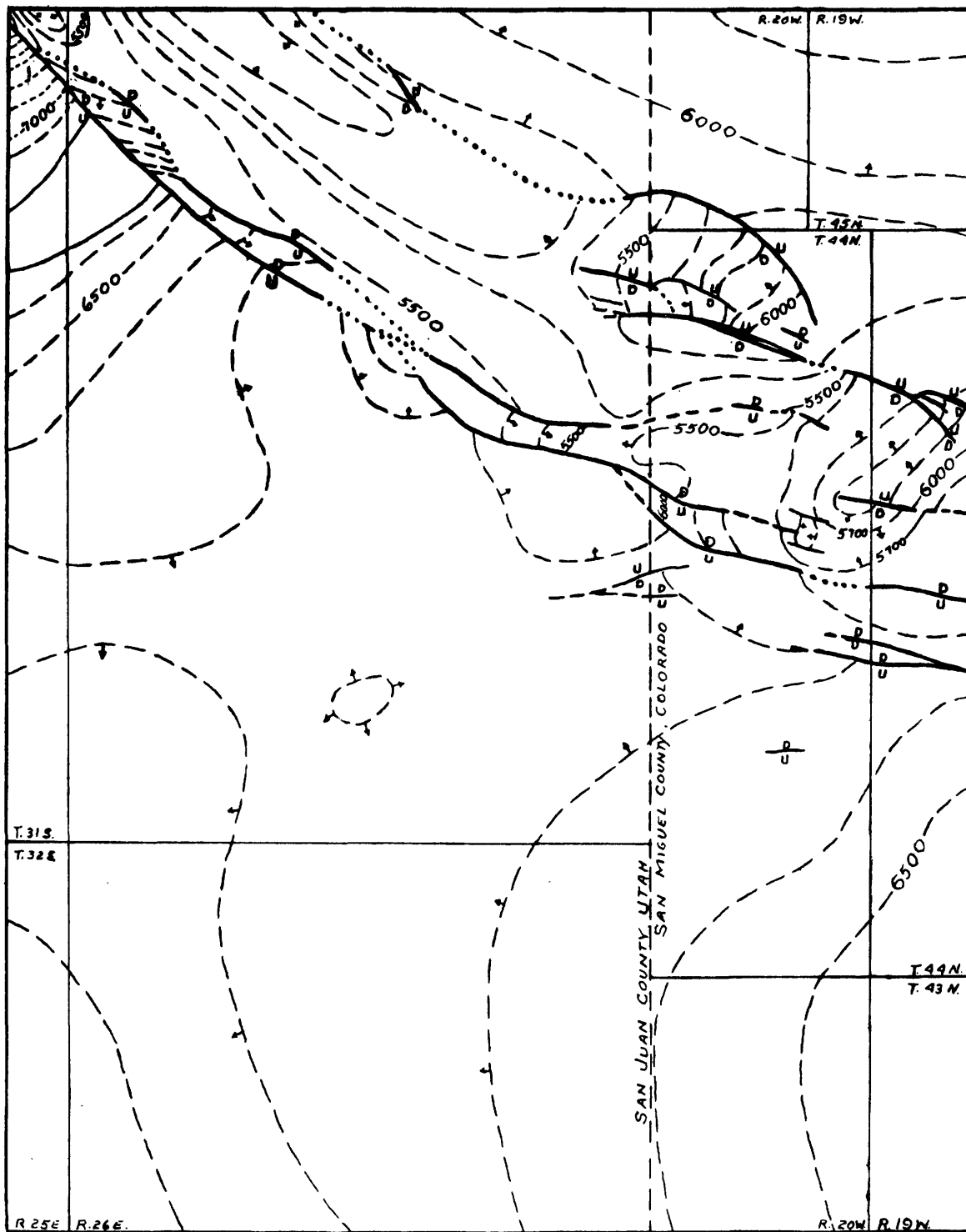


Fig. 5. Simplified Structural Map of the Mt. Peale 4 SE Quadrangle. Structure contours drawn on base of Morrison formation; dashed where approximately located; arrows indicate direction of dip. Contour interval is 100 feet; datum is mean sea level.

Dips are nearly flat except close to faults. The prevailing regional dip is north to northwest. Within the graben of Lower Lisbon Valley and McIntyre Canyon is a northwest-plunging syncline. Moderately steep dips (exceeding 10°) are common along faults bordering the syncline.

Mineral deposits

In the Mt. Peale 4 SE quadrangle uranium-vanadium deposits occur in the Chinle formation and in the Morrison formation. Occurrences of copper minerals are common in the Burro Canyon and Morrison formations--especially near faults. Figure 6 shows the locations of mines and prospects in the quadrangle.

Uranium and vanadium

The Chinle formation of Late Triassic age contains many large deposits of unoxidized uranium-vanadium ore, chiefly made up of uraninite and montroseite, in the Big Indian mining district several miles northwest of the Mt. Peale 4 SE quadrangle, but the formation does not crop out within the map area. The ore-bearing horizon at the base of the Chinle is about 400 feet below the base of the Wingate sandstone and in this quadrangle is from about 700 to several thousand feet beneath the ground surface. An unoxidized uranium-vanadium ore body in the basal Chinle, generally referred to as the "Williams lease", lies in the northwest corner of the quadrangle. This deposit is known only from drill hole data, and future exploration at this locality will determine the size of the deposit and the potential of surrounding deeply buried Chinle.

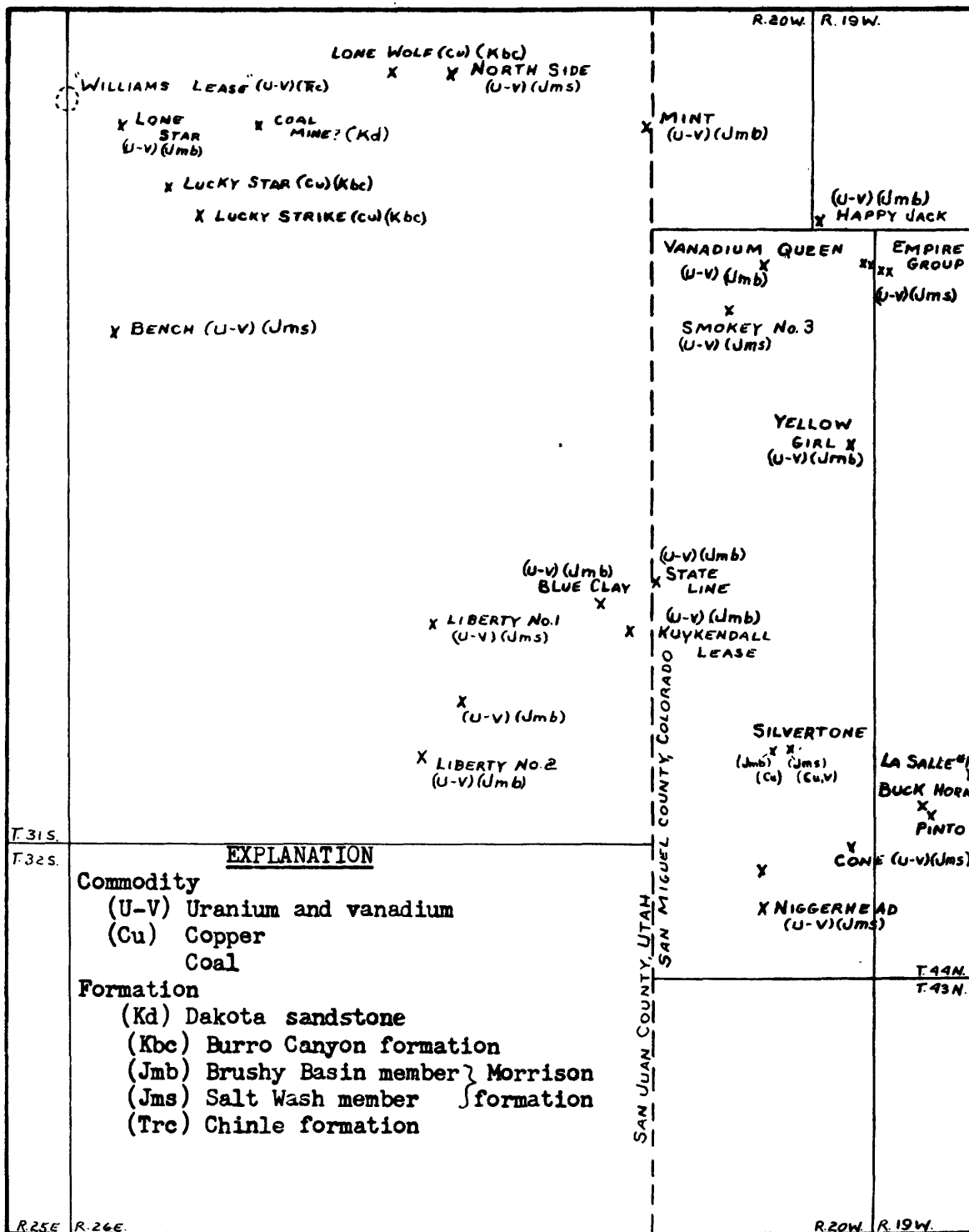


Fig. 6. Map of the Mt. Peale 4 SE quadrangle, Utah-Colorado, showing locations of mines and prospects

The uranium-vanadium deposits in the Morrison formation in this quadrangle are small. Only a few mines have produced more than several hundred tons. The deposits are oxidized and the chief ore minerals are carnotite, tyuyamunite, and vanadium mica. The deposits are both in the Brushy Basin member and the Salt Wash member.

Deposits in the Brushy Basin member of the Morrison formation occur in a dark brownish-gray pebble-conglomerate and coarse-grained sandstone lenticular bed about 50 feet above the base of the member. Plant fossils occur as macerated carbonaceous debris and as silicified logs. The ore forms irregular layers and pods in thin-bedded sandstone and conglomerate with common to abundant carbonaceous material. Examples of this type of deposit are the Happy Jack and Vanadium Queen mines near McIntyre Canyon.

Uranium-vanadium deposits in the Salt Wash member of the Morrison formation occur mainly in the top persistent bed of fine- to medium-grained sandstone. More mines and prospects have been developed in the Salt Wash than in the Brushy Basin member in this quadrangle, and the total production from the Salt Wash is larger than from the Brushy Basin; however, the average size of the deposits in the Brushy Basin member is probably larger than those in the Salt Wash member. The deposits in the two members are much alike. In the deposit in the Salt Wash, however, the uranium-vanadium ore tends to form curving cross-cutting layers. These structures are known as "rolls" and are well described by Shawe (1956) for the adjacent Slick Rock mining district to the east.

Within the Mt. Peale 4 SE quadrangle the ore horizons of the Morrison are well exposed, but the frequency and size of deposits are less than in quadrangles to the east or west. The ore-bearing sandstone is commonly thick (more than 40 feet), but interstitial and underlying mudstone are commonly red, and in places, as along the rim of Lower Lisbon Valley, the ore-bearing sandstone itself has a distinct reddish cast. These colors are not generally associated with ground favorable for ore deposits in the Morrison formation (Weir, 1952) and suggest that the uranium-vanadium ore potential of the Morrison in this quadrangle is small.

Copper deposits

Sparse carnotite and vanadium mica occur with malachite, azurite, chalcocite, and volborthite in the Burro Canyon formation near a fault at the Lucky Strike adit near the northwest corner of the quadrangle. The deposit is the only known occurrence of uranium and vanadium minerals in Cretaceous rocks in the area. Both the uranium and vanadium minerals are localized along joints. Non-radioactive occurrences of copper oxides are common in the Burro Canyon along the fault passing through the Lucky Strike deposit. Small shows of malachite and azurite are also common in the Burro Canyon along the fault near McIntyre Canyon near the east edge of the quadrangle.

At the Silvertone prospects near the southeast corner of the quadrangle malachite, azurite, and volborthite occur in breccia along a small fault in the Morrison formation. The copper minerals are found in the basal conglomeratic sandstone ledge of the Brushy Basin member and the top three sandstone lenses of the Salt Wash member. The top

sandstone lens of the Salt Wash contains thin layers of sandstone impregnated with vanadium mica near the fault. The fault has a displacement of only a few feet, but the copper-bearing breccia cement with black calcareous material in places is several feet wide; the vertical exposure of the fault is at least 200 feet. No carnotite was seen at these Morrison prospects.

At the Pinto and Buckhorn workings near the southeast corner of the quadrangle malachite, azurite, and volborthite occur with a deposit of carnotite and vanadium mica. No fault is near these deposits.

All of the copper deposits in the Mt. Peale 4 SE quadrangle are small; none suggest a mining potential. The occurrence of copper minerals with uranium and vanadium minerals suggests, however, that the uranium deposits and copper deposits of the Lisbon Valley area are the results of the same mineralizing process.

References

- Cater, F. W., Jr., 1955, Geology of the Horse Range Mesa quadrangle, Colorado: U. S. Geol. Survey Geol. Quad. Map GQ-64.
- Kelley, V. C., 1955, Regional tectonics of the Colorado Plateau and relationship to the origin and distribution of uranium: New Mexico Univ. Pub. Geology No. 5, 120 p.
- Weir, D. B., 1952, Geologic guides to prospecting for carnotite deposits on Colorado Plateau: U. S. Geol. Survey Bull. 988-B, p. 15-27.
- Shawe, D. R., 1956, Significance of roll ore bodies in genesis of uranium-vanadium deposits on the Colorado Plateau: in Page, L. R., Stocking, H. E., and Smith, H. B., Contributions to the geology of uranium and thorium by the United States Geological Survey and Atomic Energy Commission for the United Nations International Conference on Peaceful Uses of Atomic Energy, Geneva, Switzerland, 1955: U. S. Geol. Survey Prof. Paper 300, p. 239-241.

Western San Juan Mountains, Colorado

Final reports for Survey publication are in progress on the Placerville, Little Cone, and Gray Head quadrangles, which contain the known vanadium-uranium deposits of the Placerville district, Colorado. Results of the work in these quadrangles have been reported in TEI-620, p. 47-50; TEI-640, p. 47-49; TEI-690, p. 67-71; TEI-700, p. 30-33; and TEI-740, p. 20-21.

Laguna area, New Mexico
by
R. H. Moench and J. S. Schlee

The report period was devoted to preparation of the final report, for U. S. Geological Survey publication, on the uranium deposits of the Laguna district, and their relations to the regional geology.

Grants, New Mexico
by
R. E. Thaden

Restudy of field relations in the vicinity of Grants Ridge during the report period indicates that an eruption of a Tertiary volcano deposited rhyolitic pumice over a surface which sloped eastward from an elevation of 7900 feet on the south side of La Jara Mesa to about 7450 feet at the west end of East Grants Ridge. After part of this pumice had been reworked by weathering agents, a later eruption deposited more pumice over the reworked material and built a large cone. The force of the eruptions removed the country rock underlying the crater floor to a depth below the present lowest surface of erosion. Still later viscid material was extruded into the crater to form a cumulo-dome (Cotton, 1944, p. 156) covering an area of about 2 square miles.

The porphyritic rhyolite in the dome has a specific gravity of 2.05. It is light-gray, porous, and has phenocrysts of feldspar and oriented microphenocrysts of feldspar and biotite in a matrix of light colored glass. Flow banding is prominent and is associated with numerous voids as much as 2 inches by 14 inches by several feet, the long dimensions of which are in the plane of the flow layers and normal to the orientation of the microphenocrysts.

Obsidian, now largely altered to perlite, formed a chilled exterior phase of the porphyritic rhyolite body. Dense rhyolite is found at some places in the upper part of the dome on the western lip of the original pumice cone; devitrification of this rock is far advanced. This dense material just within the western lip of the cone may represent a deposit which was overridden several times by viscid masses and was degassed and devitrified by intermittent heating. On the other hand, the dense rhyolite may represent part of a chilled vitreous cap of the dome, which was devitrified by volatiles escaping vertically from the interior of the body.

At most outcrops the contact of the porphyritic rhyolite with the enclosing pumice cone is obviously intrusive. The pumice may be warped upward and crudely foliated at the contact, or it may be crushed and crudely foliated by lateral pressure; fragments of pumice are locally incorporated in the obsidian.

Ore controls

The distribution of uranium ore in the Grants area appears to be controlled mainly by pre-Dakota or later folding, and to a lesser extent by sandstone channel deposits.

Ore in the Morrison formation of Jurassic age is associated primarily with folds that developed during deposition of the Morrison, rather than

with channel sandstones; the folds trend N. 60° to 70° W. in the central and northern parts of the area, and about N. 30° W. in the eastern part (TEI-690, p. 159-160; TEI-740, p. 71-72). The trend of the channels in the Morrison is widely divergent from that of the folding; the directions of sediment transport in the Poison Canyon area are N. 70° E. for the main body of the Westwater Canyon member, N. 60° E. for the so-called Poison Canyon tongue of local usage of the Westwater Canyon, and N. 40° E. for the Brushy Basin member. Channel sandstone units in the Brushy Basin member elsewhere in the area trend close to N. 45° E. Channels in both the Westwater Canyon and Brushy Basin members can be seen on the rim outcrop, and others have been discovered by drilling (TEI-690, p. 372-375). The Francis and Evelyn uranium deposits near the northwest corner of the Grants area, and the Jackpile deposit in the Laguna area, are examples of ore bodies in these northeasterly trending channel sandstone units. It is possible that such channels contain ore only at places where the channels are in association with the pre-Dakota or younger folds mentioned above.

Many of the ore bodies in the Ambrosia Lake area that are in the Westwater Canyon member of the Morrison formation and that have no underlying confining claystone layers may be in favorable chemical environments in the bottoms of channels, where the channels intersect the folds. Many such ore bodies may contain large quantities of organic trash, the deposition of which was controlled by the configuration of the channel. Other ore bodies in folded areas, but not within well defined channel sandstone units, may not be associated with organic trash, so that their deposition was controlled by a widespread secondary concentration of degraded organic fluid in the folds. The deposits in the well defined

channels are likely to be of smaller tonnage and of lower and less predictable grade than deposits in poorly defined channels.

Measurements of the trend of intraformational folds in the Todilto limestone of Jurassic age show peak concentrations in a reticulate system, with a double peak at about N. 35° W. and N. 5° W., and a single peak at about N. 75° W. Axial planes dip mostly westerly and southerly, respectively, and fractures in both sets indicate left lateral movement. The largest intraformational folds in the Todilto trend N. 15° E. and are symmetrical. The ore, which is associated with the folds, shows no preference with respect to the fold orientations.

The large folds in secs. 4 and 9, T. 12 N., R. 9 W. (TEI-740, p. 72) have now been traced to the vicinity of sec. 25, T. 13 N., R. 10 W., where they are mostly less than 2,000 feet in width and as little as 20 feet in amplitude. These folds invariably involve the Entrada sandstone of Jurassic age, and control the position of groups of ore bodies.

In summary, the characteristics of folds in the Grants area indicate that the association of ore with them is due primarily not to the amplitude, distribution or orientation of the folds, but rather to the influence of the folds on the development of chemical environments favorable for ore precipitation.

Reference

Cotton, C. A., 1944, Volcanoes as landscape forms: Welling, New Zealand, Whitcombe and Tombs, Limited.

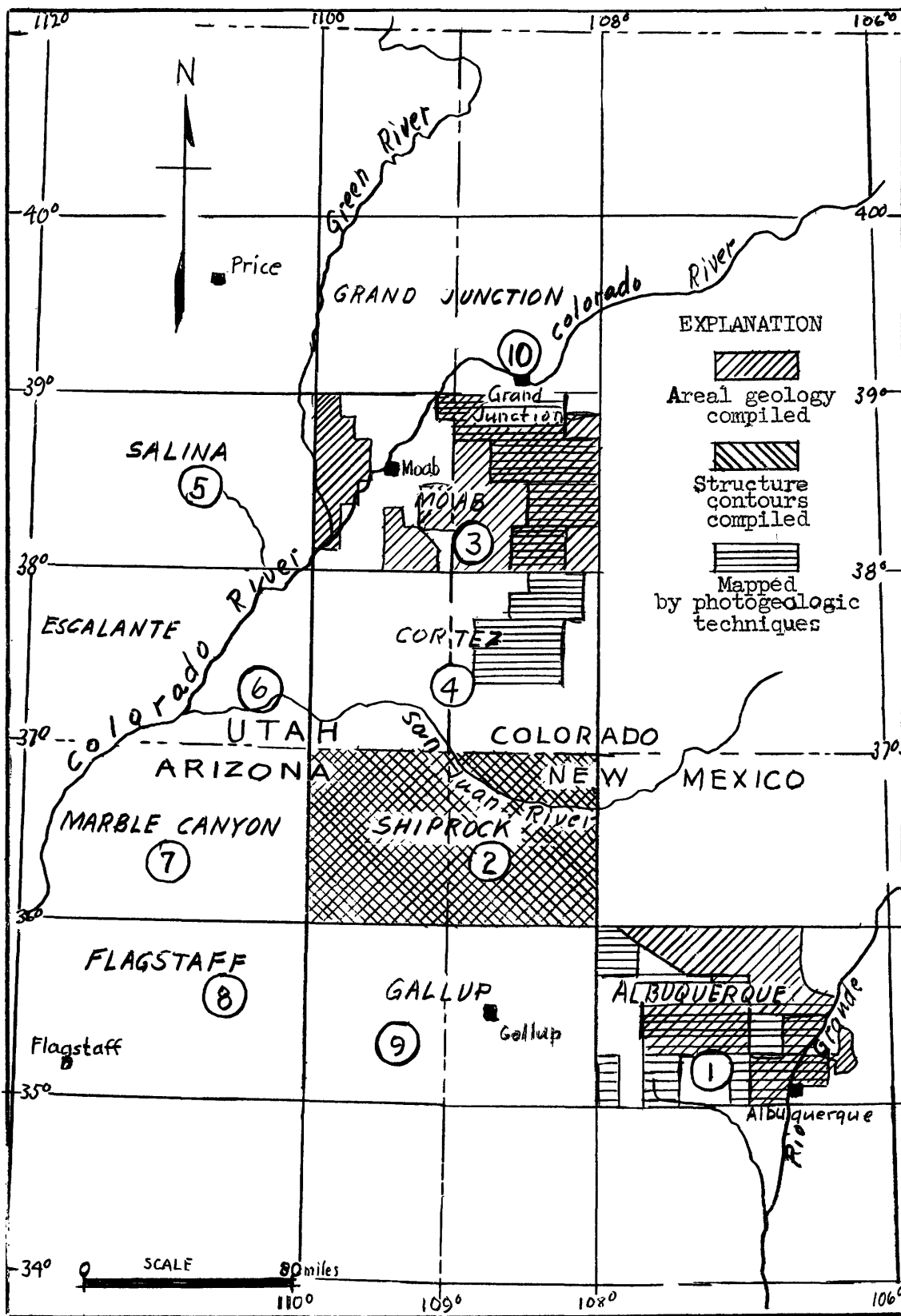


Figure 7.--Index map showing tentative order of, and progress in, compilation of 2° sheets of the Colorado Plateau geologic maps project.

Geologic maps of the Colorado Plateau
by
D. G. Wyant, W. A. Fischer, R. B. O'Sullivan,
Helen Beikman, and P. L. Williams

During the report period work continued on the Shiprock, Moab, and Albuquerque 2° sheets. (See fig. 7.) The Shiprock sheet has been completed and is now being reviewed and revised. The Moab sheet is about 70 percent compiled, and the Albuquerque sheet is about 40 percent compiled.

All photogeologic effort in the Colorado Plateau during the report period was directed toward the compilation of maps at a scale 1:62,500 for use in compilation of the 2° maps. Some of these maps will be published. The equivalent of thirty-six 7-1/2-minute quadrangles were completed during the report period: 22 in the Albuquerque sheet, 14 in the Moab sheet. In the preparation of these maps, pre-existing maps, as well as photogeologic techniques using high altitude photographs in conjunction with the radial planimetric plotter, the Zeiss Stereotope, and the Kelsh and Balplex plotters, were employed.

Brief field trips were made to check the shape of the Precambrian surface in part of the Moab sheet, and the rock types and contacts in part of the Albuquerque sheet.

During the report period photogeologic maps were published in the Survey's Miscellaneous Geologic Investigations Series of the 15-minute Escalante Forks quadrangle in Mesa, Montrose, and Delta Counties, Colorado, and of the 7-1/2-minute Cockscomb SE quadrangle in Kane County, Utah.

Central region

Black Hills, South Dakota - Wyoming

The Survey's uranium program in the northern Black Hills was completed prior to the current period, and has been reported in TEI-690, p. 230-246; TEI-700, p. 75-82; and TEI-740, p. 100-105. Investigations in the southern Black Hills during the report period are reported below.

Angostura Reservoir quadrangle, South Dakota, by Jon J. Connor

The Angostura Reservoir 7 1/2-minute quadrangle is in the northeast part of Fall River County south of the town of Hot Springs. Twenty-six hundred feet of lithified sedimentary rocks, locally overlain by unconsolidated stream-laid terrace deposits, wind-blown material, and alluvium, are exposed in the quadrangle. The sedimentary rocks range in age from Jurassic to Tertiary (?). The Inyan Kara group of Early Cretaceous age, because of its uranium deposits, has been studied in the most detail.

Pre-Inyan Kara stratigraphy.--The oldest rocks exposed in the quadrangle are the Lak and Redwater shale members of the Sundance formation of Late Jurassic age. The Lak member consists of red and white, poorly bedded very fine-grained sandstone and siltstone. A maximum thickness of 20 feet is exposed in the western part of Red Canyon. The Lak is overlain by the Redwater shale member, which is predominantly gray to green, thin-bedded shale interbedded with gray, fossiliferous, glauconitic sandstone. The Redwater shale, which is exposed at only a few places in the quadrangle, is about 130 feet thick.

The Unkpapa sandstone overlies the Sundance formation in apparent conformity and underlies the Inyan Kara group disconformably. The Unkpapa ranges in thickness from 150 to 300 feet and is subdivided into a basal sandstone unit of variable thickness and an upper siltstone unit that is locally absent, probably because of erosion before deposition of the overlying Inyan Kara group. The sandstone unit commonly weathers to a red or white, locally red and white banded, vertical cliff. The siltstone unit at the top of the Unkpapa commonly weathers to a talus-covered slope. The Unkpapa is probably continental, perhaps eolian in origin, and is believed to be of Late Jurassic age.

Inyan Kara stratigraphy.--The Inyan Kara group of Early Cretaceous age is divided into two formations, the Lakota at the base and the Fall River at the top.

The Lakota formation ranges in thickness from 375 to 475 feet and is subdivided into three members which are, in ascending order, an unnamed lower member, the Minnewaste limestone member, and the Fuson member.

The following table compares the nomenclature used in this report with that used by Darton (1902).

This Report	Darton (1902)
Fuson member	Fuson shale
Minnewaste limestone member	Minnewaste limestone
Unnamed lower member	Lakota formation

The unnamed lower member of the Lakota is approximately 300 feet in thickness but varies considerably from place to place. It is composed mainly of orange, lenticular, rim-forming sandstones that interfinger with or locally truncate gray-green, slope-forming mudstones (claystone, siltstone and thin, local sandstone). Shale, limestone, and conglomerate are rare. Together these sandstones and mudstones form a heterogeneous unit that probably was deposited by an aggrading stream system, although the minor amounts of limestone and shale are probably lacustrine and paludal, respectively. Fossils are rare in the unnamed lower member; those found were predominantly ostracods.

The Minnewaste limestone member is about 20 feet thick and consists of thin, tabular lenses of dense gray limestone interbedded with small amounts of carbonaceous siltstone and calcareous sandstone. The Minnewaste is resistant and weathers to a thin prominent ledge. Fossils are rare, but a few poorly preserved remains were tentatively identified as freshwater sponges (R. G. Rezak and P. E. Cloud, Jr., written communications, 1958).

The Fuson member of the Lakota formation, which is about 100 feet thick, is a rarely exposed sequence of variegated claystones, siltstones, and minor sandstones. The rocks comprising the Fuson member are peculiar in their general absence of sedimentary structure and in the presence of polished siliceous pebbles and cobbles sparsely distributed through the claystone beds. Though the depositional environment of the Fuson member is obscure, it was undoubtedly continental, perhaps eolian or lacustrine.

The Fall River formation is about 140 feet thick and is composed predominantly of brown, medium-to coarse-grained, well-jointed sandstone and gray to red, thin-bedded siltstone. The lower 50 feet of the formation is a sequence of interbedded, thin-bedded, locally carbonaceous siltstone

and sandstone. The rocks are commonly gray in color. The base of the formation is marked by an erosional disconformity which is recognized throughout the Black Hills. The upper part of the formation consists of brown, ledge-forming sandstones that interfinger with rarely exposed, slope-forming, siltstones. The siltstones are generally red where exposed and where not exposed may impart a red color to the soil. Locally, relatively large, cliff-forming sandstone bodies, elongate in shape, are present at or near the base of the upper unit and fill channels scoured into the lower unit. These large sandstone bodies are grouped into a middle unit of the Fall River formation. The contact of the formation with the overlying Skull Creek shale is gradational.

Post-Inyan Kara stratigraphy.---Overlying the Inyan Kara group is a sequence of marine shales and limestones about 1,750 feet thick. In ascending order these are the Skull Creek shale, Mowry shale, Belle Fourche shale, Greenhorn formation, Carlile formation, Niobrara formation, Pierre shale, and Chadron (?) formation. The Skull Creek and Mowry shales of Early Cretaceous age and the Belle Fourche shale of Late Cretaceous age are black shales and generally are not fossiliferous. The Greenhorn formation is composed of shale near the base and fossiliferous limestone at the top. The overlying Carlile formation is a gray fossiliferous shale containing a sandy member in the middle. The Niobrara formation is chalky shale; above it is the Pierre shale, a black shale containing numerous concretions. Only 230 feet of Pierre is exposed in the quadrangle.

Locally a thin conglomeratic sandstone lies in angular disconformity on the gently dipping shales. It has been mapped as the Chadron (?) formation and is Tertiary (?) in age.

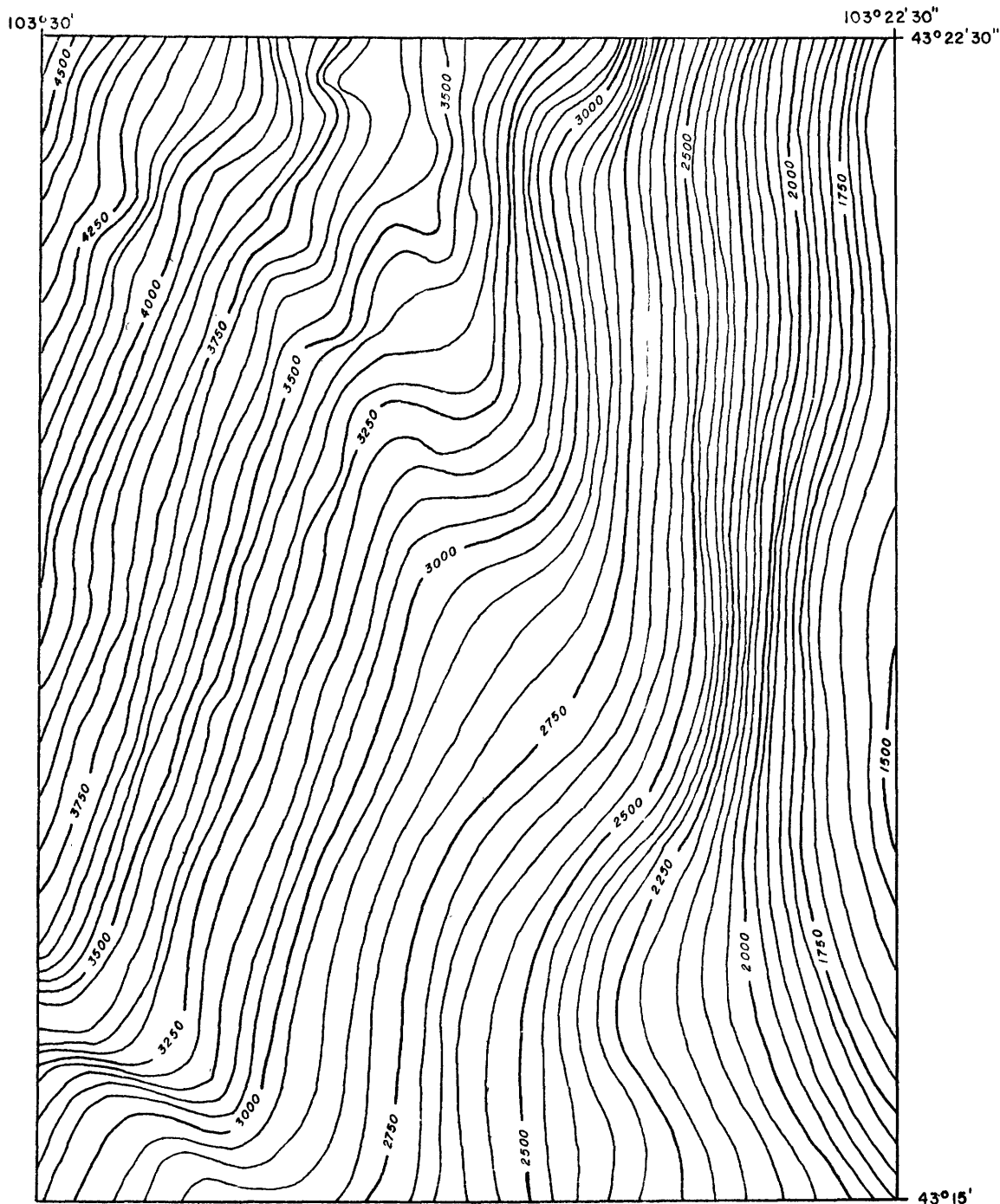


FIGURE 8. — GENERALIZED STRUCTURE CONTOUR MAP OF ANGOSTURA RESERVOIR QUADRANGLE, SOUTH DAKOTA. Contours represent the base of the Fall River formation

1 MILE

Contour interval 50 feet
Datum is mean sea level

Structure.--The quadrangle is on the gently dipping east flank of the Cascade anticline, and the structure is essentially homoclinal with an average dip of 3° to the east and southeast (see figure 8). The quadrangle has about 3,100 feet of structural relief. A number of small southeast-plunging anticlines and synclines are superimposed on the homoclinal attitude. One small fault with a throw of 15 feet is present near the north edge of the quadrangle.

Reference

Darton, N. H., 1902, The Oelrichs quadrangle, S. Dak.-Nebr.: U. S. Geol. Survey Geol. Atlas of the U. S., Folio 85.

Solution and brecciation of the Minnelusa formation, by C. G. Bowles and D. E. Wolcott

Geologic mapping in the Argyle and Hot Springs quadrangles extends to parts of five quadrangles in which gypsum has been removed by solution. The solution of anhydrite or gypsum in the upper part of the Minnelusa formation of Permian-Pennsylvanian age in the Argyle and Hot Springs quadrangles is of regional significance, and has been discussed in TEI-640, p. 111-112; TEI-690, p. 213; TEI-700, p. 83; and TEI-740, p. 89.

The distribution of collapse breccias and the localities where sections have been measured or drill-hole data are available are shown on figure 9. A correlation of various units in the upper part of the Minnelusa formation is shown on figure 10. The sections at localities 3 and 7 (fig. 10) were determined from drill-hole data, and the sections at localities 2 and 5 were compiled from both drill-hole and outcrop data. The sections at localities 1, 4, and 6 were measured on the outcrop.

Cores from a drill-hole at locality 3 contained as much as 230 feet of anhydrite and sparse gypsum. Correlative rocks, however, contain no

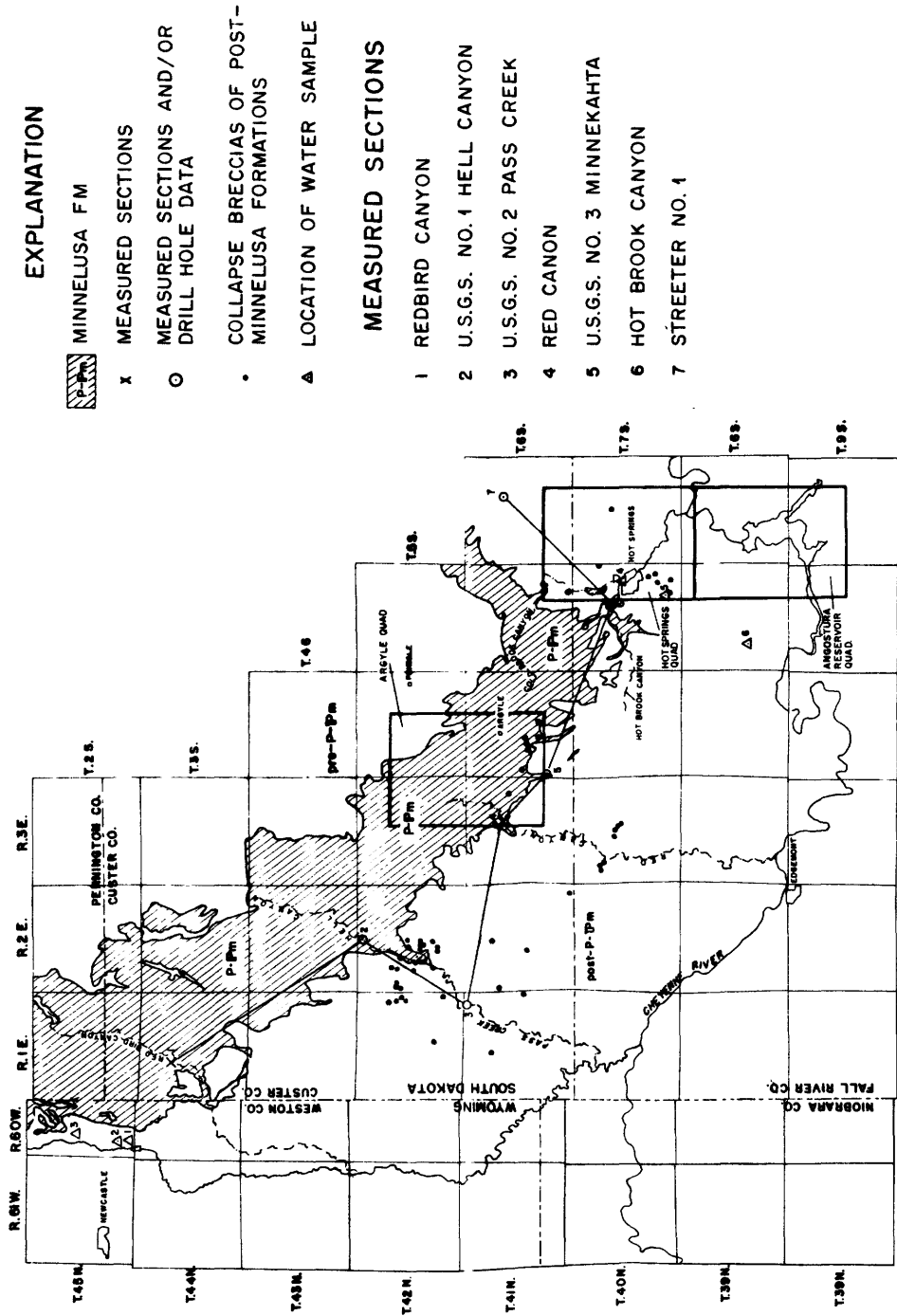


FIGURE 9 MAP OF THE SOUTHERN BLACK HILLS, SOUTH DAKOTA-WYOMING, SHOWING MINNELUSA FORMATION OUTCROP, COLLAPSES INVOLVING POST-MINNELUSA ROCKS, AND LOCATIONS OF STRATIGRAPHIC SECTIONS AND WATER SAMPLES

anhydrite or gypsum at their outcrop except at one locality (TEI-640, p. 111-112). At its outcrop the upper part of the Minnelusa formation is intensely brecciated, except at the one locality where gypsum has been observed. The presence of more than 200 feet of anhydrite in the subsurface rocks and the absence of anhydrite or gypsum in the exposed brecciated rocks indicate that the brecciation resulted from solution and removal of calcium sulfate.

The solution and removal of gypsum have resulted in varying degrees of brecciation, collapse, and crenulation of the intervening beds of sandstone, siltstone, shale, limestone, and dolomite.

This brecciation and collapse may be divided into three zones according to the intensity of brecciation. The intensity varies directly with the amount of gypsum, or anhydrite that originally was present.

The uppermost zone (fig. 10, units 1-16) is about 225 feet thick and is characterized by moderate brecciation of the first and second sandstone beds (units 1 and 3), and by intense brecciation of the rocks below the second limestone bed (unit 4). Intense brecciation has resulted in massive "beds" of breccia, in which the breccia fragments have moved very little relative to one another, but the entire block of beds has been let down as units and brecciated in the process. Also in the upper zone, but in contrast to the breccia "beds", are near-vertical breccia pipes or filled sinks (fig. 11). These breccia pipes contain individual fragments derived from several overlying beds and are cemented with calcium carbonate. The pipes range up to 40 feet in diameter and 150 feet in depth.

The middle zone, 50 to 100 feet thick, is characterized by contorted and locally brecciated "beds" and by breccia "sills". The breccia "sills"

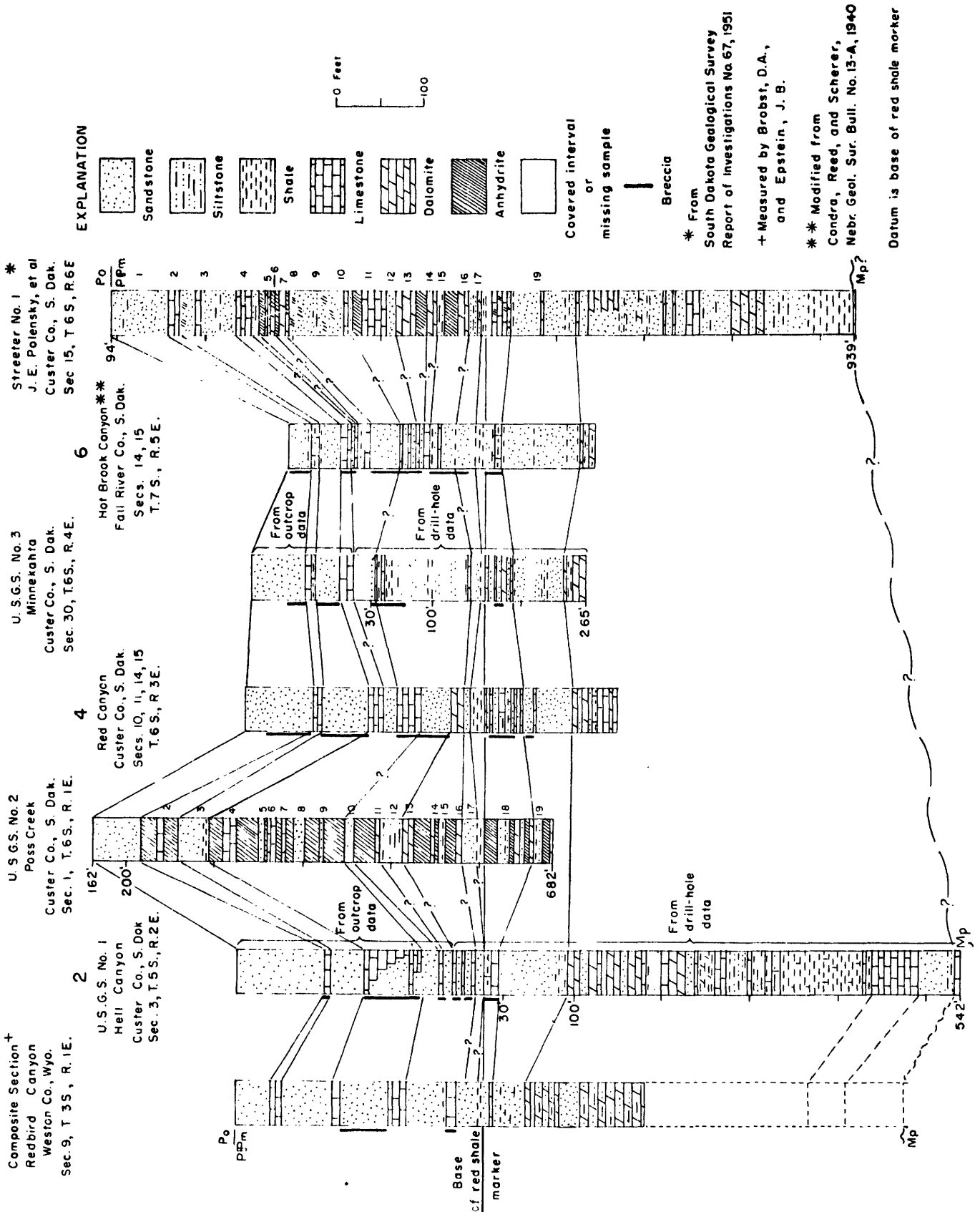


FIGURE 10.—CORRELATION OF THE UPPER MINNELUSA FORMATION IN THE SOUTHERN BLACK HILLS OF WYOMING AND SOUTH DAKOTA

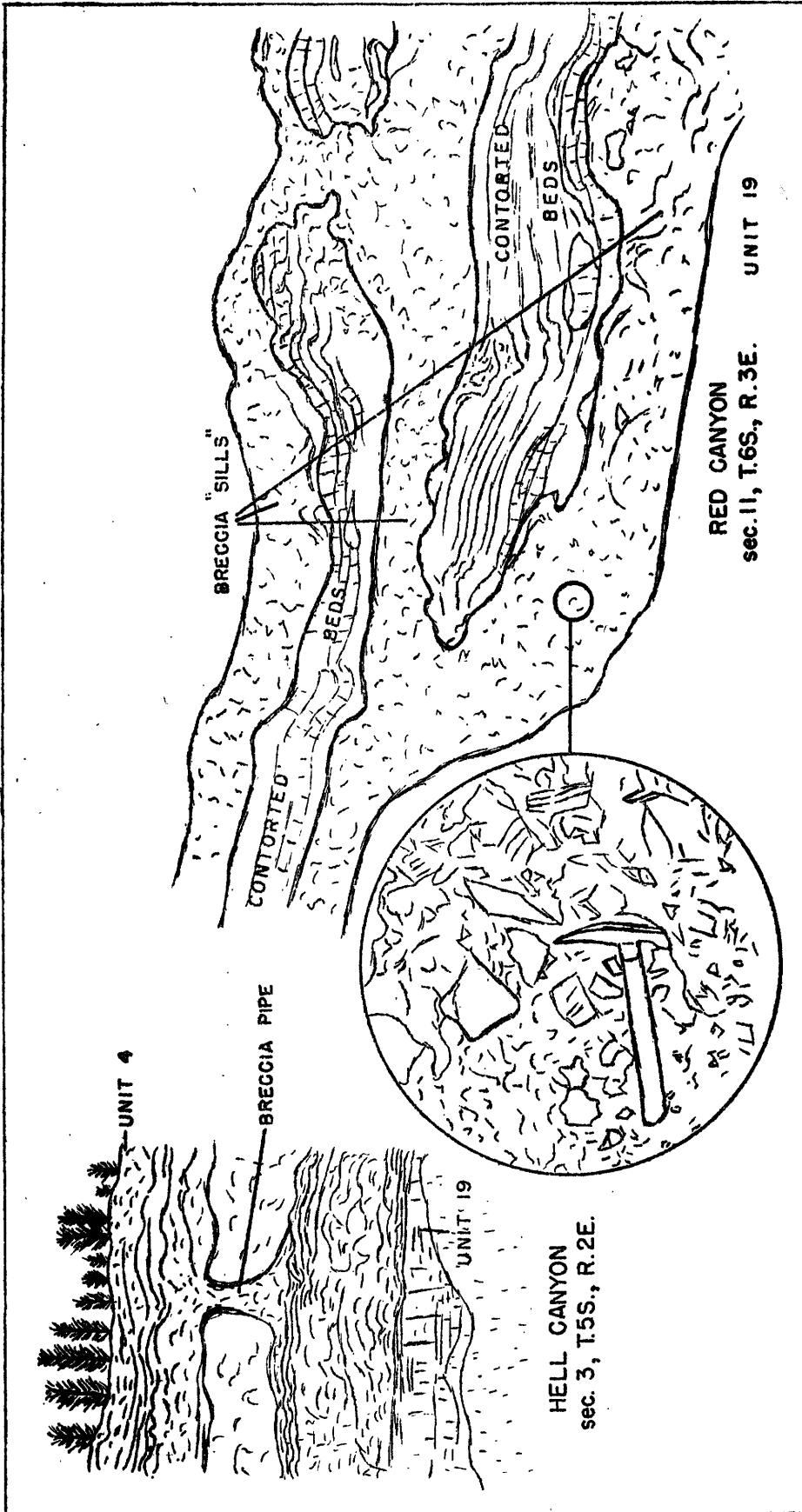


FIGURE 11.-- BRECCIA PIPES AND "SILLS" IN THE MINNELUSA FORMATION, CUSTER COUNTY, S. DAK.

presumably flowed laterally into solution caverns. The breccia "sills" are common below the red shale marker (fig. 11).

In the lower zone the beds are undisturbed, except in areas affected by solution and collapse of the underlying Pahasapa limestone of Mississippian age.

The rocks involved in the collapse and brecciation include the Minnelusa, Opeche, Minnekahta, Spearfish, Sundance, Unkpapa, Morrison, and Lakota formations. Some of the breccias in the Minnelusa formation are overlain by undisturbed gravel of White River (Oligocene) age. The earliest solution and subsidence, therefore, occurred during post-Lakota and pre-White River time. Closed depressions as much as 60 feet deep and unaffected by the present drainage system indicate that solution and subsidence have extended into recent time. This is substantiated by the relatively large quantities of CaSO_4 that are being carried by the present-day spring waters (table 2).

Table 2.--Chemical analyses of spring water presumably issuing
from the Minnelusa formation
(Surface outlets are at the base of the Minnekahta
limestone or in the lower part of the Spearfish
formation. Components in parts per million.)

Sample Number	1	2	3	4	5	6
Silica	16.	14.	13.	27.	2.4	22.2
Aluminum	0.2	0.4	0.1	0.1	0.3	0.2
Iron	0.00	0.00	0.04	0.00	0.03	0.03
Manganese	0.00	0.00	0.00	0.00	0.00	0.00
Calcium	532.	472.0	402.	252.	508.	568.
Magnesium	83.	78.	56.	51.	112.	92.
Sodium	5.4	5.5	3.8	86.	21.	54.
Potassium	2.6	2.6	1.6	9.8	15.	6.2
Lithium	.00	.00	.05	.05	.05	.00
Uranium	0.012	0.011	0.0047	0.0075	0.0063	0.0057
Bicarbonate (HCO ₃)	225.	227.	190.	232.	112.	235.
Carbonate (CO ₃)	0.	0.	0.	0.	0.	0.
Sulfate (SO ₄)	1420.	1260.	1040.	639.	1610.	1540.
Chloride (Cl)	4.0	5.0	1.0	112.	13.	62.
Fluoride (F)	0.4	0.4	0.2	0.8	0.2	0.9
Nitrate (NO ₃)	4.7	3.2	1.4	1.0	0.0	0.6
Phosphate (PO ₄)	0.00	0.00	0.00	0.00	0.00	0.00
Boron	.07	.11	.05	.24	.19	.19
B plt	7.6	7.7	7.5	7.0	7.4	7.0

Location of water samples (shown on fig. 9):

1. SE 1/4 sec. 31, T. 45 N., R. 60 W., Weston Co., Wyo.
2. NE 1/4 sec. 31, T. 45 N., R. 60 W., Weston Co., Wyo.
3. SW 1/4 sec. 17, T. 45 N., R. 60 W., Weston Co., Wyo.
4. Evan's Plunge, SW 1/4 sec. 13, T. 7 S., R. 5 E., Hot Springs, S. Dak.
5. NW 1/4 sec. 35, T. 7 S., R. 5 E., Fall River Co., S. Dak.
6. Cascade Springs, SW 1/4 sec. 20, T. 8 S., R. 5 E., Fall River Co., S. Dak.

Gas Hills, Wyoming

Field work in the Gas Hills area was completed prior to the current report period, and results have been reported in TEI-690, p. 272-276 and 508-512; TEI-700, p. 88-91; and TEI-740, p. 106-120. A final report on investigations in the Gas Hills is being prepared for publication as a USGS Professional Paper.

Eastern region

Mauch Chunk, Pennsylvania

Work on the Mauch Chunk project was completed prior to the present report period and important results were reported in TEI-690, p. 312-317; TEI-700, p. 110-113; and TEI-740, p. 121-135. A final report for Survey publication is being prepared.

GEOLOGIC TOPICAL STUDIES

Colorado Plateau region

General stratigraphic studies
by
L. C. Craig

Compilation of data on Paleozoic sedimentary rocks of the Colorado Plateau was recessed at the beginning of this report period. A summary of the progress of this work was given in TEI-740, p. 127-129.

During this report period the work on Mesozoic sedimentary rocks was confined mainly to preparation of reports; field study was restricted to brief examinations of several localities. A stratigraphic section of Cretaceous rocks near Grand Junction, Colorado, was reviewed and sampled for petrologic analysis. Mesozoic beds at Tanque Arroyo, north of Albuquerque, New Mexico, were also examined. Based on exposures at the latter locality, it is concluded that sandstones like the so-called Jackpile sandstone of local usage (Freeman and Hilpert, 1956, p. 317-318) are present at the top of the Morrison formation east of the Rio Grande in north-central New Mexico. In support of this identification of beds, it may be noted that Swift (1956) also identified similar beds at the top of the Morrison (his Deadmans Peak formation) east of the Rio Grande near San Antonio.

The relatively wide extent of the so-called Jackpile sandstone of local usage in the eastern part of the San Juan Basin was discussed in TEI-700, p. 114-115 but no mention was made in that report of possible extensions of the sandstone east of the Rio Grande.

During this report period the following paper was published:

Craig, L. C., and Cadigan, R. A., 1958, The Morrison and adjacent formations in the Four Corners Area in Guidebook to the geology of the Paradox Basin: Intermountain Assoc. Petroleum Geologists, 9th annual field Conf. guidebook, p. 182-192.

References

Freeman, V. L., and Hilpert, L. S., 1956, Stratigraphy of the Morrison formation in part of northwestern New Mexico: U. S. Geol. Survey Bull. 1030-J, p. 309-334.

Swift, E. R., 1956, Study of the Morrison formation and related strata, north-central New Mexico: unpublished MS thesis, Univ. of New Mexico.

Triassic studies

Studies of the Triassic formations in the Colorado Plateau were essentially completed before the current report period. The more important results of the Triassic study were reported in TEI-690, p. 341-351; TEI-700, p. 115-122; and TEI-740, p. 130-139.

Lithologic studies by R. A. Cadigan

Lithologic studies of sedimentary rocks of the Colorado Plateau during this report period included a petrologic study of a suite of samples from sedimentary rocks of the San Rafael group of Jurassic age. The samples were collected by the author from a measured stratigraphic section in the Paria Amphitheater area in southwestern Garfield County, Utah. The stratigraphy, including measurements and unit boundaries used in this report, was done by the Entrada stratigraphy project.

The petrologic study consisted of the grainsize analysis and microscopic compositional study of 29 sandstone, siltstone, claystone and limestone samples which represent a thickness of about 1,600 feet of sedimentary rocks. Methods used to determine composition are those reported in TEI-700, p. 124-139.

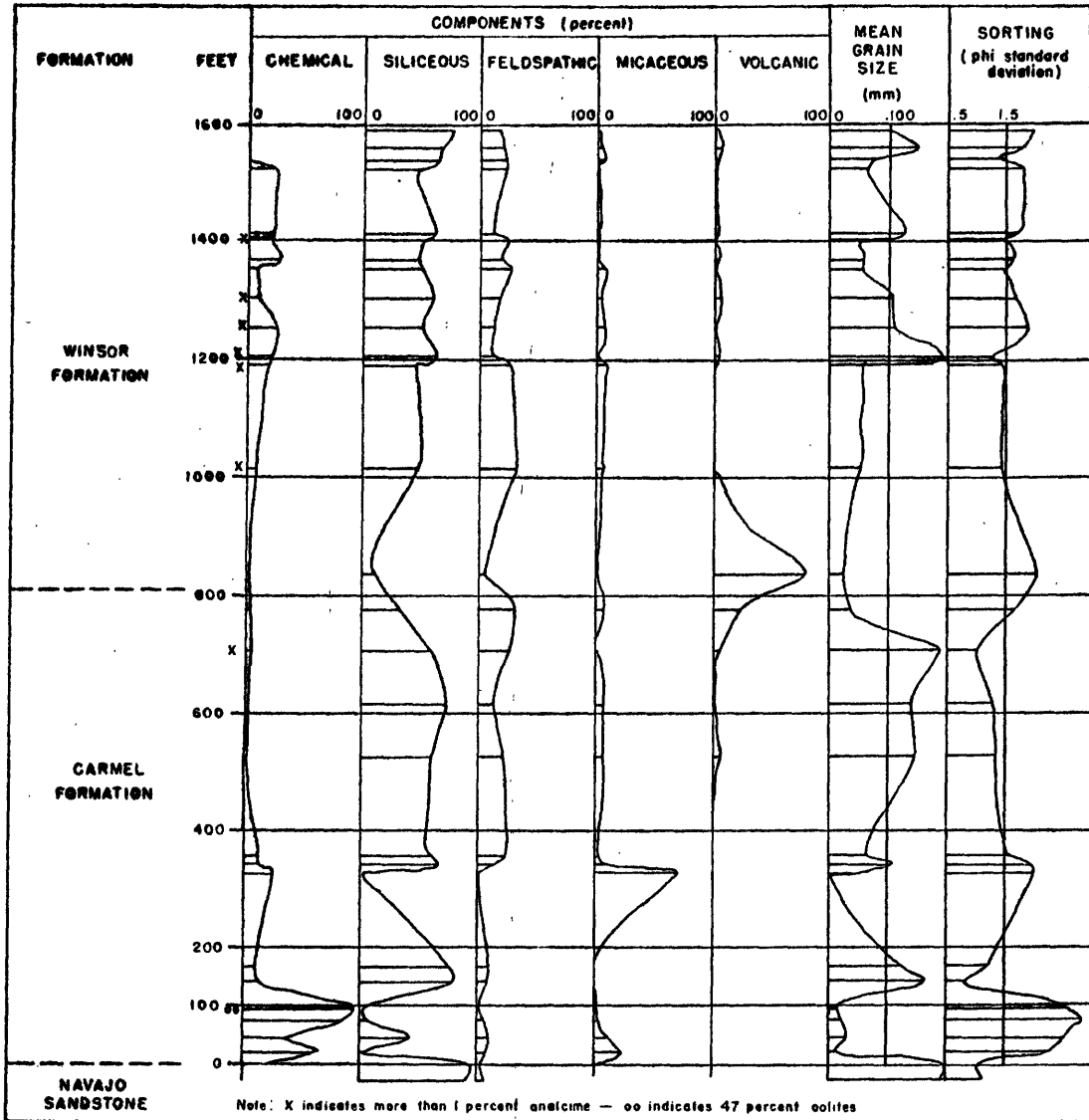


FIGURE 12. GRAPHS SHOWING THE PERCENTAGE ROCK COMPOSITION, GRAIN SIZE, AND SORTING IN SEDIMENTARY ROCKS IN THE PARIAMPHITHEATER AREA, GARFIELD COUNTY, UTAH

Data obtained as a result of the investigation are summarized in graphic form in figure 12. From left to right in columns are: the formation names; location in feet above the top of the Navajo sandstone; the 18 mineral components listed in table 3, summarized under the four headings: chemical, siliceous, feldspathic, micaceous, and volcanic components; mean grain size, in millimeters; and sorting, in terms of the standard deviation of the phi grain size distribution.

The San Rafael group in this area consists of the Carmel and Winsor formations (J. C. Wright, 1958, oral communication). A significant result of this study was the discovery of analcime in the upper Carmel and Winsor formations. Altered tuff fragments and ash are also present, giving evidence of a substantial volcanic contribution to the sedimentary rocks which make up the two formations.

Table 3.--Tabulated results of point count composition analyses of 29 samples of Jurassic rocks from a measured section of the San Rafael group in the Paria Amphitheater area, Garfield County, Utah

Distance above top of Navajo sandstone, in feet	Navajo sandstone		Carmel formation		
	-30	-2	20	45	75
Sample numbers	L2958	L2959	L3003	L2962	L2960
Chemical components (excluding silica)					
Calcite and dolomite, barite, gypsum, etc.	--	--	64.6	34.6	84.8
Red interstitial iron oxide and impregnations	0.2	--	0.4	--	--
Total	0.2	--	65.0	34.6	84.8
Siliceous components					
Quartz grains and overgrowths	92.2	97.0	3.2	43.2	6.6
Quartzite fragments	--	--	--	--	--
Chert, detrital	0.2	--	--	--	--
Chert, chalcedony, interstitial	--	--	0.2	0.2	--
Total	92.4	97.0	3.4	43.4	6.6
Feldspar and feldspar derived components					
Potassic feldspar	0.6	0.6	7.6	9.4	6.0
Plagioclase feldspar	3.0	1.4	0.2	2.4	0.6
Kaolinite and kaolinitic clays	3.2	0.6	0.6	--	--
Total	6.8	2.6	8.4	11.8	6.6
Dark mineral and micaceous rock fragments and related material					
Mica flakes and books	--	--	--	1.4	0.8
Illite and micaceous clays	0.2	--	23.0	8.4	0.6
Micaceous and basaltic rock frags.	--	--	--	0.2	--
"Heavy minerals"	--	--	--	--	--
Misc. (usually unidentified opaque minerals)	--	--	0.2	--	0.4
Total	0.2	--	23.2	10.0	1.8
Volcanic components					
Altered tuff and felsic rocks fragments	0.4	0.4	--	0.2	0.2
Montmorillonite and related clay mixtures	--	--	--	--	--
Altered ash (clay mixtures, shard relics, etc.)	--	--	--	--	--
Total	0.4	0.4	--	0.2	0.2

Table 3.--Continued

Distance above top of Navajo sandstone, in feet	Carmel formation				
	95	140	165	325	340
Sample numbers	L2961	L3004	L3005	L3010	L3011
Chemical components (excluding silica)					
Calcite and dolomite, barite, gypsum, etc.	96.0	9.8	9.6	19.0	8.6
Red interstitial iron oxide and impregnations	--	--	--	8.0	0.4
Total	96.0	9.8	9.6	27.0	9.0
Siliceous components					
Quartz grains and overgrowths	0.4	81.2	78.2	2.0	66.0
Quartzite fragments	--	--	--	--	--
Chert, detrital	--	--	0.2	--	0.2
Chert, chalcedony, interstitial	--	--	--	--	--
Total	0.4	81.2	78.4	2.0	66.2
Feldspar and feldspar derived components					
Potassic feldspar	1.6	6.8	8.6	--	10.6
Plagioclase feldspar	--	1.2	0.4	--	3.0
Kaolinite and kaolinitic clays	--	0.8	2.6	--	0.2
Total	1.6	8.8	11.6	--	13.8
Dark mineral and micaceous rock fragments and related material					
Mica flakes and books	--	--	--	1.0	--
Illite and micaceous clays	2.0	--	0.2	70.0	8.4
Micaceous and basaltic rock frags.	--	--	--	--	--
"Heavy minerals"	--	--	--	--	0.2
Misc. (usually unidentified opaque minerals)	--	0.2	--	--	0.6
Total	2.0	0.2	0.2	71.0	9.2
Volcanic components					
Altered tuff and felsic rock fragments	--	--	0.2	--	1.8
Montmorillonite and related clay mixtures	--	--	--	--	--
Altered ash (clay mixtures, shard relics, etc.)	--	--	--	--	--
Total	--	--	0.2	--	1.8
Notes on composition	47.2 percent oolites		claystone		

Table 3.--Continued

Distance above top of Navajo sandstone, in feet	Carmel formation				
	355	525	615	705	775
Sample numbers	L3012	L3006	L3007	L3009	L3008
Chemical components (excluding silica)					
Calcite and dolomite, barite, gypsum, etc.	13.4	1.2	3.8	4.4	4.2
Red interstitial iron oxide and impregnations	--	0.2	--	0.8	0.2
Total	13.4	1.4	3.8	5.2	4.4
Siliceous components					
Quartz grains and overgrowths	59.2	60.8	73.4	60.8	32.4
Quartzite fragments	--	--	--	0.4	0.2
Chert, detrital	0.2	--	0.2	--	0.4
Chert, chalcedony, interstitial	--	--	--	--	--
Total	59.4	60.8	73.6	61.2	33.0
Feldspar and feldspar derived components					
Potassic feldspar	18.0	15.8	9.2	17.6	21.2
Plagioclase feldspar	6.6	6.2	4.0	8.6	10.8
Kaolinite and kaolinitic clays	0.6	0.2	--	--	0.2
Total	25.2	22.2	13.2	26.2	32.2
Dark mineral and micaceous rock fragments and related material					
Mica flakes and books	--	0.4	--	--	0.8
Illinite and micaceous clays	1.0	5.0	7.2	1.4	4.6
Micaceous and basaltic rock frags.	--	--	--	--	--
"Heavy minerals"	0.2	--	0.2	--	0.4
Misc. (usually unidentified opaque minerals)	0.2	1.4	0.4	0.2	1.2
Total	1.4	6.8	7.8	1.6	7.0
Volcanic components					
Altered tuff and felsic rock fragments	0.6	7.8	1.2	5.6	1.0
Montmorillonite and related clay mixtures	--	1.0	0.4	0.2	22.4
Altered ash (clay mixtures, shard relics, etc.)	--	--	--	--	--
Total	0.6	8.8	1.6	5.8	23.4
Notes on composition	9.4 percent interstitial gypsum		1.6 percent analcime		

Table 3.--Continued

Distance above top of Navajo sandstone, in feet	Winsor formation				
	836	1016	1191	1206	1256
Sample numbers	L3013	L3014	L3015	L3016	L3017?
Chemical components (excluding silica)					
Calcite and dolomite, barite, gypsum, etc.	2.0	10.0	17.2	20.6	27.0
Red interstitial iron oxide and impregnations	--	0.2	0.4	--	--
Total	2.0	10.2	17.6	20.6	27.0
Siliceous components					
Quartz grains and overgrowths	10.6	48.0	43.4	63.0	50.2
Quartzite fragments	--	--	0.2	0.2	--
Chert, detrital	--	--	1.0	1.4	0.8
Chert, chalcedony, interstitial	--	--	--	--	--
Total	10.6	48.0	44.6	64.6	51.0
Feldspar and feldspar derived components					
Potassic feldspar	3.4	16.2	18.6	6.8	8.0
Plagioclase feldspar	2.0	17.2	8.6	2.8	5.2
Kaolinite and kaolinitic clays	--	--	--	--	--
Total	5.4	33.4	27.2	9.6	13.2
Dark mineral and micaceous rock fragments and related material					
Mica flakes and books	1.8	--	0.2	--	--
Illite and micaceous clays	0.2	5.0	6.8	0.4	6.4
Micaceous and basaltic rock frags.	--	--	--	--	--
"Heavy minerals"	0.2	0.2	0.2	--	--
Misc. (usually unidentified opaque minerals)	--	2.4	1.4	--	0.2
Total	2.2	7.6	8.6	0.4	6.6
Volcanic components					
Altered tuff and felsic rock fragments	0.2	0.8	1.0	4.8	2.0
Montmorillonite and related clay mixtures	79.6	--	1.0	--	0.2
Altered ash (clay mixtures, shard relics, etc.)	--	--	--	--	--
Total	79.8	0.8	2.0	4.8	2.2
Notes on composition		1.0	1.2	4.2	1.2
		percent	percent	percent	percent
		analcime	analcime	analcime	analcime

Table 3.—Continued

Distance above top of Navajo sandstone, in feet	Winsor formation				
	1306	1356	1368	1406	1412
Sample numbers	L3018	L3019	L2557	L3020	L2558
Chemical components (excluding silica)					
Calcite and dolomite, barite, gypsum, etc.	10.8	10.4	30.0	19.4	24.6
Red interstitial iron oxide and impregnations	--	--	--	0.2	--
Total	10.8	10.4	30.0	19.6	24.6
Siliceous components					
Quartz grains and overgrowths	60.4	50.0	46.6	51.2	61.4
Quartzite fragments	0.6	0.2	--	--	--
Chert, detrital	0.2	0.6	--	0.4	0.6
Chert, chalcedony, interstitial	--	--	--	--	0.2
Total	61.2	50.8	46.6	51.6	62.2
Feldspar and feldspar derived components					
Potassic feldspar	13.2	18.8	9.2	15.2	6.6
Plagioclase feldspar	4.6	9.0	8.2	9.4	2.0
Kaolinite and kaolinitic clays	--	--	0.2	--	0.4
Total	17.8	27.8	17.6	24.6	9.0
Dark mineral and micaceous rock fragments and related material					
Mica flakes and books	0.2	0.4	0.2	0.4	--
Illite and micaceous clays	3.6	7.4	0.6	1.4	--
Micaceous and basaltic rock frags.	--	--	--	--	--
"Heavy minerals"	--	0.2	--	0.2	--
Misc. (usually unidentified opaque minerals)	0.2	0.6	0.4	0.2	--
Total	4.0	8.6	1.2	2.2	--
Volcanic components					
Altered tuff and felsic rock fragments	6.2	2.4	4.6	2.0	4.2
Montmorillonite and related clay mixtures	--	--	--	--	--
Altered ash (clay mixtures, shard relics, etc.)	--	--	--	--	--
Total	6.2	2.4	4.6	2.0	4.2
Notes on composition	2.6	0.8		3	
	percent	percent		percent	
	analcime	analcime		analcime	

Table 3.--Continued

Distance above top of Navajo sandstone, in feet	Winsor formation			
	1522	1538	1561	1591
Sample numbers	L2559	L2560	L3021	L3022
Chemical components (excluding silica)				
Calcite and dolomite, barite, gypsum, etc.	27.0	--	0.2	--
Red interstitial iron oxide and impregnations	0.6	--	--	0.2
Total	27.6	--	0.2	0.2
Siliceous components				
Quartz grains and overgrowths	47.4	65.2	67.8	77.4
Quartzite fragments	--	--	0.6	0.2
Chert, detrital	--	0.2	1.0	0.8
Chert, chalcedony, interstitial	--	--	--	--
Total	47.4	65.4	69.4	78.4
Feldspar and feldspar derived components				
Potassic feldspar	17.0	19.2	15.8	13.4
Plagioclase feldspar	5.8	3.0	3.8	2.8
Kaolinite and kaolinitic clays	0.4	0.4	0.2	--
Total	23.2	22.6	19.8	16.2
Dark mineral and micaceous rock fragments and related material				
Mica flakes and books	--	--	0.4	--
Illite and micaceous clays	--	9.0	3.6	1.8
Micaceous and basaltic rock frags.	--	--	--	--
"Heavy minerals"	0.6	0.2	--	--
Misc. (usually unidentified opaque minerals)	--	--	0.4	--
Total	0.6	9.2	4.4	1.8
Volcanic components				
Altered tuff and felsic rock fragments	1.0	2.6	6.2	3.4
Montmorillonite and related clay mixtures	0.2	0.2	--	--
Altered ash (clay mixtures, shard relics, etc.)	--	--	--	--
Total	1.2	2.8	6.2	3.4
Notes on composition			0.2	
			percent	
			analcime	

The history of deposition of these sedimentary rocks may be interpreted from the compositional, textural, and stratigraphic data shown on figure 12. The following interpretations of sample analyses are in stratigraphic sequence, from bottom to top--in order of the sequence of events. The samples are identified in terms of location in feet above the Navajo sandstone.

The two samples from -30 to 0 feet (orthoquartzites), in the Navajo sandstone, represent a period of regional quiescence and probably an eolian environment. The sediments formed moderately well-sorted (standard deviation: 1.0-1.5), fine-grained sandstone with a low content of feldspathic (mostly plagioclase and kaolinite), volcanic, and micaceous components and a correspondingly high content (more than 90 percent) of siliceous (quartz) components.

The four samples from 0 to 100 feet (three limestones and one feldspathic orthoquartzite) represent the lowest 100 feet of the Carmel formation. The properties of the samples are indicative of submergence of the eolian Navajo sandstone caused by an increased rate of subsidence in either this area of deposition, or the region as a whole. This area was invaded by the sea with the result that chemical deposition in shallow water marine environment was the dominant feature; the chemical deposits are mostly calcite with some fossil shell fragments and oolite beds. Detritals deposited consist of minor proportions of poorly sorted micaceous muds; the muds contain higher proportions of potash feldspar than the previous detritals, which indicates the presence of a new source area. The poor sorting (stand. dev.: 2.0 - 4.0) of the muds suggests aqueous transport with little or no reworking.

The two samples taken between 100 and 200 feet (an orthoquartzite and a feldspathic orthoquartzite), indicate a return to conditions of quiescence in the area of deposition, brought about by a decrease in the rate of subsidence or a slight uplift which produced emergence and a beach-eolian environmental complex. Minor tectonic activity in one or more source areas continued. Because of the slow rate of deposition it is proposed that a considerable length of time which is not reflected in a proportionate thickness of the sediments passed during these events. The rocks show a large increase in proportions of siliceous to chemical components; the sediments are fine-grained, moderately well to very well sorted (stan. dev.: 0.5 - 1.0) sandstones with higher potassic feldspar and calcite contents than the similar appearing Navajo sandstone. The resemblance to the Navajo sandstone is due to their similar tectonic and geographic environments of deposition.

Six samples of the Carmel formation between 200 and 750 feet (one graywacke claystone, three feldspathic orthoquartzites, and two arkoses), indicate a major increase in the tectonic activity in the source areas and an increase in the rate of subsidence. Source area activity consisted of moderate uplift and the beginning of significant volcanic activity. The potassic feldspar-rich sediments were dominantly moderately sorted (sand. dev.: 1.5 - 2.0) to moderately well sorted fine-grained sandstone. Compared with earlier deposits, they show a large increase in feldspathic and volcanic components, including analcime. Analcime is interpreted here as a probable derivative of sodic vitric ash; it is present as an interstitial zeolite and in one sample (705 ft.) makes up 1.6 percent of the rock; it is graphed as part of the chemical components in figure 12. Gypsum occurs as an interstitial cement in

the sample from 355 feet, and composes 9.4 percent of the rock. The gypsum and low chemical components of subsequent samples suggest continued deposition on an emergent but aquatic plain.

The four samples of the Carmel and Winsor formations between 750 and 1200 feet (two arkose, one tuffaceous arkose, and one tuff) indicate an increase in the rate of subsidence and fluctuations between aquatic plain and shallow water environments of deposition; in addition, there was continued moderate uplift of the source areas and a period of relatively intense volcanic activity. Sediments deposited in this interval were mostly moderately sorted silts. A zone 705 to 1000 feet above the Navajo sandstone contains significantly larger amounts of volcanic components; the altered potassic tuff fragments and the montmorillonite and montmorillonite-hydromica clays compose as much as 80 percent of the rock. The volcanic zone represents a period of rapid deposition and subsidence as indicated by the moderate to poor sorting. After deposition of the volcanics, the rate of deposition of detrital materials decreased, that of chemical components increased, and deposition probably continued in a shallow water environment as the presence of fossil shell fragments at 1016 feet suggests.

The eleven samples of the Winsor formation between 1200 and 1600 feet (two arkose and nine feldspathic orthoquartzite) indicate an increased rate of subsidence with a resulting increase in the rate of deposition of detrital sediments; moderate uplift continued in the granitic source areas and tectonic uplift possibly began a new quartzitic source area. The sediments deposited on the aquatic plain were fine to very fine grained, moderately sorted to moderately well sorted sands--coarser and

less well sorted than the previous sediments. Although the sands were predominantly feldspathic, the proportion of siliceous components increased at the expense of the feldspathic components. The sediments continued to contain significant proportions of volcanic components including analcime, and increased amounts of chemical components.

Based on the petrologic analysis of 29 samples, the San Rafael group in the Paria Amphitheater area represents a series of tectonic events which can be summarized in order of occurrence as follows:

- (1) submergence of the eolian depositional plain on which the Navajo sandstone was being deposited thus ending a long period of regional quiescence;
- (2) minor tectonic uplift of source areas which produced micaceous and feldspathic sediments;
- (3) major tectonic uplift of (probably the same) source areas, which produced arkosic sediments;
- (4) a period of volcanism which began at the time of the major uplift, reached a peak sometime later, but continued at a reduced but moderate rate through the remainder of the period of deposition of the San Rafael group;
- (5) tectonic uplift of a quartzitic source area during deposition of the upper part of the San Rafael group.

The uranium ore potential of the San Rafael group at the location sampled is considered to be poor. As has been pointed out in previous reports (TEI-490, p. 47-48 and TEI-700, p. 124-139) 15 to 35 percent kaolinite (and hydromica) in a quartzitic or feldspathic sandstone is required to form conditions favorable for uranium deposition. The maximum proportion of kaolinite observed in the 22 samples classifiable as sandstones or sandy siltstones is in a sample of Navajo sandstone in which well-crystallized kaolinite composes 3 percent of the rock.

The maximum proportion of hydromica observed in these sandy rocks is in a sample from the upper part of the Winsor formation in which poorly crystallized mixed hydromicamontmorillonite and well crystallized fibrous hydromica compose 9 percent of the rock.

Analcime zeolite which occurs in significant quantities in nine of the samples was identified by optical and X-ray properties. The D-spacing in Angstrom units of the three strongest lines for the concentrated material are, in order of prominence: 5.60, 3.43, 2.93 (100, 80, 65).

San Rafael (Entrada) studies
by
D. D. Dickey and J. C. Wright

The distribution and lithologic nature of the San Rafael group were outlined in TEI-740, p. 139-146. That report suggested that a complete reorientation of sediment-transport direction occurred in late Jurassic time. Sediment-transport had been westward during deposition of the earlier San Rafael formations; it was northeastward during deposition of later formations. This marked reorientation is significant because it implies the uplift at that time of a new source-area in the location that had long been the site of the Cordilleran geosyncline. Studies of crossbedding in the Curtis formation, completed in this report period, have confirmed that this formation was deposited by northeastward-flowing currents.

The crossbedding occurs in a conglomeratic sandstone at the base of the Curtis formation. This sandstone, which is present over most of the San Rafael Swell in Emery County, Utah, ranges in thickness from

1 to 15 feet. It is coarse-grained, poorly sorted, and pebbly. It contains not only glauconite and fragmental marine fossils, but also carbonaceous debris of twigs and small branches.

The sets of cross-strata are only one to four feet thick, but are large areally; they are scores of feet long parallel to their strike, and tens of feet broad across the strike. They have only slight curvature; the strike at the ends of a set seldom differs as much as 10 degrees from the strike at the axis.

The crossbeds have remarkably consistent dip-direction at individual localities, both within small areas and throughout the region. Measurements of crossbeds were made at seven localities, each about 10 miles apart; and from 10 to 47 dip observations were made at each locality. The estimated average dip-direction at each locality is indicated by an arrow on figure 13. The estimate of average dip-direction is the computed average of the sample of crossbeds measured at the locality. Associated with each arrow is a sector, which indicates the estimated reliability of the average. If, for instance, this sector spreads 12 degrees on either side of the arrow it indicates that, at the 95 percent probability level, the estimated average dip-direction is within 12 degrees of the true average dip-direction. The estimated reliability has been computed by Stein's method as described by Cochran (1953, p. 59):

$$r_e = \frac{t_{.05s}}{\sqrt{n}}$$

where r_e = the estimated reliability in degrees

$t_{.05}$ = t-value from Student's "t" table at the 95 percent probability level.

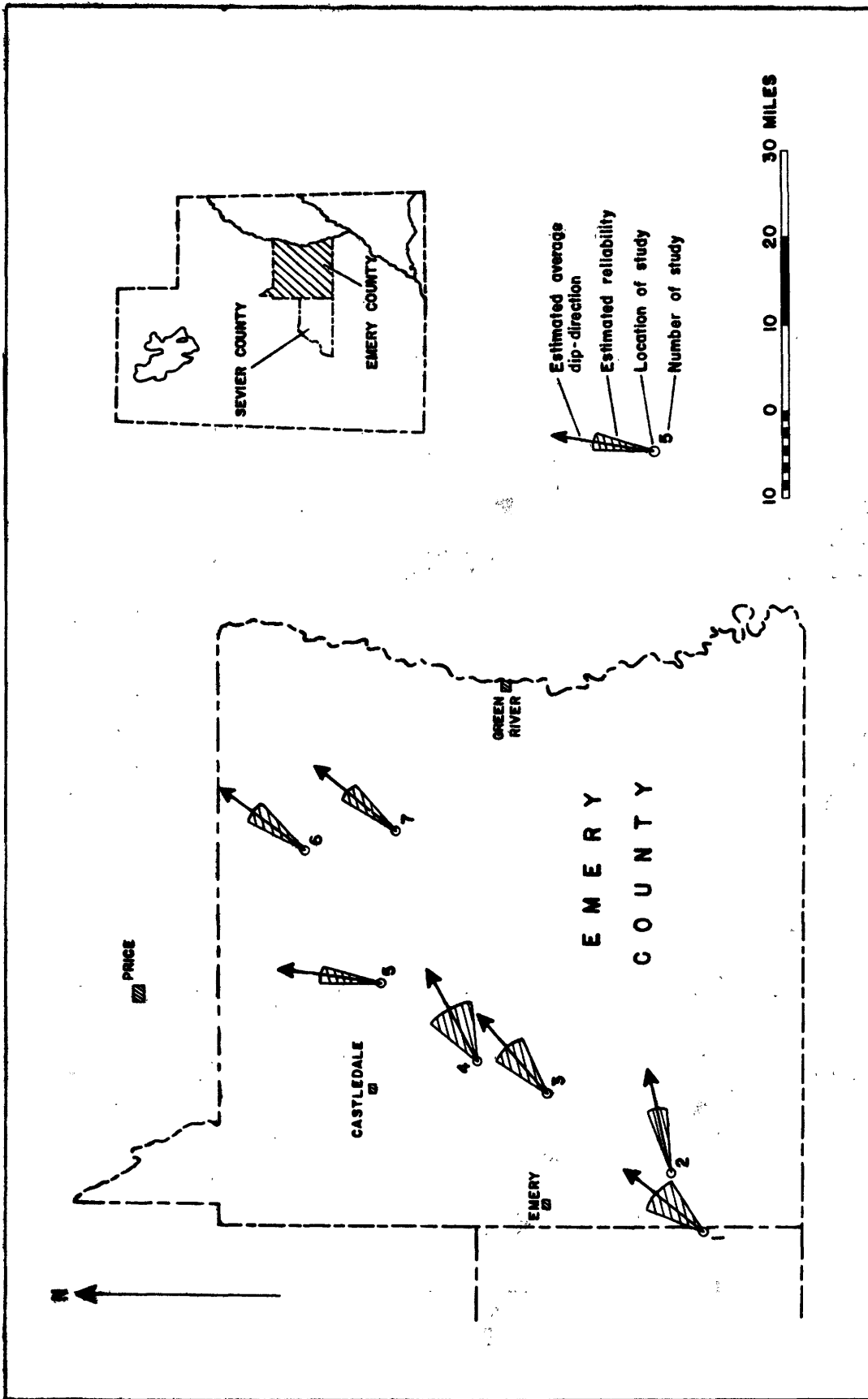


FIGURE 13.— DIP-DIRECTION OF CROSSBEDS IN BASAL PART OF CURTIS FORMATION, EMERY AND SEVIER COUNTIES, UTAH

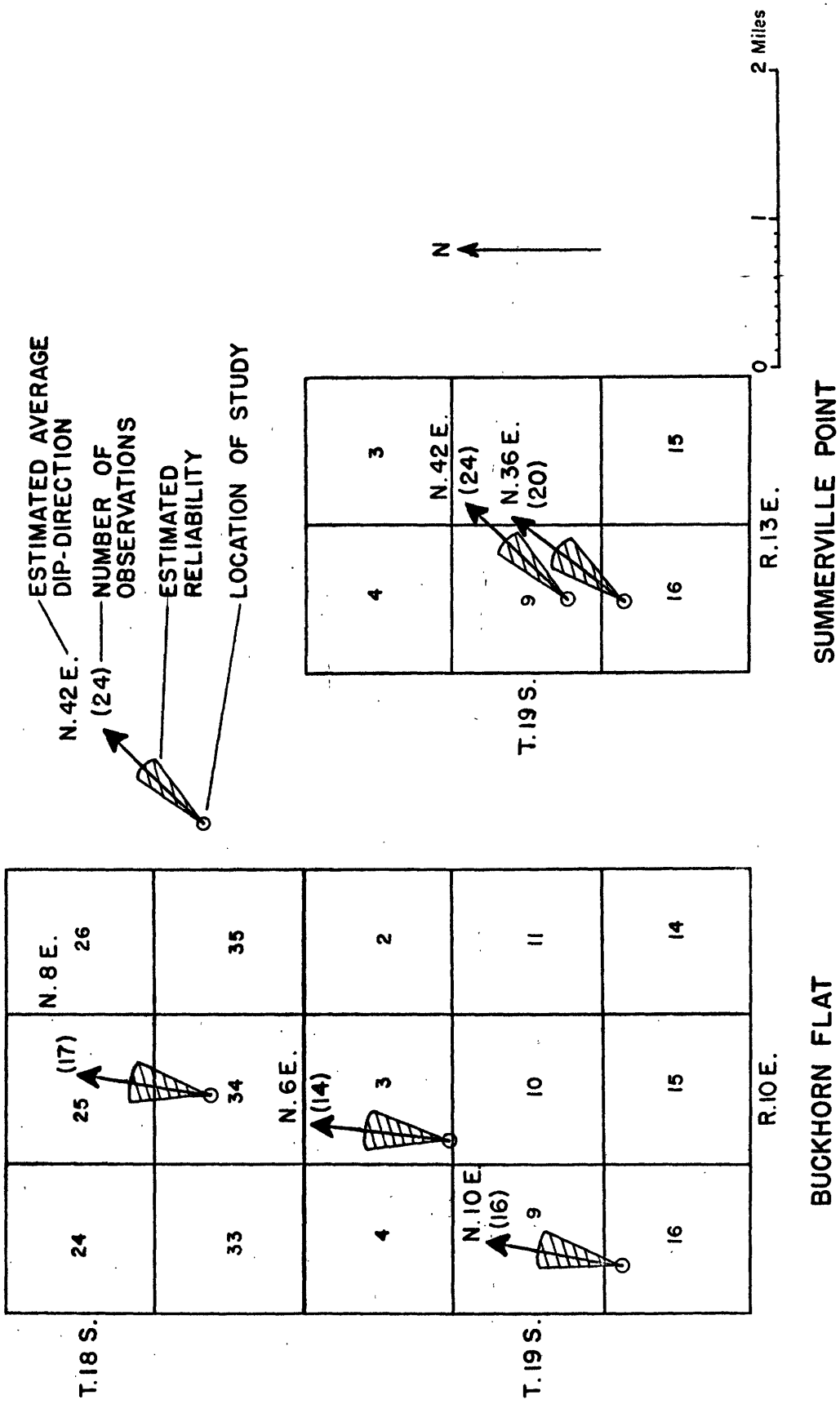


FIGURE 14.-- CROSSBEDDING CONSISTENCY, BASAL BEDS OF CURTIS FORMATION, EMERY COUNTY, UTAH

s = estimate of standard deviation, determined from the half-spread (in degrees) about the estimated average that will include two-thirds of all the observations.

n = the number of observations.

The samples appear to approximate normal distributions for which the statistic is designed. The values of the estimated reliability (table 4) indicate (at the 95 percent probability level) that the estimated average dip-direction at each locality is within 22 degrees or less of the true average dip-direction at the locality.

As a test of the consistency over slightly larger areas, studies at two of the major localities were divided into sub-localities spaced a fraction of a mile from each other. The results, shown on figure 14, indicate that the dip of the cross beds is extremely consistent over areas of a few square miles.

Finally, it should be noted (table 4) that the estimated average dip-directions for all seven localities are included within a sector only 69 degrees wide.

This high consistency at several levels indicates that the conglomeratic sandstone in the basal Curtis formation was deposited from currents which did not meander and which probably flowed on relatively steep slopes from a source area in southwest Utah or southern Nevada. This area is close to the position of the ancient, persistent Cordilleran geosyncline. It is believed that this geosynclinal area (which persisted as a sedimentary trough until at least mid-Jurassic time) was uplifted just prior to deposition of this conglomeratic sandstone; the pattern of later formations indicates that the area continued as a source-terrane throughout the remainder of the Mesozoic.

Table 4.--Measurements of dip-direction, crossbeds in basal part of Curtis formation

Study	Location	Number of Measurements	Estimated average dip-direction	Estimated reliability (95% level)	Estimated average dip (below horizontal)
1. Last Chance	Sec. 12, T.25S., R.5E. (unsurveyed)	11	N.38°E.	± 18°	23°
2. Willow Springs	Sec. 19, T.24S., R.7E. (unsurveyed)	10	N.77°E.	± 9°	22°
3. Drunk Mans Point	Secs. 9 & 10, T.22S., R.8E.	18	N.48°E.	± 17°	21°
4. Horn Silver Gulch	Sec. 31, T.20S., R.9E.	19	N.61°E.	± 22°	26°
5. Buckhorn Flat	T. 18 & 19S., R. 10E	47	N. 8°E.	± 8°	21°
5a. South	Sec. 16, T.19S.,R.10E.	16	N.10°E.	± 14°	21°
5b. Middle	Sec. 3, T.19S.,R.10E.	14	N. 6°E.	± 15°	21°
5c. North	Sec. 34, T.18S.,R.10E.	17	N. 8°E.	± 15°	21°
6. Humbug Wash	Sec. 19, T.17S.,R.13E.	30	N.36°E.	± 11°	21°
7. Summerville Point	T.19S., R. 13E.	44	N.38°E.	± 9°	21°
7a. South	Sec. 16, T. 19S., R. 13E.	20	N.36°E.	± 14°	21°
7b. North	Sec. 9, T. 19S., R. 13E.	24	N.42°E.	± 11°	21°

Significant new information on the petrology of the sediments of the San Rafael group is reported in the section on Lithologic studies, pages 46-59 of this report.

Reference

Cochran, W. G., 1953, Sampling techniques: New York, John Wiley and Sons, Inc.

Ambrosia Lake area, New Mexico

A study of the uranium ore deposits in the Ambrosia Lake area, New Mexico, was started in the summer of 1958. The emphasis of the program is on mine mapping, both surface and underground, and such related geochemical and petrographic work as may be necessary for an understanding of the occurrence and origin of the almost unique uranium ore bodies in the area. The progress of the investigations will be reported in future Semiannual reports.

Central region

Inyan Kara group, Black Hills, Wyoming

by W. J. Mapel and C. L. Pillmore

Correlations of sandstone beds in the Fall River formation given in TEI-700 (p. 154), have been modified as a results of recent field work on the west side of the Black Hills between Newcastle and Sundance. The Fall River formation, which with the underlying Lakota formation makes up the Lower Cretaceous Inyan Kara group, is about 135 feet thick in this area and consists of interbedded sandstone, siltstone, and silty shale. One or more massive rim-forming sandstone beds crop out in the upper part of the formation and may be traced for about 45 miles (fig. 15). The principal rim-forming bed in the northern part of the area is as much as 40 feet thick and generally is 80 to 90 feet above the base of the

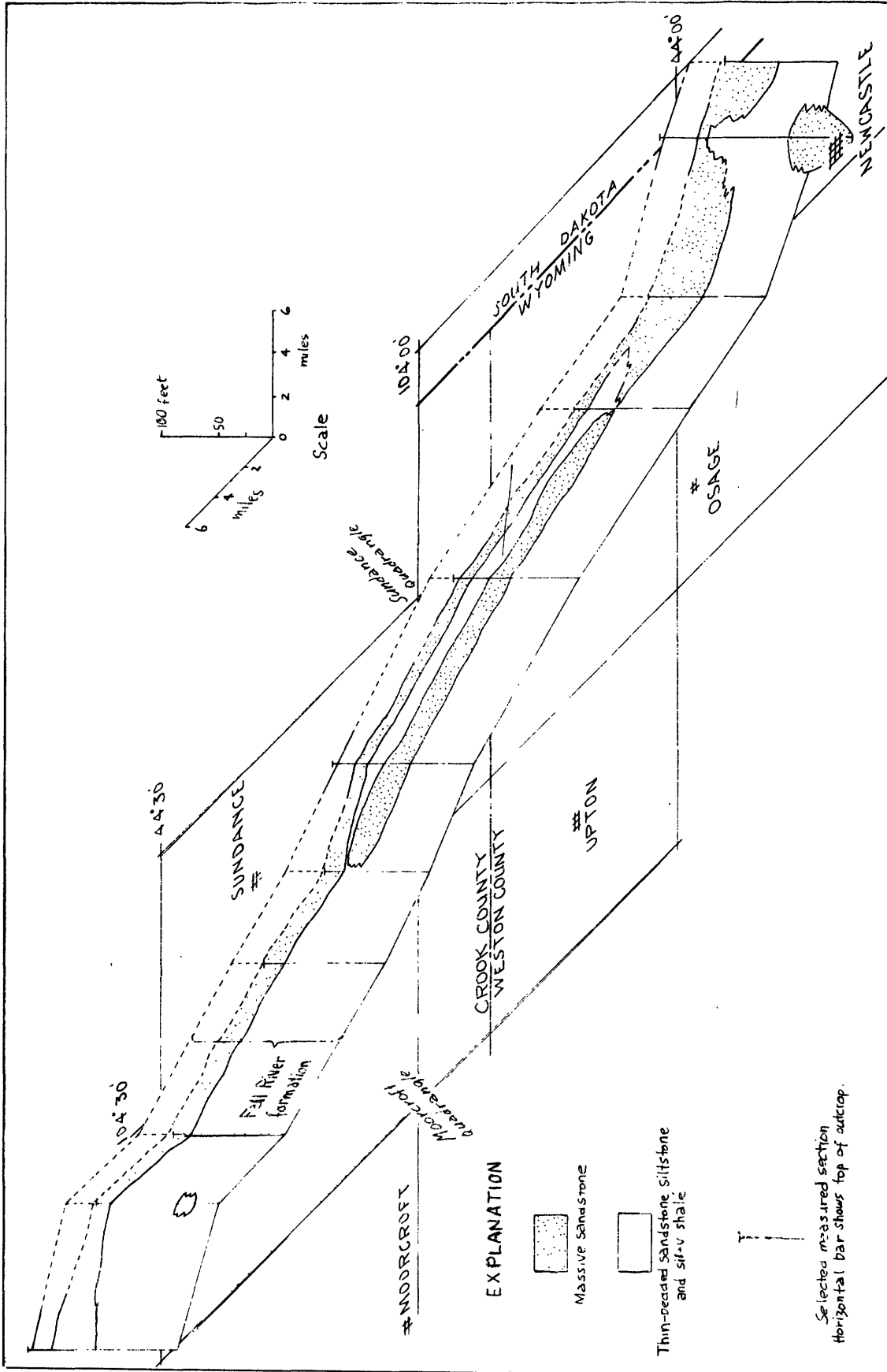


Figure 15. Generalized restored section showing correlation of massive rim-forming sandstone in the Fall River formation, west side of the Black Hills, Wyoming.

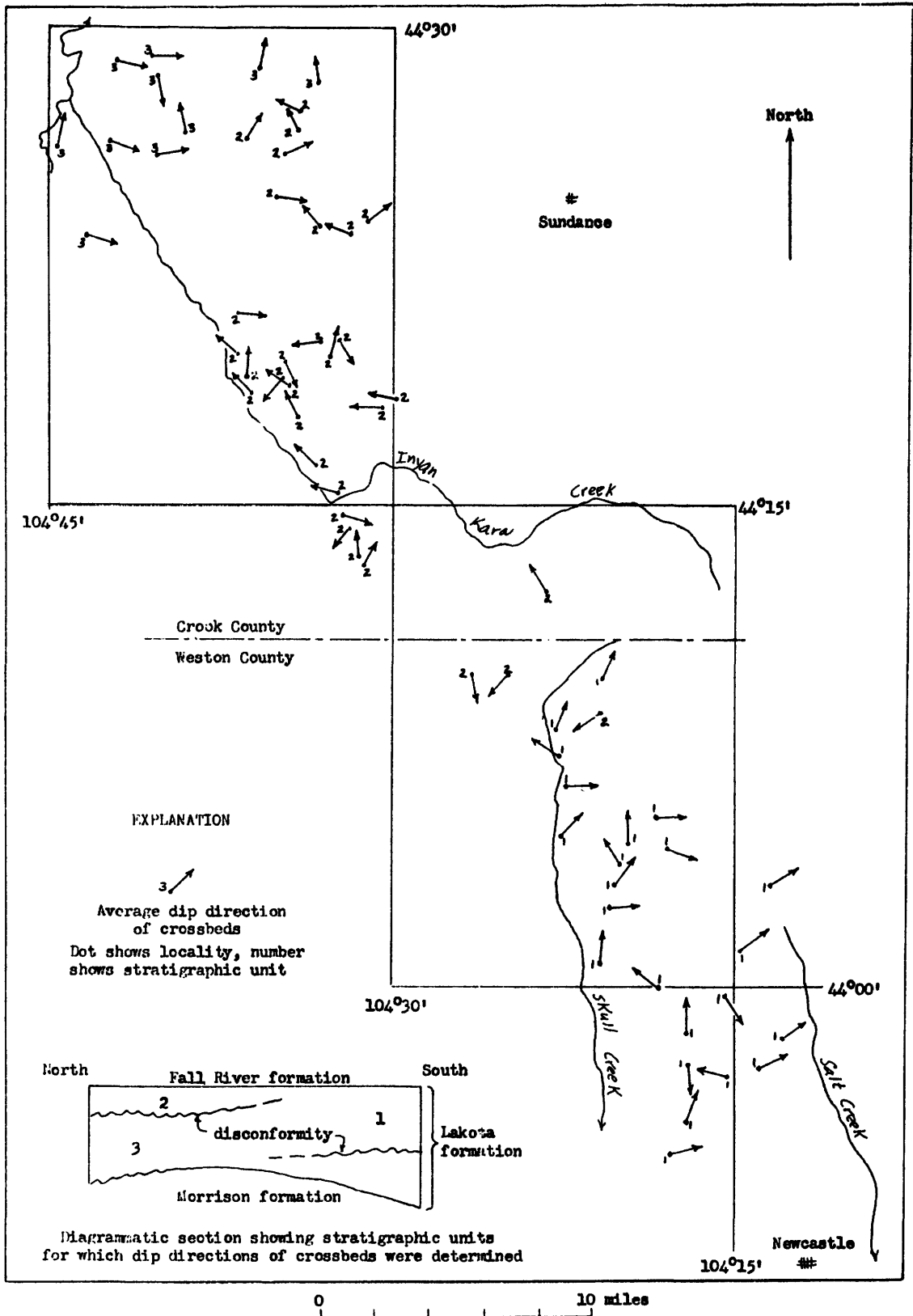


Figure 16. Map showing average dip direction of crossbeds in the Lakota formation, west side of the Black Hills, Wyoming.

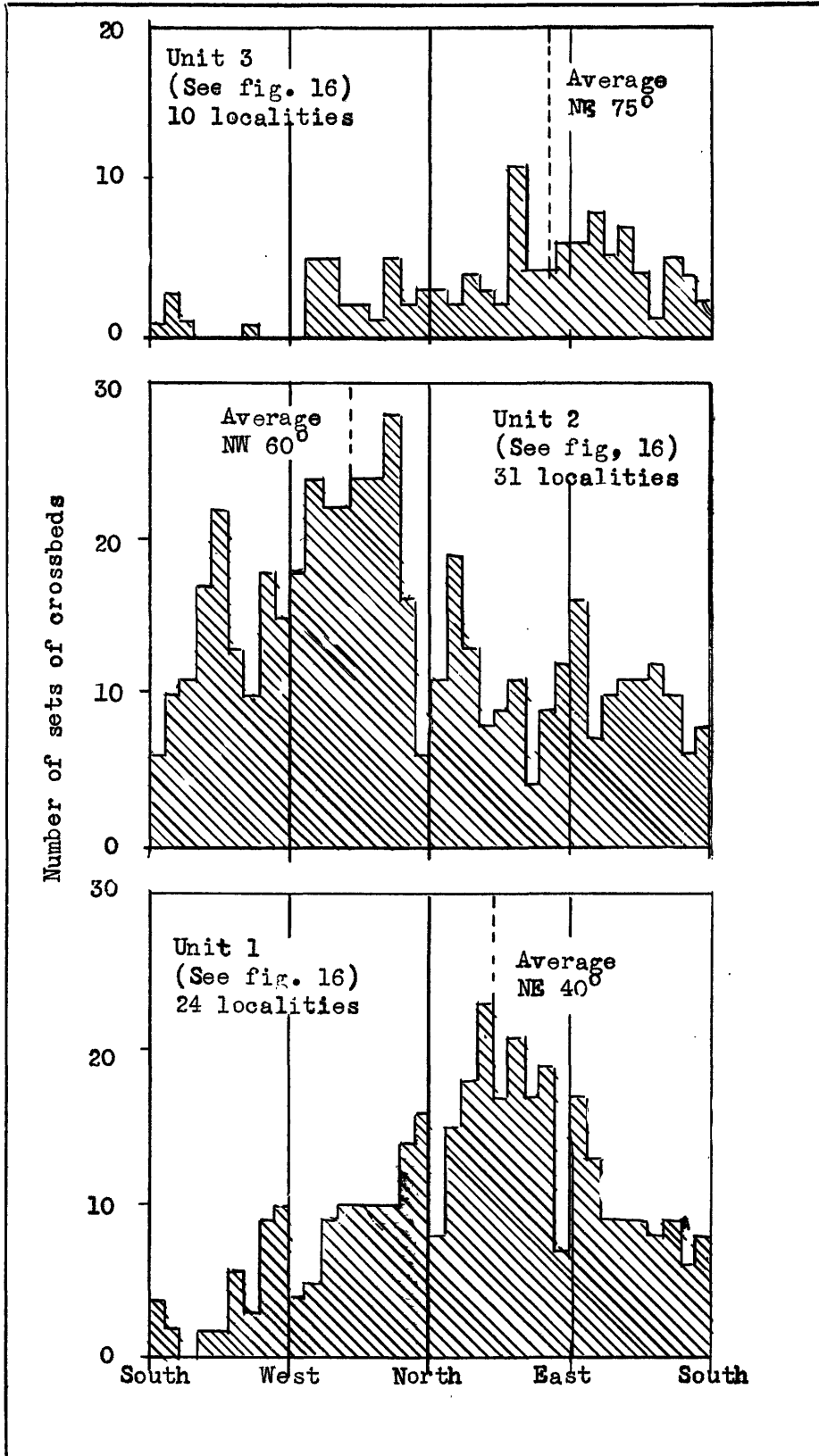


Figure 17.--Diagrams showing dip direction of crossbeds in the Lakota formation, west side of the Black Hills, Wyoming.

formation. A stratigraphically lower bed in the southern part of the area is locally 65 feet thick and generally is 50 to 65 feet above the base of the formation. Both beds crop out for several miles midway between Newcastle and Sundance in the Sundance-3 15 minute quadrangle.

The Lakota formation consists of sandstone, siltstone, and claystone and is 100 to 250 feet thick. Dip directions of crossbeds in sandstone of the Lakota formation were determined at 65 localities to establish the average direction of flow of stream currents responsible for deposition of the sand (see figs. 16 and 17). Readings on at least 10 sets of crossbeds were averaged in calculating the dip-direction at each locality. The resultant dip-direction for all readings is N. 8° E. The data suggest that meandering streams flowing generally from south to north deposited the crossbedded sandstone in the Lakota formation. Brobst (TEI-640, p. 102-108) presents the same conclusion for areas in the vicinity of Edgemont in the southern Black Hills.

Regional synthesis, Montana and the Dakotas

Field work on the Regional synthesis project was recessed on July 1, 1958, and a final report for Survey publication is being prepared. The more important results of the project were reported in TEI-700, p. 160-171, and TEI-740, p. 188-201.

Alaska

Reconnaissance for uranium in Alaska

by E. M. MacKevett, Jr.

Since 1955 the reconnaissance for uranium in Alaska project has consisted mainly of a detailed study of the Bokan Mountain uranium-thorium

area on the southern part of the Prince of Wales Island. As of November 1958 about 72 square miles has been mapped in detail and maps have been made of the Ross-Adams mine, the numerous nearby uranium-thorium prospects, and some of the copper and gold prospects. The area is principally underlain by a wide variety of intrusive rocks that range from ultramafic types to alkali granite and syenite. Volcanic and metamorphic rocks are less extensively distributed. Probably the principal conclusion from study of the area is that almost all of its uranium-thorium deposits are genetically related to the alkali granite that forms a small stock or boss centered near Bokan Mountain.

Various aspects of the Bokan Mountains uranium-thorium area have been described in earlier reports. These include a description of the alkali granite (MacKevett, 1957), a preliminary map of the area, accompanied by a brief text (MacKevett, 1957a), a description of the Ross-Adams deposit (MacKevett, 1958) and summaries in previous semiannual reports.

As far as known, there were no significant new uranium discoveries in Alaska during the report period. Prospector interest seems to be at a low ebb, although there were local prospecting activities and efforts to interest mining companies in known prospects.

The following report was published during the period:

MacKevett, E. M., Jr., 1958, Geology of the Ross-Adams uranium-thorium mine, Alaska: Proc. Int. Conf. on Peaceful Uses of Atomic Energy, Geneva, 1958.

References

- MacKevett, E. M., Jr., 1957, Sodium-rich granite from the southern part of Prince of Wales Island, Alaska: (Abs.) Geol. Soc. America Bull., v. 68, no. 12, p. 1834-1835.
- MacKevett, E. M., Jr., 1957a, Preliminary geologic map of part of the Bokan Mountain uranium-thorium area, Alaska: U. S. Geol. Survey open file report.

GEOPHYSICAL INVESTIGATIONS

Colorado Plateau regionRegional geophysical studies
by

H. R. Joesting, P. Edward Byerly and J. E. Case

Regional geophysical surveys have been made of part of the Colorado Plateau (see figure 18) to gain information on regional geology, buried basement rocks, and possible regional controls of the occurrence of uranium. The surveys will also provide basic geologic information to aid in exploring for petroleum.

Compilation of aeromagnetic maps covering about 22,000 sq. mi. has been completed, except for parts of the Mt. Ellen, Mt. Pennel, and Orange Cliffs 30 minute quadrangles in the western part of the area for which suitable base maps are not yet available. Gravity field work was also completed during the past field season. Compilation of last season's data is now underway.

Regional gravity surveys were made from May through September, 1958. The following areas in Utah were covered: Salt Valley and the Thompson area in Grand County, Green River Desert and the San Rafael Swell in Emery County, the Orange Cliffs in Wayne County, and the Abajo Mountains in San Juan County. A gravity traverse was also made from a landing on the Colorado River 18 miles south of Moab, Utah, to Meander anticline, near the junction of the Colorado and Green Rivers. Late in the season a reconnaissance gravity survey was made of the Ute Mountains, in Montezuma County, Colorado. Gravity work carried out during the past field season is summarized in Table 5.

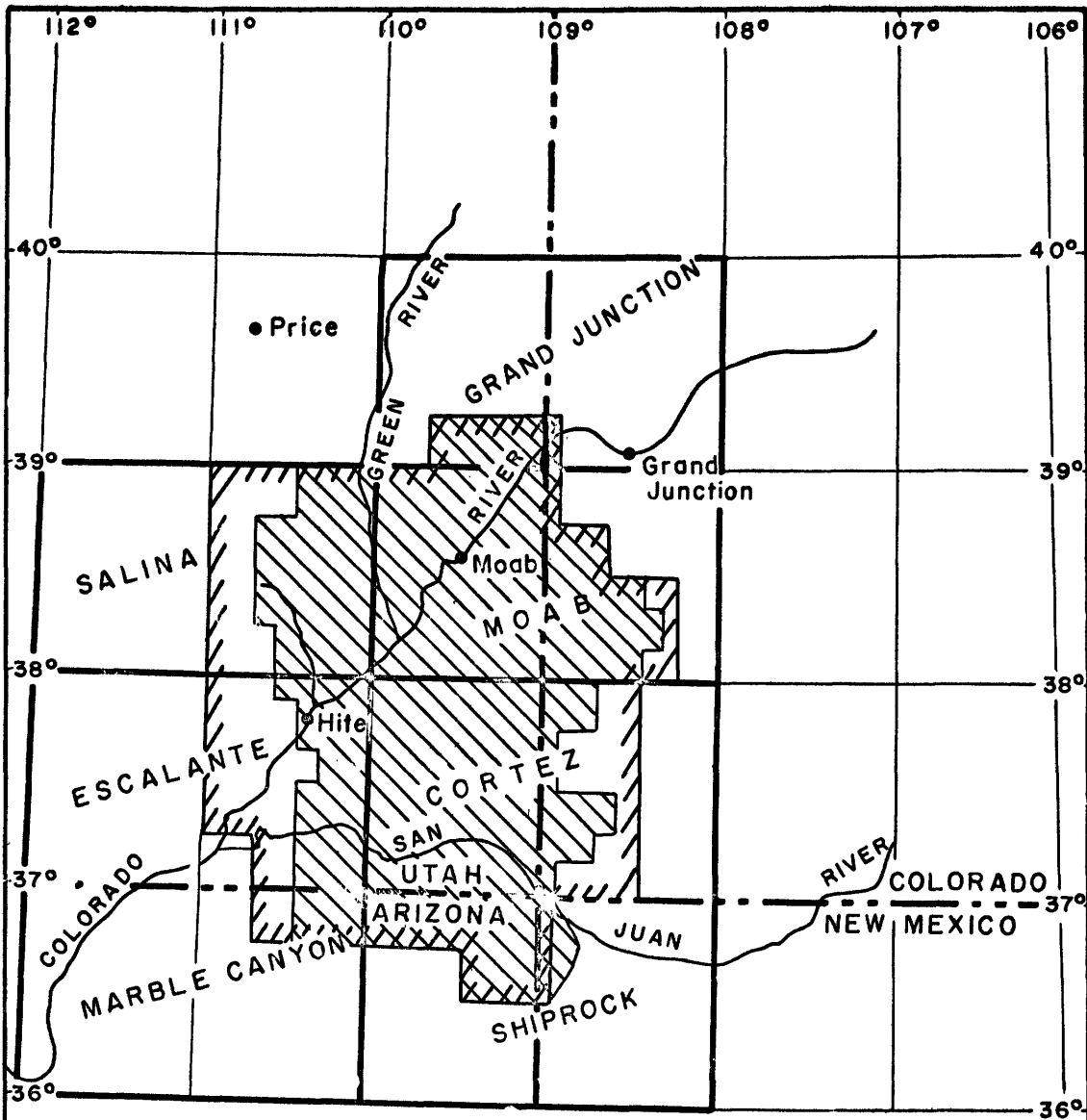


Fig. 18.--REGIONAL GEOPHYSICAL SURVEYS
IN CENTRAL COLORADO PLATEAU



Boundary of geo-
magnetic survey



Boundary of
gravity survey

Table 5

Regional Gravity Field Work Completed

May through September, 1958

MOAB 2° QUAD.

Quad or area	No. of 7 1/2' quads	Area sq. mi.	Stations		Total	Sta.per sq. mi.	Sq.mi. per sta.
			Base	Old ^{1/} New			

Moab 30' quad	8	400	3	22	105	127	0.32	3.2
Carlisle 30' quad	7	350	-	118	57	175	0.50	2.0
Mt. Waas 30' quad	4	200	1	30	32	62	0.31	3.2

CORTEZ 2° QUAD.

Verdure 30' quad	4	200	4	60	50	110	0.55	1.8
Elk Ridge 30' quad	2	100	3	26	9	35	0.35	3.3
Ute Mountains	5	250	3		52	52	0.21	4.8

SALINA 2° QUAD.

Tidwell 30' quad	16	800	14	5	201	206	0.26	3.9
Stinking Springs Creek 30' quad	4	200	3		86	86	0.43	2.3
Mt. Ellen 30' quad	6	300	7	3	96	99	0.33	3.0
Orange Cliffs 30' quad	16	800	11	83	84	167	0.21	4.8

ESCALANTE 2° QUAD.

White Canyon 30' quad	3	150	5	9	34	43	0.29	3.5
Mt. Pennell 30' quad	1	50			6	6	0.12	8.4

TOTALS	66	3,800	54	356	812	1,168		
--------	----	-------	----	-----	-----	-------	--	--

^{1/} Includes stations previously established.

A summary of regional gravity surveys made on the Colorado Plateau through 1958 is given in Table 6. As shown in the table, gravity stations were established in an area of 13,650 square miles. Distribution of stations is reasonably uniform, except in a few inaccessible areas. Regional gravity surveys now cover most of the area within the bounds of the aeromagnetic survey for which suitable topographic maps are available (see figure 18), so that no additional field work is planned at this time. The gravity coverage now includes four of the laccolithic mountains of the Colorado Plateau: the Carrizo, Abajo, La Sal and Ute Mountains. Adequate aeromagnetic surveys are available only for the Abajo and La Sal Mountains.

A precise vertical angle stadia traverse was made into the crater of Upheaval Dome in San Juan County, Utah, to check altimetry and spot elevations on which the Bouguer gravity anomalies are based. Spot elevations were found to be in good agreement with elevations established by transit and stadia, whereas altimetric elevations failed to agree by as much as 16 feet. This discrepancy is not excessive for altimetry, considering the difficulties related to rough terrain and scant control in the area. The resulting correction reduced the positive gravity anomaly in Upheaval Dome by about 1 milligal.

A vertical magnetic survey was also run in Upheaval Dome to check a small apparent aeromagnetic anomaly indicative of a shallow igneous intrusion. No corresponding anomaly was found by the ground survey; the apparent airborne anomaly evidently resulted from small locational errors in the airborne traverses. The new evidence therefore indicates that Upheaval Dome is not caused by a shallow igneous intrusion, but must be caused by an intrusion of salt. The gravity anomaly associated with a

small salt plug of the dimensions indicated by the structure would be too small to measure by the methods used in the regional gravity survey.

Simple Bouguer anomalies have been computed for most of the gravity stations established during the past summer, except those of the Ute Mountain survey. Topographic corrections for selected stations in the Moab 2° quadrangle are also being prepared, and a final Bouguer gravity map of the area has been started.

A negative gravity anomaly of about 30 milligals has been found over Salt Valley anticline in Grand County, Utah. On the basis of the large gravity anomaly and the probable low density contrast between the core of the anticline and the flanking sedimentary rocks, Salt Valley anticline may be one of the largest salt anticlines in the Paradox Basin. A low density contrast is considered likely because the evaporite core of the anticline may contain a comparatively high proportion of clastic material. The source of the clastics would be the buried northwestern extension of the Uncompahgre Plateau, northeast of Salt Valley, which was uplifted and strongly eroded during late Pennsylvanian and Permian times.

A 6 milligal negative anomaly was found near Tenmile Wash, along the northwestern extension of the Moab Valley fault system. The anomaly indicates the presence of a thickened salt mass on the strike of the salt core of the Moab anticline, but separated from the main salt intrusion. A rather large structural relief on the top of the salt would be required to produce the observed gravity anomaly, as upper Cretaceous rocks are exposed at the surface and the salt may be several thousand feet beneath the surface.

The Colorado Plateau geologic maps project will furnish information to aid in preparation of generalized geologic maps of the areas covered

Table 6

Summary of regional gravity surveys on Colorado Plateau
through September, 1958

MOAB 2° QUAD.

	No. of 7 1/2' quads.	Area sq.mi.	Bases	Total sta.	Sta. per sq. mi.	Sq. mi. per sta.
Moab 30' quad	16	800	32	344	0.43	2.3
Carlisle, 30' quad	16	800	17	350	0.44	2.3
Mt. Waas 30' quad	14	700	25	459	0.66	1.5
Mt. Peale 30' quad	16	800	63	662	0.83	1.2
Paradox 30' quad	21	1,050	21	617	0.59	1.7
Gateway 30' quad	—	—	—	—	—	—
TOTALS	83	4,150	156	2,432	0.59	1.7

CORTEZ 2° QUAD.

Cedar 30' quad	2	100		81	0.81	1.2
Verdure 30' quad	16	800	16	460	0.58	1.7
Elk Ridge 30' quad	16	800	21	286	0.36	2.8
McElmo 30' quad	5	250		52	0.48	2.1
Aneth 30' quad	16	800	18	458	0.57	1.7
Bluff 30' quad	<u>16</u>	<u>800</u>	<u>17</u>	<u>284</u>	<u>0.36</u>	<u>2.8</u>
TOTALS	71	3,550	72	1,621	0.46	2.2

SHIPROCK 2° QUAD.

Shiprock 30' quad	8	400	43	95	0.24	4.2
Carrizo 30' quad	16	800		488	0.61	1.6
Setsiltso springs 30' quad	8	400	41	225	0.56	1.8
TOTALS	32	1,600	84	808	0.50	2.0

SALINA 2° QUAD

Tidwell 30' quad	16	800	14	206	0.26	3.9
Stinking Springs Creek 30' quad	4	200	3	86	0.43	2.3
Mt. Ellen 30' quad	6	300	7	99	0.33	3.0
Orange Cliffs 30' quad	<u>16</u>	<u>800</u>	<u>11</u>	<u>167</u>	<u>0.21</u>	<u>4.8</u>
TOTAL	42	2,100	35	558	0.37	2.7

Table 6 (continued)

Summary of regional gravity surveys on Colorado Plateau
through September, 1958

ESCALANTE 2° QUAD.

	No. of 7 1/2' quads.	Area sq. mi.	Bases	Total sta.	Sta. per sq. mi.	Sq. mi. per sta.
White Canyon 30' quad	15	750	14	207	0.27	3.7
Clay Hills 30' quad	16	800	9	223	0.28	3.6
Mt. Pennel 30' quad	1	50		6	0.12	8.4
Navajo Mountain 30' quad	<u>2</u>	<u>100</u>	<u>—</u>	<u>7</u>	<u>0.07</u>	<u>14.3</u>
TOTALS	34	1,700	23	443	0.26	3.8

MARBLE CANYON 2° QUAD.

Agathla Peak 30' quad	11	550	23	189	0.34	2.9
-----------------------	----	-----	----	-----	------	-----

External Base loop:

Dove Creek to Shiprock

8

Grand Junction to Gateway

8

Others

7

23

GRAND TOTALS	273	13,650	393	6,074	0.44	2.3
--------------	-----	--------	-----	-------	------	-----

by the regional geophysical surveys. Additional material will be obtained as needed from published sources. Compilation of subsurface information has been resumed to guide interpretation of geophysical data. Isopach and structure maps of the Mississippian rocks and of the evaporite member of the Hermosa formation have been brought up to date.

Bottom cuttings of wells penetrating crystalline rocks have been submitted for determination of their magnetic susceptibilities and densities. Additional samples of dioritic rocks from the La Sal Mountains were also collected for analysis.

The following papers were published during the period:

- Joesting, H. R., and Plouff, Don, 1958, Geophysical studies of the Upheaval Dome area, San Juan County, Utah: Intermountain Assoc. Petroleum Geologists Guidebook, 9th Annual Field Conference, p. 86-92.
- Shoemaker, E. M., Case, J. E., and Elston, D. P., 1958, Salt anticlines of the Paradox Basin: Intermountain Assoc. Petroleum Geologists Guidebook, 9th Annual Field Conference, p. 39-59.

Central region

Texas Coastal Plain geophysical and geologic studies
by
J. A. MacKallor, D. H. Eargle, and R. M. Moxham

The principal uranium ore-bearing unit in the Karnes County area, Texas, is the Stones Switch sandstone member of the Whitsett formation of the Jackson group. The location of the area is shown in figure 19; figure 20 shows the outcrop of the Stones Switch sandstone through the principal uranium-bearing area, with generalized surface and subsurface contours drawn on the base of the member. Isopachs indicating the thickness of the member in the subsurface show that it is thickest in three general areas: (1) along the outcrop in the vicinity of the San Antonio River;

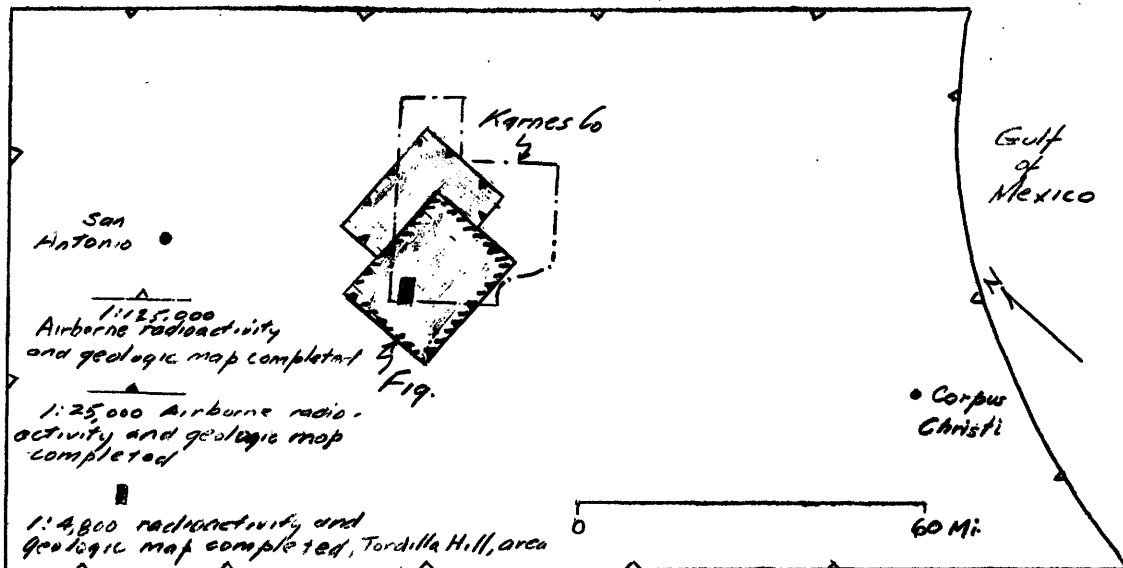


FIG. 19 -INDEX MAP OF CENTRAL TEXAS COASTAL PLAIN

(2) in an elongate area generally parallel to the strike about 8 to 12 miles down dip from the outcrop; and (3) locally on downthrown blocks along northeast-trending fault lines. The thickest sections are 60 to 70 feet thick, and the thinner ones average 40 feet thick. The thicker area along the outcrop is believed to be a deltaic deposit, in part reworked by longshore currents. The downdip thick area is believed to have been an offshore bar. The thinner area between the two is most likely a lagoonal deposit, a conclusion which is confirmed by the ecology of the fossils in the member. Downdip from the offshore bar the Stones Switch sandstone member thins and about 15 miles from the outcrop the sands give way to clays.

The thicker areas on the downthrown side of faults are believed to be accumulations in troughs that formed contemporaneously with sedimentation.

An anomalously thin area lies on the downthrown block southeast of the Coy City fault and coincides with the crest of the Coy City gas field anticline. It is likely that the anticline was present as a topographic

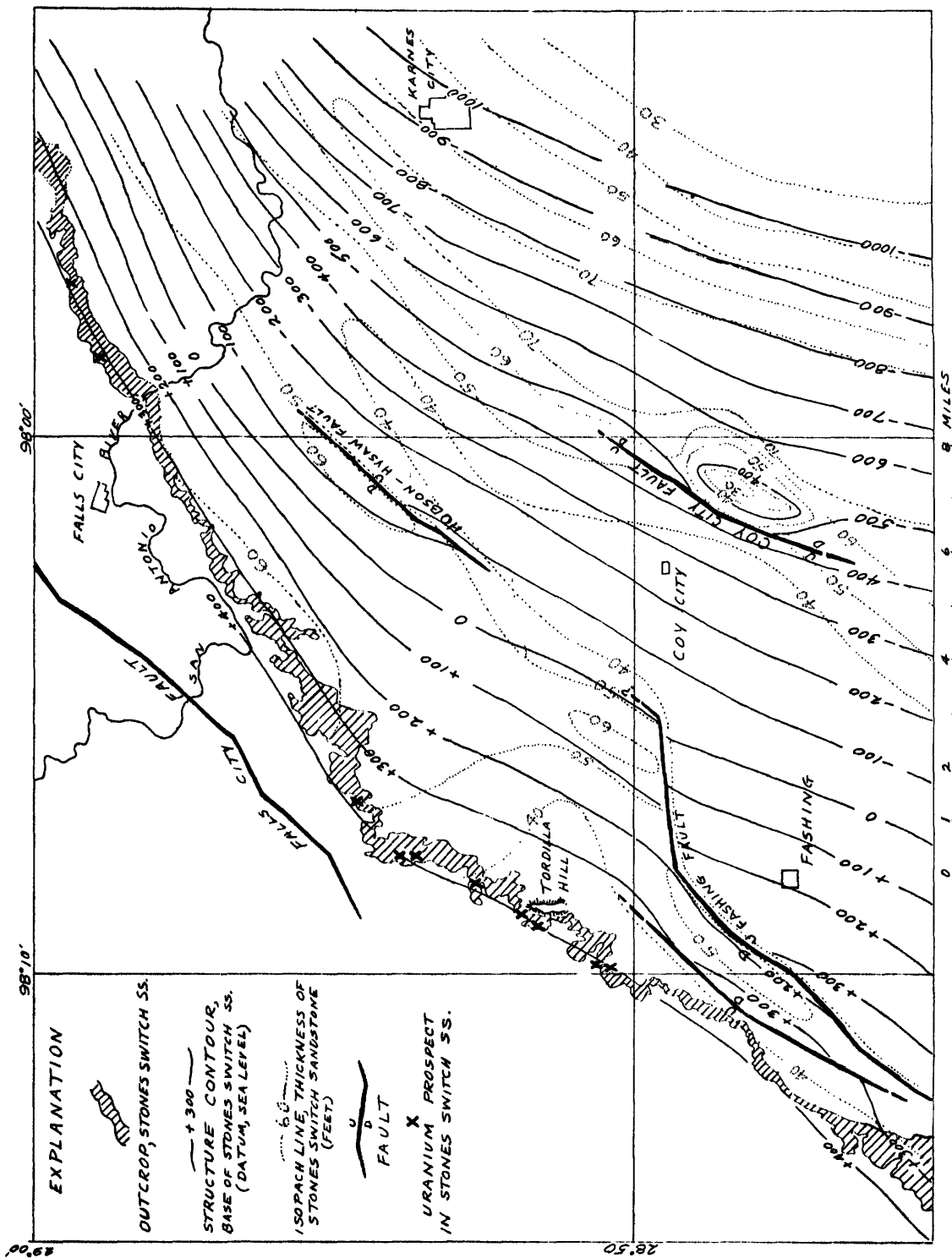


FIG. 20.- STRUCTURE AND THICKNESS OF STONES SWITCH SANDSTONE, KARNES COUNTY AREA, TEXAS

ridge when the sediments were accumulating, and that a smaller volume of sand was deposited on the ridge than in the trough adjoining the fault.

Deposition of the sandstone of the Stones Switch member was followed by chiefly non-marine tuffaceous siltstones, sandstones, and clays. These accumulated to a thickness of about 100 feet before another littoral or marine sandstone was deposited.

Tordilla Hill area

The first major uranium deposits found in the central Texas Coastal Plain are in the Tordilla Hill area, western Karnes County (see fig. 19).

Stratigraphy.--The geologic section in the vicinity of Tordilla Hill is summarized in Table 7. It should be noted that the stratigraphic nomenclature has been revised (Eargle, 1959); the Jackson has been raised to group status, in accord with present usage.

Deposition of the tuffaceous sediments of the Jackson group was characterized by rapid lateral and vertical changes from sand through silt to mudstone. Such facies changes, accompanied by typical shoreline sedimentary structures and supported by paleontological evidence, indicate that the rocks of the Jackson in this area were deposited in a near-shore environment, probably similar to that now existing on the Texas Gulf coast.

Most of the rocks within the area are friable and poorly indurated, but small areas of silicified sandstone and, to a less extent, silicified tuff are common. With rare exceptions, silicification is confined to within 20 feet, and usually to within 5 feet, of the surface. Considerable evidence has been obtained to show that silicification developed on a pre-Recent land surface under climatic conditions somewhat different from the present (fig. 21).

Table 7.--Stratigraphy of the Jackson group of Eocene age in the vicinity of Tortilla Hill, Karnes County, Texas

<u>Formation</u>	<u>Member</u>	<u>Thickness, feet</u>	<u>Lithology</u>
Whitsett	Dubose	110-120	Upper 30 feet is sandstone; lower part consists of intercalated thin beds of tuffaceous sandstone, siltstone, and clay.
	Stones Switch sandstone	20-50 (only 20' at Boso deposit, normal thickness 40-50)	An upper bed contains casts of plant roots; middle part at many places contains silt or clay; lower part changes progressively downward from fine to very fine sand, to silt to the underlying Conquista clay
	Conquista clay	75-90	Contains a fossiliferous sandstone unit 10 feet thick. Clay is reddish-brown in oxidized zone, within 20 to 30 feet of surface, and bluish black at greater depths.
McElroy	Dilworth sandstone	-/10	Only upper plant root sandstone bed is exposed, but auger drill holes indicate clay and sandstone beneath.

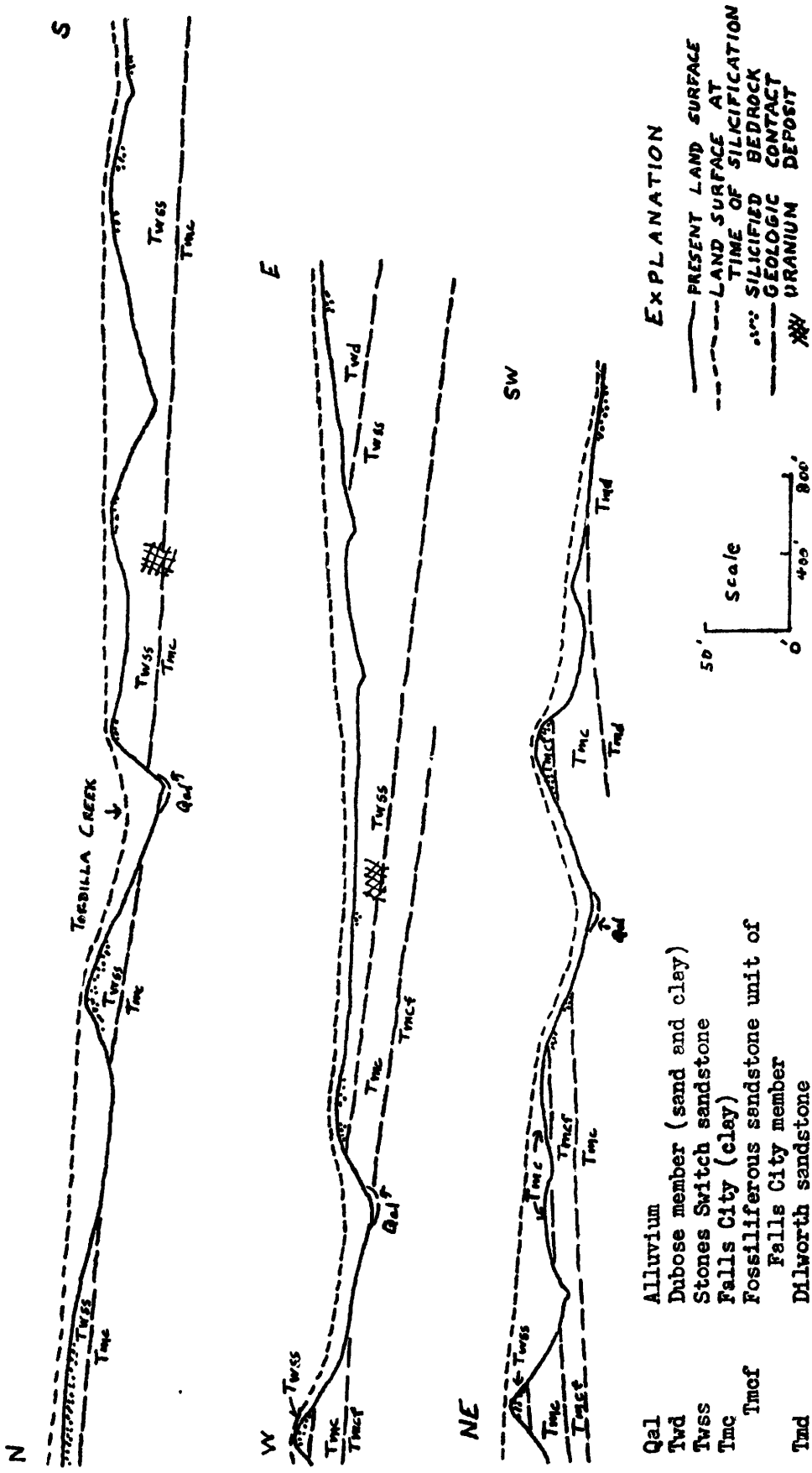


FIG. 21.-CROSS-SECTIONS SHOWING RELATIONSHIP BETWEEN SILICIFICATION AND LAND SURFACE

Structure

The rocks of the mapped area strike generally NNE, but locally, as in the Continental deposit in the northeast part of the area, the strike is ENE. The rocks dip gently toward the southeast at about 100 to 300 feet per mile. Local variations in strike and dip result from very gentle anticlinal and synclinal flexures. The dip of the beds in the area of uranium deposits flattens significantly with respect to the regional dip (TEI-740, p. 222).

No faults were observed within the immediate Tordilla Hill area, nor were any detected by seismic and resistivity surveys. If faults exist, they have small displacements. It should be noted, however, that the lenticularity of the beds effectively prevents detection of small faults, either by subsurface geological or by geophysical methods.

The silicified outcrops usually have well developed sets of vertical joints which commonly strike NNE, less commonly ESE.

Ore deposits and controls

The ore minerals exposed in the shallow prospect pits and trenches are almost exclusively secondary, high-valent minerals (Weeks, A. D., personal communication). These include uranyl phosphates, phosphate-arsenates, silicates, phosphate-silicates, molybdates, and vanadates. One of the uranium molybdates is the only uranium mineral found in the area that may be in part low-valent. No uraninite or coffinite has been found in the Karnes County near-surface deposits.

With the exception of some uranium in medium-grained sandstone on the Boso property, all of the known deposits in the area are in fine- to

very fine-grained sandstone in the lower part of the Stones Switch member of the Whitsett formation and/or in the upper few feet of clayey silt of the Conquista member of the McElroy formation.

Lithology apparently is the most important ore control but structure has a subsidiary part. Two lithologic features are involved: (1) a mudstone "channel" within the Stones Switch member and (2) a middle facies of the Stones Switch consisting of intercalated sandstone, siltstone, and clay (TEI-700, p. 188; TEI-740, p. 224-227).

The mudstone channel has been traced, mainly in the subsurface, from the Continental deposit generally southwestward, parallel to the strike of the beds, for more than 3 miles. It is 300 to 400 feet wide, from 20 to 40 feet thick in the center, and has steep sides. The top of the channel is in the upper half of the Stones Switch member, and the base is near the Stones Switch-Conquista contact, usually above it but at some places below it.

The intercalated sandstone-siltstone-clay facies of the middle Stones Switch apparently is closely related, both spatially and in origin, to the mudstone channel.

All of the known major uranium deposits of Karnes County area lie within a few hundred feet up dip from the mudstone channel, and most are within the area of intercalated sand, silt, and clay.

It is postulated that the mudstone channel and associated facies of the Stones Switch greatly decreased the gross permeability of the Stones Switch sandstone member and impeded the normal, downdip (i.e. E SE) flow of uraniumiferous ground water. The mudstone channel changed the direction of the hydraulic gradient to a more southerly direction. It is further postulated that the accompanying changes in velocity and pressure took place in the

presence of a reducing agent, resulting in precipitation of uranium along a SSW-oriented trend.

The shapes of the individual ore bodies appear to be controlled by vertical jointing. The deposits are elongated in a direction parallel to the strike of a major joint set and have extensions or protuberances parallel to the strike of the other important joint set.

Results of these studies suggest the following theory of origin. The sediments of the Jackson containing a substantial amount of uraniferous tuff were deposited in a near shore terrestrial environment or in shallow water. Rapid burial apparently inhibited loss of uranium to the sea. Later, with regression of the sea, sodium carbonate ground-water, perhaps similar to present-day ground-water of the area, leached uranium from the sediments, released silica and promoted zeolitic alteration (Weeks, 1958). Precipitation of uranium took place where such waters entered a favorable physical environment provided by the structural and lithologic elements described above. A superimposed reducing environment could have been provided by H_2S gas, as cores obtained from mineralized holes give a strong H_2S odor. The most logical source of a substantial supply of H_2S is the Edwards gas-distillate field of Cretaceous age which lies along the Fashing fault, at a depth of about 11,000 feet below the uranium deposits.

The following papers were published during the period:

- Eargle, D. H., 1958, Regional structure and lithology in relation to uranium deposits, Karnes County area, Texas: Econ. Geol., vol. 53, no. 7 (abs.).
- MacKallor, J. A., and Bunker, C. M., 1958, Ore controls in the Karnes County uranium area, Texas: Econ. Geol., vol. 53, no. 7, (abs.).
- Manger, G. E., 1958, A comparison of the physical properties or uranium bearing rocks in the Colorado Plateau and Gulf Coast of Texas: Econ. Geol., vol. 53, no. 7, (abs.).

- Moxham, R. M., 1958, Geologic evaluation of airborne radioactivity data: Proc. 2nd U. N. Conf. on Peaceful Uses of Atomic Energy, Geneva, 1958.
- Weeks, A. D., Levin, Betsy, and Bowen, M. J., 1958, Zeolitic alteration of tuffaceous sediments and its relation to uranium deposits in the Karnes County area, Texas: Econ. Geol., vol. 53, no. 7, (abs.).

References

- Eargle, D. H., 1959, Stratigraphy of the Jackson group, south-central Texas: A. A. P. G. Bull., in press.
- Ellisor, A. C., 1933, Jackson group of formations in Texas with notes on Frio and Vicksburg: Bull. Amer. Assoc. Petrol. Geol., v. 17, no. 11, p. 1293-1350.
- Weeks, A. D., 1958, Zeolitic alteration of tuffaceous sediments and its relation to uranium deposits in the Karnes County area, Texas: Econ. Geology, v. 53, no. 7, November 1958, p. 928.

General investigations

Physical properties of ore and host rock

Field work on the Physical properties of ore and host rock project was completed prior to this report period, and a final report for Survey publication is in preparation. Most of the studies were made in two areas; part of the Colorado Plateau, and the Texas coastal plain. The most important results of the Colorado Plateau studies were reported in TEI-690, p. 461-472; those of the Texas coastal plain investigations in TEI-740, p. 228-237.

Geophysical studies in uranium geology
by
R. M. Hazlewood

The results of the regional gravity survey of the Black Hills of South Dakota have been discussed in TEI-640, p. 112, TEI-690, p. 471, TEI-700, p. 194, and TEI-740, p. 237-238.

During June an additional 400 gravity stations were occupied in the northern Black Hills of South Dakota. The reduction of this data, necessary terrain corrections, and interpretation of the data have been started.

Electronics laboratory
by
W. W. Vaughn

The possibility of using the gamma-neutron reaction from Ra²²⁸ and beryllium for a portable beryllium detector was investigated. Two ounces of thorite containing 22 percent ThO₂ was used with a sample of beryllium which weighed 4 ounces and contained 50 percent BeO. A neutron yield of 24.42 counts per minute was observed. The neutron yield per second per curie from a 1 gm target of Be at 1 cm is 3.5×10^4 for Ra²²⁸ and 19×10^4 for Sb¹²⁴. However, if Ra²²⁸ can be obtained in a concentrated-capsule form the lower neutron yield from Ra²²⁸ may be offset by the fact that it has a longer half-life than Sb¹²⁴ by a factor of about 40.

A thorough search was made for thin foils (gold, aluminum etc.) that could be used as alpha windows in alpha counting systems. A sandwich composed of mylar-aluminum-mylar with a total thickness of approximately 1 mg/cm^2 seems to be the best available at the present time.

The Grand Junction instrument shop has been discontinued. The gamma-ray logging equipment and other radiation detection equipment was moved to Denver and integrated into the Electronics Laboratory.

Two portable alpha counters were constructed for use in localizing radioactive zones in a high environmental radiation flux on a mine face. Due to the high source to background ratio inherent in alpha counters the instrument is ideal for this application.

The U. S. Fish and Wildlife Service consulted with the Electronics Laboratory about the possibility of using radiation techniques to study the underground habits of gophers. It was suggested that a small source of radiation be attached to an animal in an escape proof enclosure and that a sensitive scintillation probe be used to determine to what depths the animal could be detected.

The following paper was published during the period:

Vaughn, W. W., Rhoden, V., and Wilson, E. E., 1958, Development in radiation detection equipment for geology: Proc. Int. Conf. on the Peaceful Uses of Atomic Energy, Geneva.

Gamma-ray logging

The gamma-ray logging project as such was recessed on July 1, 1958, and its functions incorporated in a general program on geophysical and radiometric techniques. Important results of the gamma-ray logging project were reported in TEI-700, p. 199-201, and TEI-740, p. 239-245.

Correlation of airborne radioactivity data
and areal geology
by
R. B. Guillou

Field investigation of the correlation of airborne geophysical data with geology in the Wausau area, Wisconsin, has been completed. The findings are summarized below:

The Wausau area is in the northernmost part of the driftless area in central Wisconsin and is covered by residual soil and locally by glacial debris or loess. Bedrock consists of a Precambrian complex of metamorphosed volcanic and sedimentary rocks and intrusive gabbro, syenite, and granite. Airborne traverses totaling about 1000 miles were flown in June, 1956, to determine the relationship between areal geology and airborne radioactivity and magnetic data.

Airborne radioactivity units having a difference in level of less than 200 counts per second usually are not defined on the ground through the use of standard field scintillometers. Changes in rock or soil types or changes in the amount of outcrop or float, however, generally were observed on the ground in about the same positions as the boundaries of the airborne radioactivity units. Large areas of syenite in Stettin and Maine townships and the quartzite of Rib Mountain are accurately outlined by the radioactivity data, but other rock types in the area are not so well defined.

Areas of quartzite, granite, hornblendite, diabase, and volcanic rock can be delineated by their respective aeromagnetic patterns. These data are related directly to the susceptibility of the rocks. Some individual diabase dikes more than 50 feet wide could be traced for as much as 12 miles. The remanent fields of some dikes greatly exceed their indicated fields and are inversely polarized.

The following paper was published during the period:

Bates, R. G., and Allingham, J. W., 1958, Correlation of airborne geophysical data with geology in the Wausau area, Wisconsin: Geophysics (abs., in press).

GEOCHEMICAL INVESTIGATIONS

Distribution of elements

by

A. T. Miesch

Work on the Distribution of elements project during the report period consisted of preparation and revision of final reports for Survey publication. Summaries of these reports were given in TEI-690, p. 478-490; TEI-700, p. 205-212; and TEI-740, p. 250-254.

RADIOACTIVITY INVESTIGATIONS

Radiogenic Daughter Products

by

Frank E. Senftle

A method for determining the thick source counting rates of powdered rock samples without the use of a standard sample has been found. Using an ionization chamber, a plot is made of the counting rate versus the discriminator bias. The linear portion of the curve is extrapolated to zero bias and the value thus obtained is the true thick source counting rate.

At low discriminator settings the activity measured is due not only to alpha particles but also to beta and noise pulses. As the discriminator level is raised these pulses are gradually eliminated but so also are the pulses due to the low energy alpha particles. Since the alpha particle spectrum of a thick source is a continuum from zero energy to about 7.9 Mev, a change in discriminator bias will result in a linear change in the counting rate until a sharp cut-off point is reached at about 7.9 Mev. Thus, the extrapolation of the linear portion of the curve to zero bias gives the true thick source activity.

From complete chemical analyses for eight monazite samples the thick source counting rates were calculated using the Bragg-Kleeman law. The experimental results checked to within 10 percent with the theoretical calculations.

The design and construction of a sample holder has been completed. The activity of the eight monazite samples at 77° K will be measured to determine the effect of emanation on the counting rates.

RESEARCH PROGRAMS

Physical Behavior of Radon

by

Allan B. Tanner

The technique of locating faults by measurement of the radon²²² content of ground water (A. S. Rogers, in preparation) was applied to an area of valley fill between Grantsville and Erda, Tooele County, Utah (fig. 22). Discordant water levels in a few water wells in the central part of the area had led to the inference of a fault west of the boundary between Townships 4 and 5 West.

Water samples taken from 27 wells and 2 springs were analyzed for radon. The radon concentrations in the well waters ranged from 2.7 to 5.7×10^{-10} curie per liter (270 to 570 c/l). Water from the Mill Pond Spring producing from the Erda fault less than a mile from the Oquirrh Mountains to the east, contained 8.2×10^{-10} c/l; water from the Sixmile Creek Spring, producing from deep valley fill, contained only half as much.

Previous work (TEI-540, p. 270-271) has established that radon content was anomalously high in well waters in the vicinity of a fault zone in valley fill similar to that of the Grantsville-Erda area. No systematic variation of radon concentration with location was observed in the Grantsville-Erda area, however, nor were anomalously high radon concentrations observed in water in the vicinity of the inferred faults. It was therefore necessary to conclude that the fault, if present, could not be located by the radon method. Subsequent measurements of water levels in more wells than were investigated originally have yielded evidence that the piezometric surface (not shown on figure 22) is continuous and undeformed in the area of the inferred fault and that the fault probably does not exist (H. D. Goode, oral communication).

No correlation could be found between radon concentration in well waters and the depths to the zones producing the waters. The depth to the producing zone in these wells varied from 145 to 445 feet. The radon content of water from several wells located within the same square mile and producing from the same 12-foot depth zone showed nearly the extreme range of concentrations observed in the well water samples. These findings support those of Rogers, who did not find a correlation between radon concentration and depth in waters from about 130 wells ranging in depth from 80 to 600 feet.

The following paper was published during the period:

Tanner, A. B., 1958, Increasing the efficiency of exploration drilling for uranium by measurements of radon in drill holes: Proc. Int. Conf. on the Peaceful Use of Atomic Energy, Geneva, 1958.

Distribution of uranium in igneous complexes

Uranium in some volcanic rocks
by
David Gottfried

During this report period additional suites of volcanic rocks were obtained for the purpose of relating uranium content to chemical composition. These include basaltic and rhyolite rocks from Iceland; basalts from New Jersey; and basalts, andesites, dacites and rhyolites from the Strawberry Mountains of Oregon. Petrologic and field studies on the volcanic rocks from New Jersey and Oregon are being carried out by others.

Uranium analyses on the different rock types from the same volcanic province show that the more siliceous rocks generally contain greater amounts of uranium than the mafic rocks. To show the differences in uranium content between

the different petrographic provinces, the uranium analyses have been plotted on a variation diagram of the type proposed by Larsen (1938).

Figure 23 shows the distribution of uranium in the volcanic rocks of the Modoc area of northern California. The data for these rocks were presented by Gottfried and Larsen in *TEI-740*, p. 282-283. There is about a 10 fold increase in uranium in the rhyolitic obsidians over the basalts.

Figure 24 shows the distribution of uranium in the volcanic rocks of the Strawberry Mountains, Oregon. The increase of uranium in the more siliceous rocks is less than for similar rocks from the Modoc area.

The distribution of uranium in some volcanic rocks of the Hinsdale formation and the Potosi volcanic series of the San Juan Mountains, Colorado is shown in figure 25. The data are discussed more fully elsewhere by Larsen, Gottfried and Molloy (1958). The rocks of the Hinsdale formation are more alkalic than the volcanic rocks of the Potosi volcanic series. Although based on fewer data the distribution of uranium in the Hinsdale formation is more systematic than for the Potosi series. This may in part be due to the greater complexity of the Potosi series as compared to the Hinsdale formation. The rhyolitic rocks of the Hinsdale formation contain nearly twice the uranium in similar rocks from the Potosi series.

The distribution of uranium in volcanic rocks from the Valles Mountains, New Mexico is shown in figure 26. These rocks are similar in age and composition to those of the Hinsdale formation. The increase in uranium from the basalts to rhyolites is greater than for any of the other volcanic provinces discussed here.

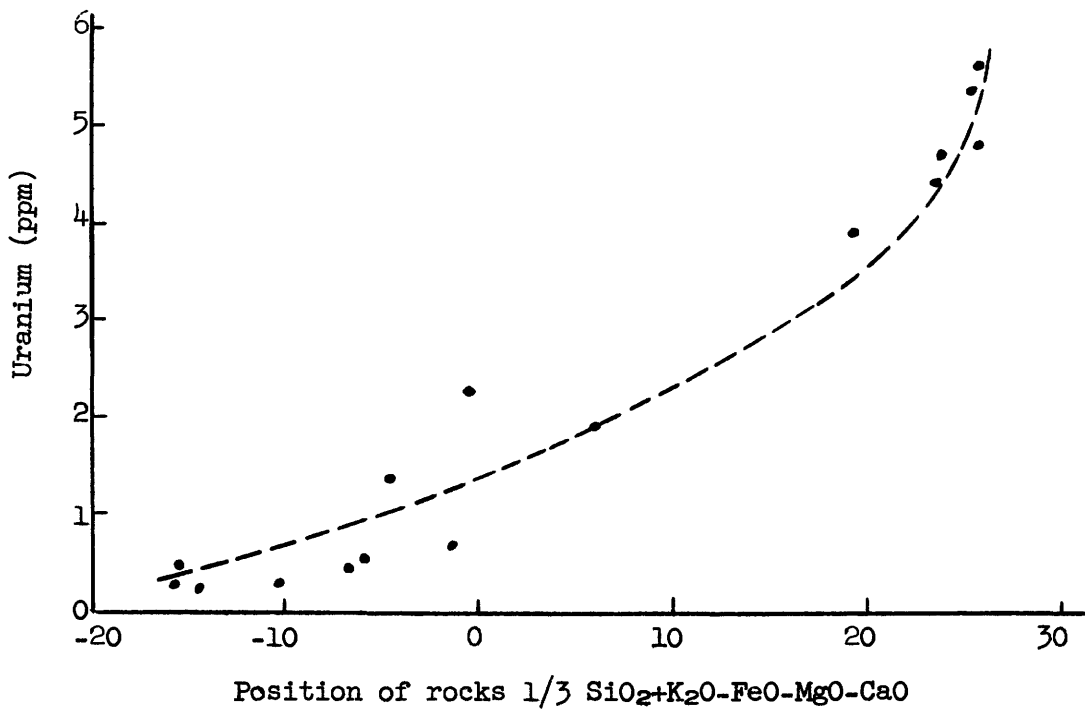


Figure 23.--Distribution of uranium in the volcanic rocks of the Modoc area, northern California.

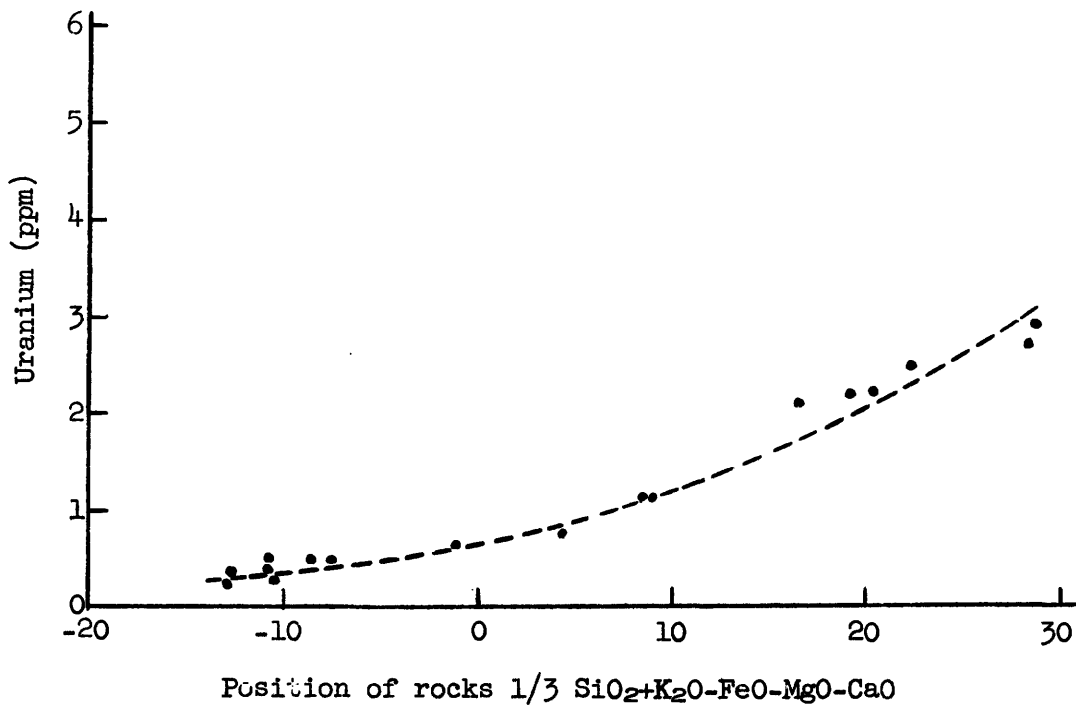
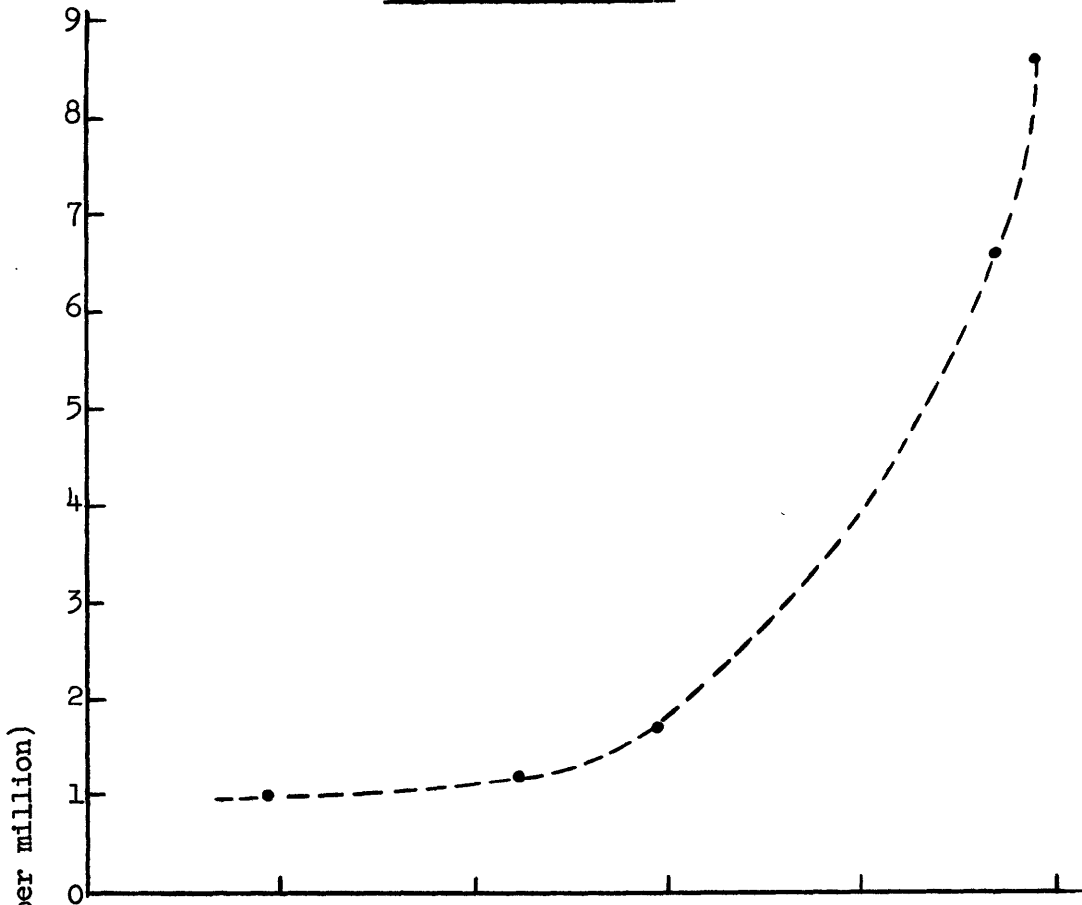


Figure 24.--Distribution of uranium in the volcanic rocks of the Strawberry Mountains, Oregon.



Potosi volcanic series

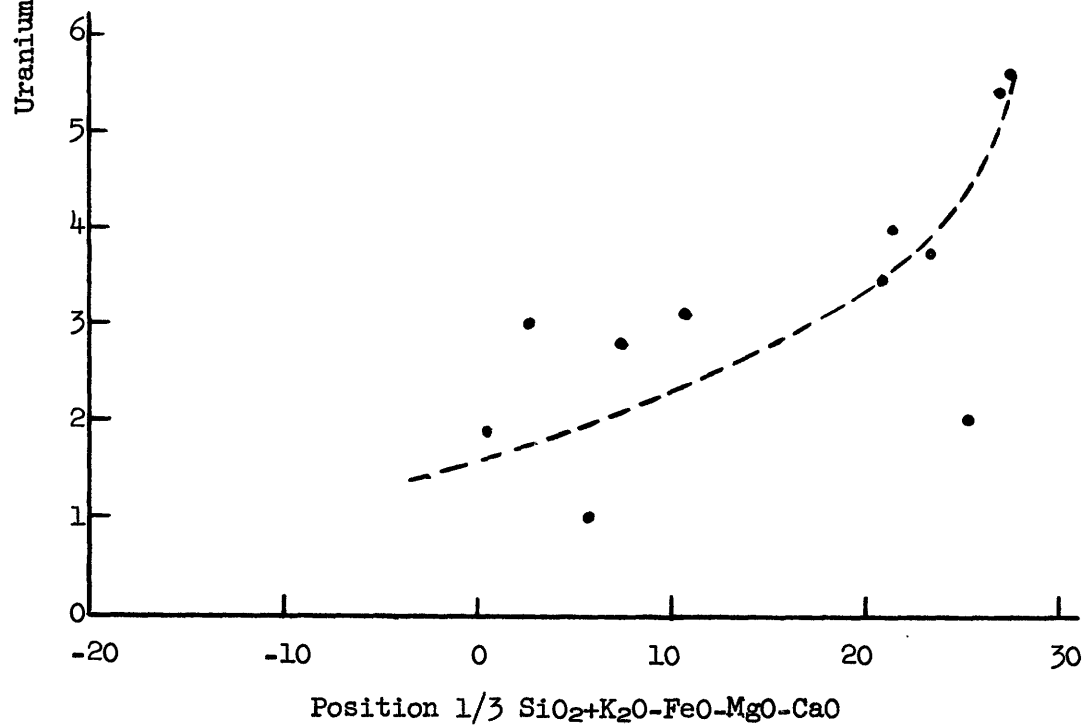


Figure 25.--Distribution of uranium in some rocks of the Hinsdale formation and Potosi volcanic series.

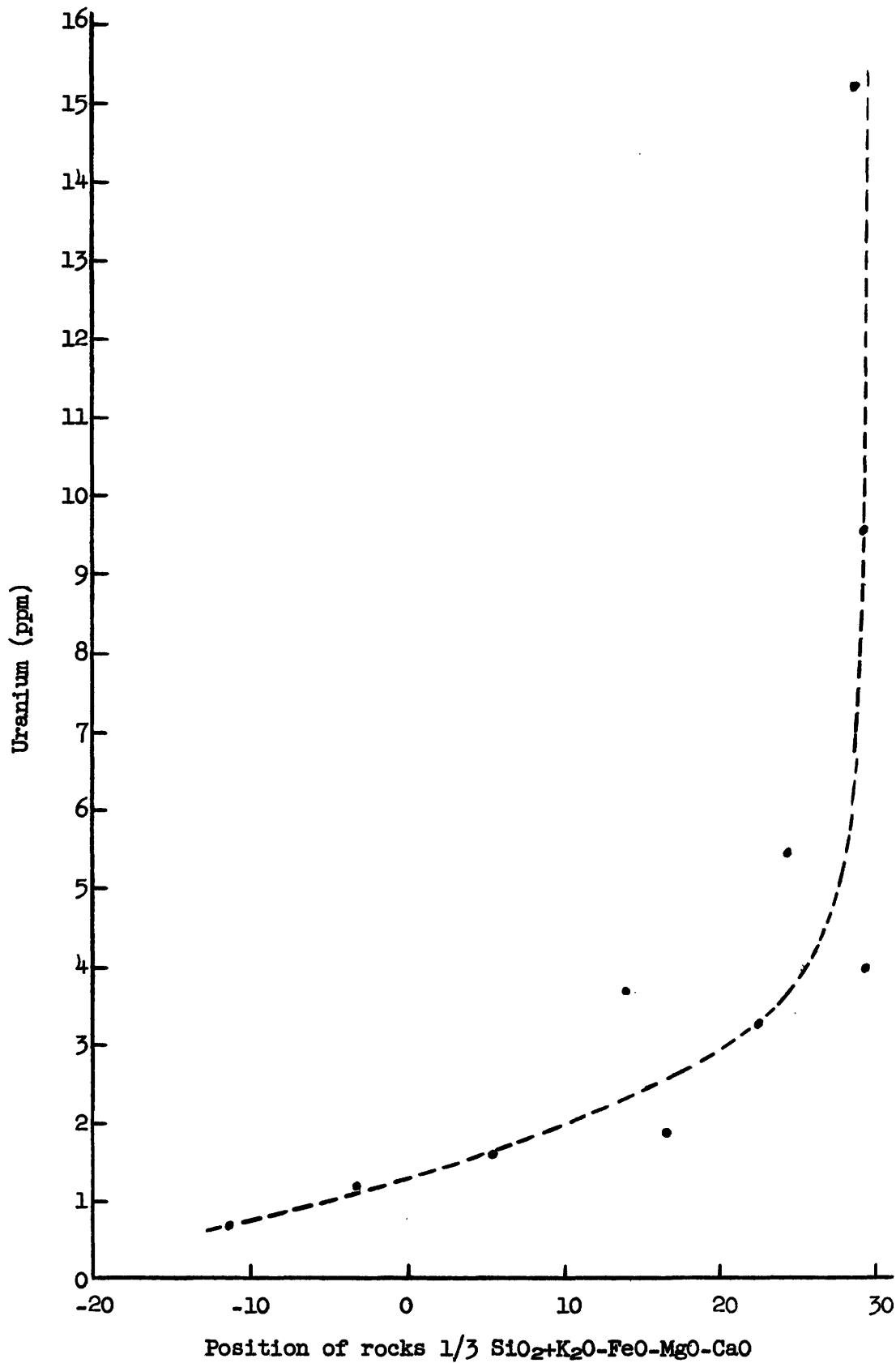


Figure 26 --Distribution of uranium in volcanic rocks of the Valles Mountains, New Mexico.

The basaltic rocks from the area known as the Watchungs in New Jersey are of Triassic age and are of the tholeiitic magma type. Twenty-five samples were analyzed for uranium. They range from 0.56 to 2.8 parts per million of uranium and average 1.0 part per million. Chemical analyses are not available for the samples on which uranium was determined; therefore it is not possible at present to correlate the uranium determinations with chemical composition.

The basaltic rocks from Iceland which were analyzed for uranium are predominately Quaternary in age. Although rock analyses were not made on these samples, they are believed to be tholeiitic (George Faust, 1958, personal communication). The samples range from 0.05 to 0.69 parts per million of uranium and average 0.22 parts per million. Eleven samples of quaternary volcanic rocks consisting mainly of obsidian and pumice of rhyolitic composition average 2.4 parts per million of uranium.

A comparison of the average uranium content of the volcanic rocks of the New Jersey and Iceland provinces is given on Table 8. The average uranium content of the basaltic rocks of New Jersey is significantly greater than the average uranium content of the basaltic rocks from Iceland. The rhyolitic rocks from Iceland appear to be low in uranium as compared to rhyolitic rocks from other petrographic provinces.

Table 8. Uranium content of volcanic rocks from New Jersey and Iceland

Locality	Rock type	No. of samples	Uranium content (ppm)	
			Range	Average
New Jersey ^{1/}	basaltic	25	0.56-2.8	1.0
Iceland ^{1/}	basaltic	16	0.05-0.69	0.22
Iceland ^{2/}	rhyolitic	11	1.2-3.3	2.4

^{1/}Samples supplied by George Faust, U. S. Geological Survey

^{2/}Samples supplied by Irving Friedman, U. S. Geological Survey

The following report was published during the period:

Larsen, E. S. Jr., Gottfried, David, and Malloy, Marjorie., 1958, Distribution of uranium in the volcanic rocks of the San Juan Mountains, southeastern Colorado: Proc. Int. Conf. on the Peaceful Uses of Atomic Energy, Geneva, 1958.

Reference

Larsen, E. S., Jr., 1938, Some new variation diagrams for groups of igneous rocks: Jour. of Geology, v. 46, p. 505-520.

Evaluation of the lead-alpha (Larsen) method for
determining the age of igneous rocks
by

David Gottfried, Howard W. Jaffe, and Frank E. Senftle

The age of an igneous rock can be determined from the lead-alpha activity ratios of certain accessory minerals (zircon, monazite, xenotime, and thorite) provided that, (1) these minerals crystallized contemporaneously with the enclosing rock-forming minerals, (2) essentially all of their lead is of radiogenic origin, formed by decay of uranium and thorium after formation of these minerals, and (3) they have neither lost nor gained parent nor daughter products since the time of crystallization. ^{Perhaps} the largest single source of analytical error is in the lead analysis; this is particularly true for minerals which contain less than 10 ppm of lead. For zircon and other accessory minerals that contain more than 10 ppm of lead the analytical precision is 4 to 10 percent of the mean of duplicate measurements.

Comparisons between the alpha emission measured by thick source alpha counting and that calculated from quantitative determinations of the uranium and thorium content of zircon and monazite indicate that the alpha activity measurements have an accuracy of ± 5 percent.

Where the method has been applied to a large number of samples of post-Precambrian suites of igneous rocks, the scatter of the age data is what would be expected from the experimental errors. In general, the standard deviation from the mean age is approximately 10 percent or less for minerals from suites of rocks older than Cretaceous. For younger rocks, which contain zircon with very low lead content, the standard deviation from the mean is considerably greater than 10 percent but is less than 10 million years.

Inasmuch as zircon, monazite, and xenotime from the same rocks give ages which agree within the limits of error of the method, it appears that the presence of common lead or the loss or gain of parent or daughter products do not contribute significantly to the errors in the age measurements of most of the post-Precambrian rocks tested.

Age determinations have been made on a large number of geologically well dated rocks in order to test the validity of the method by use of geologic evidence. With few exceptions, the age data agree with the geologic sequence of events and with the Holmes B geologic time scale.

Lead-alpha ages are in good agreement with many of the ages determined by the lead isotope, Ar^{40}/K^{40} , and Sr^{87}/Rb^{87} methods on minerals from unmetamorphosed post-Precambrian igneous rocks. However, the agreement with other methods is poor for zircon from Precambrian rocks, inasmuch as the lead-alpha age corresponds to the Pb^{206}/U^{238} age which is commonly lower than the Pb^{207}/Pb^{206} age and concordant Ar^{40}/K^{40} and Sr^{87}/Rb^{87} ages on mica.

When concordant lead isotope ages are obtained on Precambrian zircon, the lead-alpha age will also agree within the limits of error of the method. As yet

no satisfactory explanation has been found for the wide discrepancies in the measured ages of Precambrian zircon, but it appears likely that lead has been lost by partial or complete recrystallization in response to metamorphic processes.

Lead-alpha ages determined on metamorphosed igneous rocks will generally not correspond to the true age of igneous activity, but may approach the age of metamorphism.

Uranium and thorium in the Laramide intrusives of the Colorado Front Range
by
George Phair

The Laramide intrusives of the Colorado Front Range make up an "alkalic" (more accurately, CaO-poor) series which can be subdivided and systematically classified on the basis of CaO-Na₂O-K₂O relationships. These components exercise a fundamental control on the mineralogy of the rocks. Although the subdivision is basically chemical, as any quantitative classification applicable to both phaneritic and aphanitic rocks must be, dividing lines between the major rock groups have been so drawn as to coincide approximately with distinct changes in mineralogy. In perhaps 8 out of 10 instances thin-section study will suffice to place a given fresh rock in its proper chemical group. In lieu of a chemical analysis, X-ray determination of the orthoclase content of the alkali feldspar phenocrysts is necessary to separate the CaO-poor sodi-potassic rocks from the CaO-poor highly potassic types. These CaO-poor rocks are among the most radioactive known; a field geiger counter is commonly all that is required to separate the group as a whole from all others.

Although the general trend of differentiation is toward end products enriched in $\frac{K_2O \ Na_2O}{CaO}$, $\frac{Fe}{Mg}$, and SiO_2 the path followed is complicated by two factors:

(1). Magma was tapped from a hydrous, slowly differentiating deep magma into shallow hearths where it underwent further differentiation at a more rapid rate and under drier conditions. The path of deep differentiation was one of stronger reaction characterized by mildly to strongly potassic end products of moderate CaO-content; that of shallow differentiation was one of strong fractionation brought about by filter pressing, leading to sodi-potassic end products conspicuously lacking in CaO.

(2). Differences from one region to another in amount of filter pressing and in the stage at which it took place, as well as differences in environmental conditions surrounding the separate shallow hearths, gave rise to seven more or less distinct local magma trends (petrographic sub-provinces). To a considerable degree the regional and local differentiation pattern, followed by the major constituents is repeated in the distribution of the trace constituents, uranium and thorium.

The deep magma cycle largely preceded the major interval of Laramide fracturing and probably preceded that of uplift. It is characterized by the hydrous mafic minerals biotite and hornblende even in rocks as "early" as gabbro and peridotite, and by alkali feldspars (64-68 percent Or) which crystallized originally at relatively high temperatures but which upon slow cooling exsolved and inverted to lower temperature forms (orthoclase microperthite).

Scattered late pegmatites are present, but the intrusives are unaltered hydrothermally, as are their wall rocks, and aside from magmatic segregations of titaniferous magnetite in the Caribou complex most are not associated in space with ore deposits. Apparently these deeper stocks were intruded under sufficient confining pressure to insure a relatively closed system; most of the H_2O content became locked up in the hydrous rock forming silicates.

The shallow magma sequence was intruded during the rising tide of Laramide fracturing and was characterized by a reversal in stability on the part of the mafic minerals, hydrous hornblende and biotite breaking down to anhydrous aegerine augite. The sequence is characterized also by alkali feldspars (50-68 percent Or) which were more quickly cooled and hence retain higher temperature properties (intermediate between sanidine cryptoperthite and orthoclase microperthite), and by porphyritic-aphanitic textures. This sequence, including its end products, is commonly altered, and throughout the mineral belt shows a strong spatial association with hydrothermal veins and actual ore deposits. Apparently these rocks were intruded under conditions (fracturing plus de-roofing) which permitted the escape of aqueous fluids.

The end-products of deep differentiation are quickly quenched glassy biotite rhyolites approaching normal calc-alkalic compositions. They are post-ore and the youngest intrusives in the region. The end-products of shallow differentiation are quartz bostonites extremely poor in CaO, having K_2O in slight excess of Na_2O , extremely depleted in CaO and enriched in uranium and thorium by as much as 20-fold over normal calc-alkalic rhyolite. They are the youngest of the pre-ore intrusives, and their emplacement immediately preceded the deposition of pitchblende, the earliest stage of Laramide metallization.

The quartz bostonite was intruded in dikes that are very narrow but up to $5\frac{1}{4}$ miles long, suggesting low viscosity at time of intrusion. That these end products of shallow differentiation represent a low-melting highly liquid residuum is indicated by (a) bulk composition: most compositions fall in the low melting trough in the system Ab-Or-Q, petrogeny's residual system. In their low iron and extremely low MgO and CaO these rocks represent about as close an approach to the laboratory system as has been found in nature. (b) Alkali feldspars: phenocrysts range from types intermediate between sanidine cryptoperthite and orthoclase micropertthite to types as "low" as microcline. Not only is the higher temperature feldspar commonly rimmed by the low, but low temperature albite and microcline are abundant in the groundmass. In addition low temperature albite locally forms rims on some of the higher temperature potassic phenocrysts. (c) Interstitial fluorite: fluorite is a late state introduction in the groundmass; generally the more the fluorite the higher the uranium and thorium contents of the containing rock.

Actually the sparse phenocrysts in these rocks were found to have compositions appropriate to those of the feldspar first formed in the dry system Ab-Or, rather than to those in the ternary system Ab-Or-Q with or without H₂O. It strengthens the conclusion based upon texture that much of the quartz, like the fluorite, is a late magmatic introduction. The interpretation is that these long narrow dikes were ideally shaped to serve as flues and collectors for volatiles released from large volumes of cooling magma at depth. The fact that

volatiles were constantly being lost from the dikes was more than counter-balanced by accessions of volatiles from below.

Within the Front Range Mineral Belt most of the known showings and deposits of pitchblende show close space, time, and geochemical relationships to uraniferous quartz bostonite; the larger the volume of quartz bostonite cropping out in a particular area the greater its pitchblende potential. The largest center of intrusion of uraniferous quartz bostonite is at Central City, the next largest at Jamestown-Gold Hill.

This region is almost unique among mining districts for the number and strength of the ties linking well-defined rock types with specific types of ore deposit. These ties, however, give only part of the story. The quartz bostonite and quartz bostonite magma provides a source of uranium-bearing solutions; other factors were involved in the migration and precipitation of the uranium.

The separation of uranium from the late magma and its entrance into the derived aqueous liquids was probably facilitated by a shift toward more oxidizing conditions in the magma converting U^{+4} to U^{+6} and rendering it soluble. This change is reflected chemically in high Fe_2O_3 compared to FeO in these late rocks and mineralogically in abundant iron oxides as the only mafic minerals. Th^{+4} having essentially fixed valence remained in the magma through its final crystallization. It is absent from the veins. Thus the Th/U ratio of the bulk rock may give a crude indication of just how much uranium was released to the hydrothermal solutions by the crystallizing rock. For approximately comparable uranium content the Th/U ratios of the quartz bostonites in the Central City district average about 7; the similar rocks in the Jamestown-Gold Hill districts have a

Th:U ratio close to 2. On this basis also the Central City district has the largest uranium potential of any district in the Mineral Belt.

The conclusion is that solutions emanating from centers of intrusion of quartz bostonite mingled with the regional gold- and silver-bearing solutions and upon cooling and consequent reduction deposited uranium at no great distance from its igneous sources, and with further cooling, deposited other sulfides. The quartz bostonites, like most alkalic rocks, are enriched in ZrO_2 ; the pitchblende from the adjacent veins, unlike the scattered pitchblende ores in the Mineral Belt not associated with quartz bostonites, contains up to 7.0 percent ZrO_2 . No other analyzed pitchblende or uraninite is reported in the literature as containing as much as 1.0 percent ZrO_2 .

Uranium and thorium content of three early
Paleozoic plutonic series in New Hampshire

by

John B. Lyons and Esper S. Larsen, 3d

Radiometric, chemical uranium and thorium, and other chemical and spectrochemical data have been obtained on suites of rocks of the Highlandcroft (Late Ordovician), Oliverian (Middle Devonian), and New Hampshire (Middle to Late Devonian) plutonic series. These are calc-alkaline, and show a normal distribution of total radioactivity and of uranium, the diorites and quartz diorites containing the least amounts of uranium, and the granites, aplites and pegmatites the most. The analytical data for thorium and uranium contained in the rock types of each of the plutonic series are given in Tables 9 to 11. In view of the wide range in thorium content in many of the rock types, more thorium

Table 9. Uranium and thorium contents of rocks from
the Highlandcroft plutonic series

Rock types	<u>U R A N I U M</u>			<u>T H O R I U M</u>				
	No. samples analyzed	Chem. U. (ppm)		No. samples analyzed	Chem. Th. (ppm)		Th/U Ratio ^{1/}	
		Mean	Range		Mean	Range		A
Quartz monzonite	6	3.7	2.7-4.9	2	11.6	3.1-3.9	3.5	3.1
Granodiorite	1	3.0	--	0	--	--	--	--
Sodaclase-tonalite	1	3.1	--	0	--	--	--	--

^{1/} The Th/U ratios in column A are the means of the individual ratios for each rock; they are derived only from those samples analyzed for thorium.

Column B gives the ratio of mean Th:mean U.

Table 10. Uranium and thorium contents of the major rock types of the Oliverian plutonic series

Rock types	<u>U R A N I U M</u>			<u>T H O R I U M</u>			Th/U Ratio ^{1/}	
	No. samples analyzed	Chem. U. (ppm) Mean	Chem. U. (ppm) Range	No. samples analyzed	Chem. Th. (ppm) Mean	Chem. Th. (ppm) Range	A	B
Granite	14	5.7	1.8-13.0	5	14.1	7.5-21.	3.9	2.5
Quartz monzonite	6	3.5	1.1-5.5	4	10.8	6.2-21.	3.9	3.1
Granodiorite	14	2.2	0.8-6.8	4	15.4	6.2-38.	7.5	7.0
Quartz diorite	16	2.1	0.8-5.0	2	9.0	3.1-14.8	3.2	4.3
Pegmatite	2	6.9	1.3-12.4					
Aplite	3	9.3	2.1-15.9					
Wallrocks and inclusions	7	1.2	0.6-1.8					

^{1/} The Th/U ratios in column A are the means of the individual ratios for each rock; they are derived only from those samples analyzed for thorium.

Column B gives the ratio of mean Th:mean U.

Table 11. Uranium and thorium contents of the major rock types of the New Hampshire plutonic series

Rock types	U R A N I U M				T H O R I U M				Th/U Ratio ^{1/}		
	No. samples analyzed	Chem. U. (ppm)		No. samples analyzed	Chem. Th. (ppm)		A	B	A	B	
		Mean	Range		Mean	Range					
Granite	7	4.3	2.8-5.8	1	10.7			2.5	2.5	2.5	2.5
Quartz monzonite (chiefly Kinsman)	16	3.5	1.6-6.3	4	16.5	14.1-19.4		7.9	4.7	4.7	4.7
Quartz monzonite to granodiorite (Bethlehem gneiss)	29	3.4	2.2-5.2	9	14.5	11.7-18.1		5.1	4.3	4.3	4.3
Quartz diorite	2	3.1	2.9-3.4	0	--	--		--	--	--	--
Pegmatite	3	16.7	5.0-39.	0	--	--		--	--	--	--
Aplite	3	7.2	3.6-14.2	-	--	--		--	--	--	--
Wallrocks and inclusions	5	3.3	0.9-5.0	0	--	--		--	--	--	--

^{1/} The Th/U ratios in column A are the means of the individual ratios for each rock; they are derived only from those samples analyzed for thorium. Column B gives the ratio of mean Th:mean U.

analyses are needed to more than suggest that thorium increases with uranium in some of the rock series.

The mean thorium and uranium content, and mean Th/U ratio of the rock types in each series, are similar to those of the Southern California batholith. In the Highlandcroft and Oliverian series, these values have a much greater deviation from the mean than do the rocks of the Southern California batholith. In the New Hampshire plutonic series the deviations from the mean are small and the Th/U ratios seem significantly high to characterize this as a slightly thorium-enriched series.

In the Highlandcroft series the uranium is distributed chiefly among sphene, epidote, and the major rock forming silicates. In the Oliverian series as much as 75 percent of the uranium in the rocks is contained in sphene and epidote. The New Hampshire plutonic series lacks sphene and epidote, but is characterized by accessory monazite and xenotime; its uranium and thorium, however, are chiefly held in the major rock forming silicates. Temperature of crystallization and/or metamorphism have been important factors in determining the distribution of radioactivity.

Uranium and thorium in these rocks is associated with trivalent or quadrivalent transition-group elements having ionic radii and electro-negativities approximating those of uranium and thorium. These elements concentrate in the residual members of the various calc-alkaline suites largely because they do not fit into the structures of the major silicate minerals.

Synthesis and Solution Chemistry of Uranium

Studies of a reduced mineral from Ningyo-Toge mine, Japan

by

T. Muto, R. Meyrowitz, and A. M. Pommer

Physical and chemical studies of a new hydrated calcium uranous phosphate mineral from the Ningyo-Toge mine of Japan were completed. Its structure was established as $U_{1-x}R.E._{2x}(PO_4)_{2.1-2}H_2O$, where x is about 0.1 to 0.2. Its X-ray pattern resembles that of rhabdophane. Upon heating at 800° to 900°C in argon, both the natural mineral and the synthetic compound change to a monazite-type rather than a xenotime-type structure.

Mineral synthesis

by

A. M. Pommer and J. C. Chandler

Potassium and sodium analogs of a hydrated uranium silicate mineral from the Thomas range, Juab County, Utah, were prepared. Attempts to prepare the calcium analog were unsuccessful. Glass exposed to hot alkaline solutions was employed as source of silica in the preparation of this silicate. This approach was used to simulate natural conditions in which this or other minerals, (e.g., boltwoodite) may form by the action of hot uranium-bearing solutions on quartz or silicate minerals. Uranophane could not be prepared by this method.

Solution chemistry of uranium
by
A. M. Pommer and I. A. Breger

A program was developed for study of the effect of chelation by naturally occurring organic substances on the stability of the uranyl ion in aqueous solution. Such organic substances are extremely complicated polyelectrolytes for which no thermodynamic data are available. In the initial phase of this program an attempt is being made to determine if experimental titration curves for the neutralization of humic acid are related to the colloidal properties of the acid or if they truly represent chemical neutralization. If pH shifts during titration are controlled by the electrolytic properties of the humic acid solution, it will be possible to calculate complexing constants for the interaction between humic acid and the uranyl ion. A preliminary study has indicated that it is feasible to determine the isoelectric point for humic acid from changes in the electrophoretic mobility of quartz particles in humic acid solutions at differing hydrogen ion concentrations.

Association of uranium with coalified logs
by
Irving A. Breger

Complete coal analysis data have been assembled for 62 coalified logs from the Colorado Plateau containing from 0 to 16.5 percent uranium. A sufficient number of analyses is now available to permit comparison of logs from Jurassic sediments with those from Triassic and Eocene formations. Calculations confirmed the radiochemical dehydrogenation previously reported;

the relationship of high organic sulfur to high uranium content is apparent only in the Temple Mountain area (Triassic) indicating that mineralization took place under somewhat different conditions at that locality than in other regions.

Uranium in impregnated sandstones
by
Irving A. Breger and John C. Chandler

Sink-float (S. G. 1.75) was used to isolate approximately 1 g. of organic matter from the impregnated sandstone of the Jeep No. 6 claim, Ambrosia Lake area, New Mexico. Comparison of the infrared spectrum of this material with that of coalified wood from the region indicates the two to be related. This isolate is being supplemented by a large isolate to be used for complete chemical analysis. Thus far, chemical treatment of 950 g. of ore to remove silica has led to the isolation of 9.6 g. of organic material (1.0 percent) and 16.3 g. of pyrite (1.7 percent).

Similar study of an impregnated ore from the Fanny Mae Mine, Gas Hills area, Wyoming, led to the isolation of about 250 mg. of organic material by sink-float. Chemical solution of silica from a 1000-g. sample yielded 80 g. of an organic-pyrite isolate which, when sink-floated in bromoform, provided 14 g. (1.4 percent) of organic material.

The following papers were published during the period:

- Feinstein, H., 1958, Laboratory aid to speed up filtration: *J. Chem. Ed.* 35, 509.
Breger, I. A., 1958, Geochemistry of coal: *Econ. Geol.* 53, 823-842.

Stable Isotope Analysis
by
Irving Friedman and Betsy Levin

Deuterium analyses of the leaves, stems and roots of willow and rush plants collected by John H. Feth in California show that the inter-cellular water removed by drying at 110°C is enriched in deuterium in the leaves of willow and rush stems. The roots of both plants and the stem of the willow concentrate deuterium to a very small extent compared to the original ground water. The organic hydrogen, collected by burning the dried samples in oxygen, has about the same isotopic composition as the ground water. These studies will be useful in tracing the course of water in phreatophyte studies.

The deuterium analysis of hydrous minerals continued. The water content of analyzed samples of biotite as determined by the technique now in use is higher by a factor of almost two from the results of chemical analyses. This points up the fact that water determined by the Penfield method is a very poor approximation to the actual value.

Nuclear Geology
by
Frank E. Senftle

Work on the isotopic analyses of copper was completed during the report period. Tests were made to determine the isotopic fractionation of copper from adsorption on quartz and sphalerite. A solution of copper sulfate of known isotopic composition was passed through a column packed with the quartz and sphalerite. The copper which came through the column first was of somewhat lower gravity than that in the original solution. These preliminary tests of

the effect of adsorption require substantiation by a more thorough study. The study was terminated, at least temporarily, to devote time to more profitable research, and considerable effort was made to expand studies involving magnetic susceptibility measurements.

Wide variations have been quoted in the literature for the magnetic susceptibility of rutile (TiO_2). There is also a lack of similar data for the anatase and brookite forms of TiO_2 . As TiO_2 is of interest as a semi-conductor, a good value of the magnetic susceptibility is needed. Careful measurements were therefore undertaken to determine the magnetic susceptibilities of the three crystallographic forms of TiO_2 (See Fig. 27). The magnetic susceptibility of rutile was found to be $(0.0667 \pm 0.0015) \times 10^{-6}$ emu per gram and is temperature-independent from 77°K to 372°K . Anatase has a magnetic susceptibility of $(0.039 \pm 0.003) \times 10^{-6}$ emu per gram and is essentially temperature-independent from 175°K to 302°K . As the temperature was lowered below 175°K the magnetic susceptibility of anatase increased rapidly to about 0.35×10^{-6} emu per gram at 77°K . The reason for this large change is not clear. Only natural impure specimens of brookite were obtainable for these measurements. The magnetic susceptibility was measured as 1.15×10^{-6} emu per gram, but this value is probably high. It is planned to make more measurements on these materials before publication of the results.

A study is also being made of the magnetic susceptibility of tektites and other volcanic glasses. The tektites have susceptibilities which cluster about a value of $(6 \text{ or } 7) \times 10^{-6}$ emu per gram (see Table 12). However, although chemical analysis shows the presence of iron, the tektites show no ferromagnetic

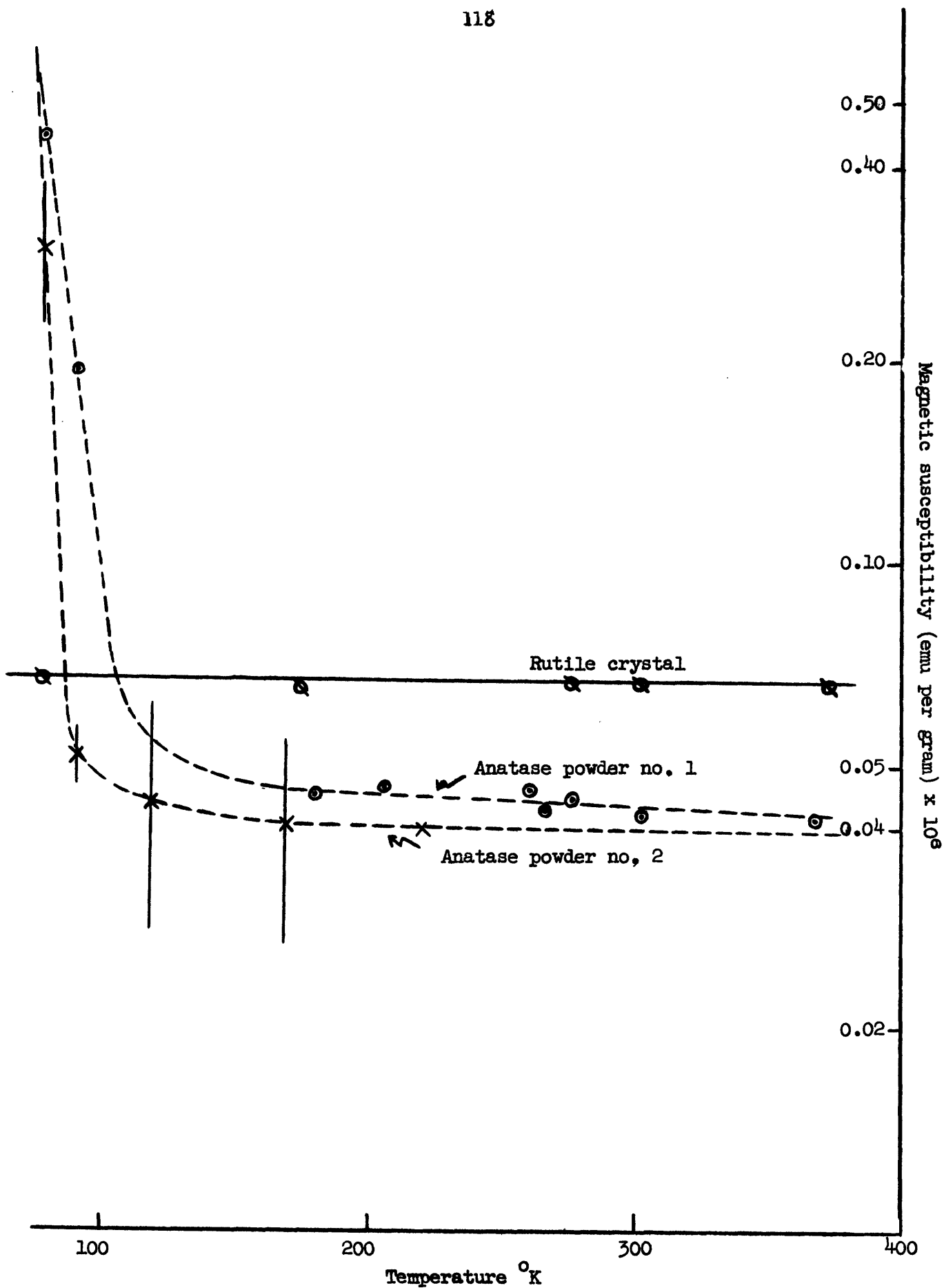


Figure 27 .--Magnetic susceptibilities of the three crystallographic forms of TiO_2 .

Table 12. Magnetic Susceptibilities

		<u>Tektites</u>	
Source			Magnetic Susceptibility (x 10 ⁻⁶ emu _g ⁻¹ per gram)
Indo-China	(a)		7.46
Indo-China	(b)		5.37
Indo-China	(c)		6.13
Australia	(a)		6.27
Australia	(b)		6.52
Australia	(c)		6.00
Bohemia			2.34
Philippines	(a)		7.57
Philippines	(b)		7.55
Philippines	(c)		6.40
Philippines	(d)		6.00
Peru			0.529
Texas			6.70
Libyan Desert Glass			-1.99
		<u>Obsidians</u>	
New Zealand	(a)		8.54
New Zealand	(b)		1.78
New Zealand	(c)		6.40
California	(a)		1.24
California	(b)		6.43
California	(c)		1.15
California	(d)		0.855
California	(e)		0.23
California	(f)		2.04
California	(g)		9.14
Arizona			0.486
Utah			10.24
Nevada			11.25
New Mexico			9.20

l/ electromagnetic units

impurity. For comparison the magnetic susceptibility of a number of specimens of obsidian samples were measured. In general the susceptibility of the obsidians is lower, but in some cases it overlaps the susceptibilities of the tektites. However, almost without exception the obsidians have a large contribution of ferromagnetic impurity. We are currently attempting to determine the significance of this difference.

An effort was made also to determine the magnetic susceptibility of a number of pure uranium minerals. We are studying the feasibility of using the magnetic susceptibility as a method of determining the formula of unknown minerals. To check the method we are applying this technique to the formula of coffinite, $(1-x) \text{USiO}_4 \cdot x \text{U(OH)}_4$. By knowing the susceptibilities of USiO_4 and U(OH)_4 , it is hoped that a reasonably good value of x can be obtained. The magnetic susceptibility of synthetic USiO_4 has been determined as $(6.63 \pm 0.09) \times 10^{-6}$ emu per gram at 29°C . The magnetic susceptibility of natural coffinite, on the other hand, is about half that of the synthetic mineral.

Nuclear Irradiation
by
Carl M. Bunker

Seven simulated subsurface formations have been constructed at the Denver Federal Center for the purpose of calibrating density logging equipment. Materials having densities in the range of 8.74 to 85.23 have been placed in 55-gallon drums. A center pipe of thin aluminum permits the logging probe to be placed within the material. The logging probe contains a 600-millicurie cobalt-60 source which emits gamma-radiation into the formation. Some of the radiation

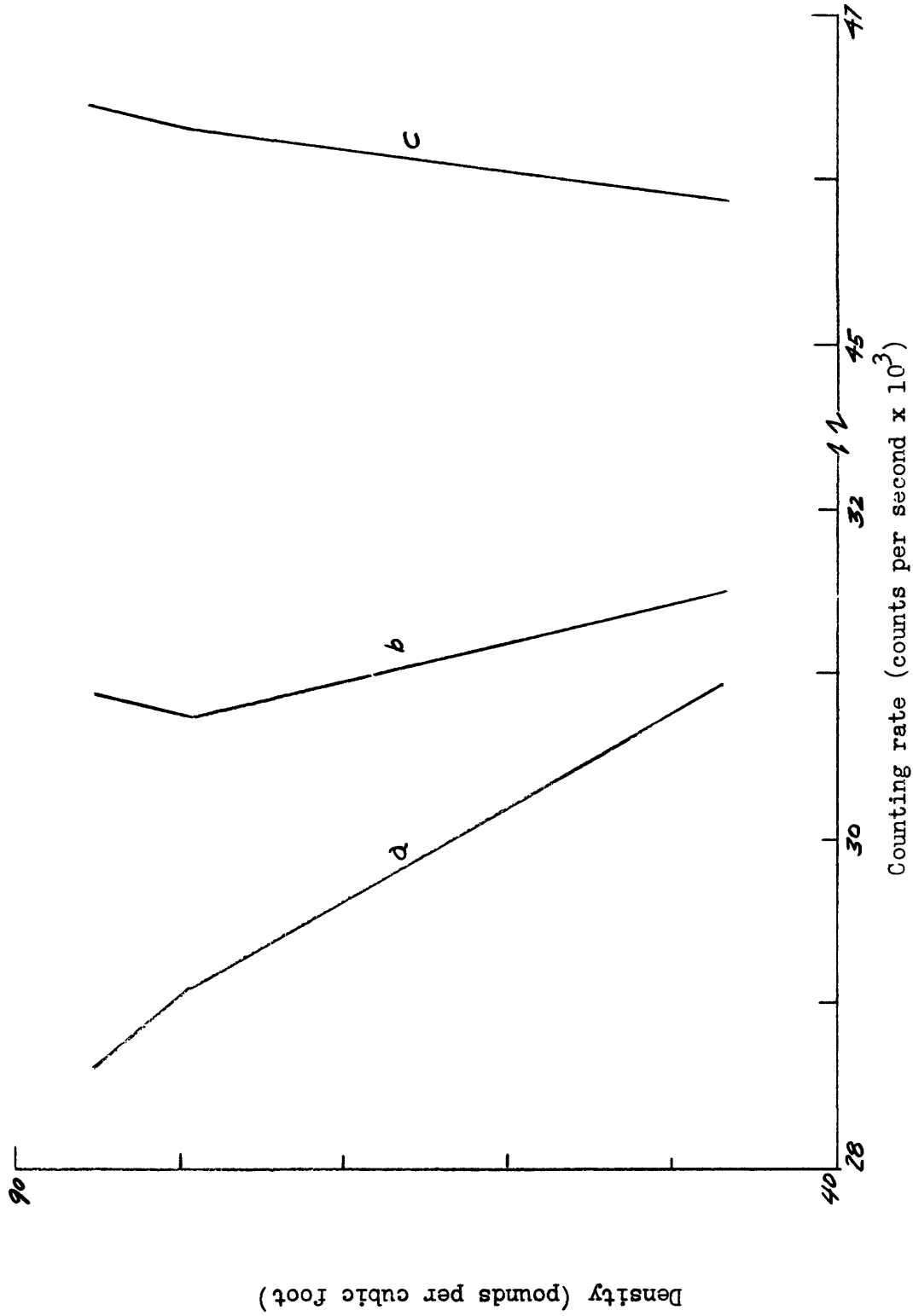


FIG. 28. RESPONSE OF DENSITY LOGGER IN SIMULATED FORMATIONS. CURVES SHOW EFFECTS OF VARIOUS SHIELDING CONFIGURATIONS AND SPECTRAL RESPONSE.

not absorbed by the formation reaches the scintillation detector and is measured with a single-channel pulse height analyzer and ratemeter. Preliminary measurements have been made using various amounts of lead shielding between the source and the detector. Various ranges of gamma-ray energies incident on the detector are being measured to determine their affect on calibration. Some of the results of the work are shown in figure 28.

Of the three curves shown in figure 28, curve "a" is the most desirable as there is greater change in counting rate with a change in density than is shown in the other curves. During the next six months calibration will be continued. An attempt will be made to obtain a calibration curve which has a slope less than that of curve "a". A method of standardization to retain the laboratory calibration while making field measurements will be investigated. Field measurements will be made in drill holes penetrating formations of known density prior to making geophysical investigations with the equipment.

Geochronology
by
Lorin R. Stieff

During this report period, the manuscript "Original Radiogenic Lead, An Additional Correction for Lead-Isotope Age Calculations: Part I" was completely rewritten. The objectives of Part I are (1) to re-emphasize (particularly for uranium ores) the importance of one of Kovarik's (Bulletin 80, NRC, 1931) fundamental prerequisites for valid lead isotope age calculations, i.e., the absence of, or correction for, original radiogenic lead, and (2) to present in more detail the mathematical analysis of this problem. The graphical treatment

of the correction for original radiogenic lead discussed in the literature is incomplete and obscure. The single algebraic solution of the original radiogenic lead problem proposed requires isotopic data that are frequently unavailable and that are very tedious mathematically.

To remedy this situation, a completely new set of age equations were derived accompanied by their graphical equivalents. With the new equations it is possible to calculate a concordant age (i.e. $Pb^{206}/U^{238} = Pb^{207}/U^{235} = Pb^{207}/Pb^{206}$ age) from discordant age data for a single sample containing either common lead or original radiogenic lead, given only the Pb^{207}/Pb^{206} ratio of the contaminating lead. It is not necessary to know either the amount of the contaminating lead or to use the index isotope (Pb^{204} or Pb^{208}) in the calculation of the common lead correction as was previously the case. For samples containing very large amounts of common lead these equations permit a substantial reduction in the uncertainty introduced by this correction.

In areas where discordant isotopic age data are available for two, three, or four samples from the same deposit, analogous equations have been developed which permit, as the number of samples increases, the calculation of concordant ages without knowledge of the amount or the ratios of the contaminating common lead and original radiogenic lead. In addition, these equations have been programmed for the Survey's digital computer. If the degree of these equations is three or greater, and if the lead-uranium and lead-lead ratios have geologically possible values, the equations will have two positive real roots. As the degree of the equations increases, the smaller root rapidly approaches the exact, concordant age corrected for original radiogenic lead. The larger root

approaches more slowly the concordant age corrected for loss of lead or gain of uranium. With this concordant age data it is then possible to calculate the Pb^{207}/Pb^{206} ratio of the original radiogenic lead, or the Pb^{207}/Pb^{206} ratio of the lead lost in the time interval represented by the two positive roots. It is also possible to obtain the isotopic composition of the lead originally present and the isotopic composition of the contaminating common lead. These calculated ages and isotopic ratios may then be compared with the measured isotope ratios obtained on the lead extracted from associated nonradioactive minerals in the same deposit. The calculated concordant ages should also be compared to the best available geological data on the age of the enclosing rock. These comparative studies coupled with the geologic field relations and mineralogic relations can be used in an evaluation of the discordant age results and ultimately in the calculation of the most probable age of the samples.

Modified second degree equations which may be used when computing facilities are not available were also developed. For most geologic problems and with a little experience, only two trial calculations need be made to come within one or two percent of the exact concordant age corrected for original radiogenic lead. Separate calculations, however, must be made to obtain the "concordant" lead loss age."

For the first time, adequate graphical and algebraic methods are now available for the calculations of concordant ages corrected from common lead, original radiogenic lead, loss or gain of lead, selective loss of radioactive daughter products, or loss or gain of uranium. In addition, the requirements

of these equations should help to guide not only the selection of the type of sample to be collected but also the number of samples that are necessary for a useful lead-isotope age study. Finally, uncertainties in the algebraic solution of the concordant ages are far smaller than the errors inherent in the determination of the half-life of U^{235} , the isotopic analyses and the quantitative determinations of lead and uranium. Thus, there are new incentives to improve our physical constants, analytical techniques, and sampling methods in order that we may derive all of the useful geologic information that is available in a comprehensive lead-isotope age study.

Isotope geology of lead

by

R. S. Cannon, Jr.

The most significant new development this period has been the decision to establish a lead isotope laboratory at the Denver Federal Center. Staff and facilities are being developed to integrate mass spectrometry with the other phases of lead isotope work already being done there. Plans for the new laboratory, which will combine adjoining facilities for chemistry and mass spectrometry, are aimed at achieving the best possible accuracy, precision, and sensitivity in lead isotope analysis and freedom from contamination in chemical handling of samples. For the guidance of this program advice has been sought at the University of Minnesota from Prof. A. O. Nier and Dr. J. H. Hoffman. Advice has been sought likewise at Oak Ridge where, as a result of arrangements made by the Division of Research with Dr. A. E. Cameron, ORNL, Antweiler and Pierce of the project staff spent two weeks

studying mass assay facilities and techniques. W. D. Harman at Oak Ridge is also working closely with Pierce in an effort to improve the quality of lead isotope analyses.

The discovery of anomalous concentrations of lead in igneous rock contiguous to lead-zinc mineralization in the Coeur d'Alene district, Idaho, as reported here earlier, has now been confirmed by quantitative analysis. Antweiler has analyzed a specimen of lead-rich monzonite from a dump of the Success mine, and also lead-rich feldspar from this monzonite, with the following results:

	Monzonite Id-Sudg-2A	Feldspar Id-Sudg-2Af
Pb	.197	.164
SiO ₂	63.24	64.25
Al ₂ O ₃	19.02	18.76
Fe ₂ O ₃	1.06	.05
FeO	2.07	.15
MgO	.79	.03
CaO	3.16	.46
Na ₂ O	4.55	1.78
K ₂ O	3.85	13.19
H ₂ O+	1.10	.24
H ₂ O-	.17	.04
TiO ₂	.35	.01
P ₂ O ₅	.14	.01
MnO	.11	.01
CO ₂	.03	.01

Lead contamination in the laboratory poses difficult obstacles to studies of abundance and isotopic composition of trace-lead in rocks and minerals. New information on these complications is obtained from time to time, and we are anxious to compare our findings with those obtained by other investigators. Some experiments on contamination from laboratory ware were made recently by

Antweiler to test the relative merits of different materials and cleaning methods. In general, it appears hazardous to use laboratory vessels made of silica-rich materials. Lead tends to accumulate on the surfaces, thus affording opportunity for contamination and for lead loss from the sample. Antweiler found that there is far less hazard in using gold or polyethylene than in using pyrex or porcelain. Platinum was inferior to gold. Cleaning laboratory vessels in boiling 1:1 HNO_3 was found to be far more effective than other conventional cleaning techniques that were tried.

A new technique of separating and concentrating galena from complex sample materials involves an elutriating device that Irving C. Frost designed and tested for this project several months ago. Heterogeneous samples of closely sized mineral grains can be separated into fractions of different specific gravities in accordance with Stokes' Law. Thus heavy minerals like galena, zircon, or gold, or light minerals like mica or feldspar, can be rapidly concentrated from samples of sand or crushed rocks and ores. The elutriating tube is made of segments of tubing graduated in diameter so that a rising current of water gives diminishing lift to falling mineral particles. Regulation of rate of flow of the elutriating fluid permits the heaviest mineral fraction to settle for collection at the foot of the tube, or the lightest mineral fraction to be collected by overflow at the top. Water is the most convenient fluid to use in this apparatus, and it has advantages over heavy liquids that are likely to be expensive, unstable, corrosive to certain metal sulfides, and more or less toxic. With this simple apparatus many mineral separations (at least on samples of 10 grams or less) can be made rapidly and effectively.

The following papers were published during the period:

Cannon, R. S., Jr., Stieff, L. R., and Stern, T. W., 1958 Radiogenic lead in non-radioactive minerals: a clue in the search for uranium and thorium: Proc. Int. Conf. on Peaceful Uses of Atomic Energy, Geneva, 1958.

Pierce, A. P., Mytton, J.W., and Barnett, P. R., Geochemistry of uranium in organic substances in petroliferous rocks: Proc. Int. Conf. on Peaceful Uses of Atomic Energy, Geneva, 1958.

Natural Radioactivity of the Atmosphere

by

Hilton B. Evans

The vehicle-mounted air monitor unit was operated during most of the summer field season, primarily to investigate the degree of correlation between the radon content of air and the lithology of areas traversed.

A number of traverses were carried out over known geologic sections in Emigration Canyon and also north of Park City, Utah. These areas are located approximately 8 miles east of Salt Lake City and 25 miles southeast of Salt Lake City respectively.

The Emigration Canyon traverse is in a deep, narrow canyon that cuts eight geologic contacts in a distance of about $2\frac{1}{2}$ miles. Fig. 29, showing lithologic units traversed and gamma-ray and air-sample count per sample interval, reveals a fair correlation between gamma-ray and air-sample peaks. However, there appears to be some displacement of air sample maxima due to vehicle motion, wind movement, or both. The vehicle speed during the traverse of fig. 29 was about 10 m.p.h., and a reduction of velocity resulted in better definition of sample peaks. Sampling over the traverse line in two directions provides more information concerning the effect of wind on radon displacement relative to the source.

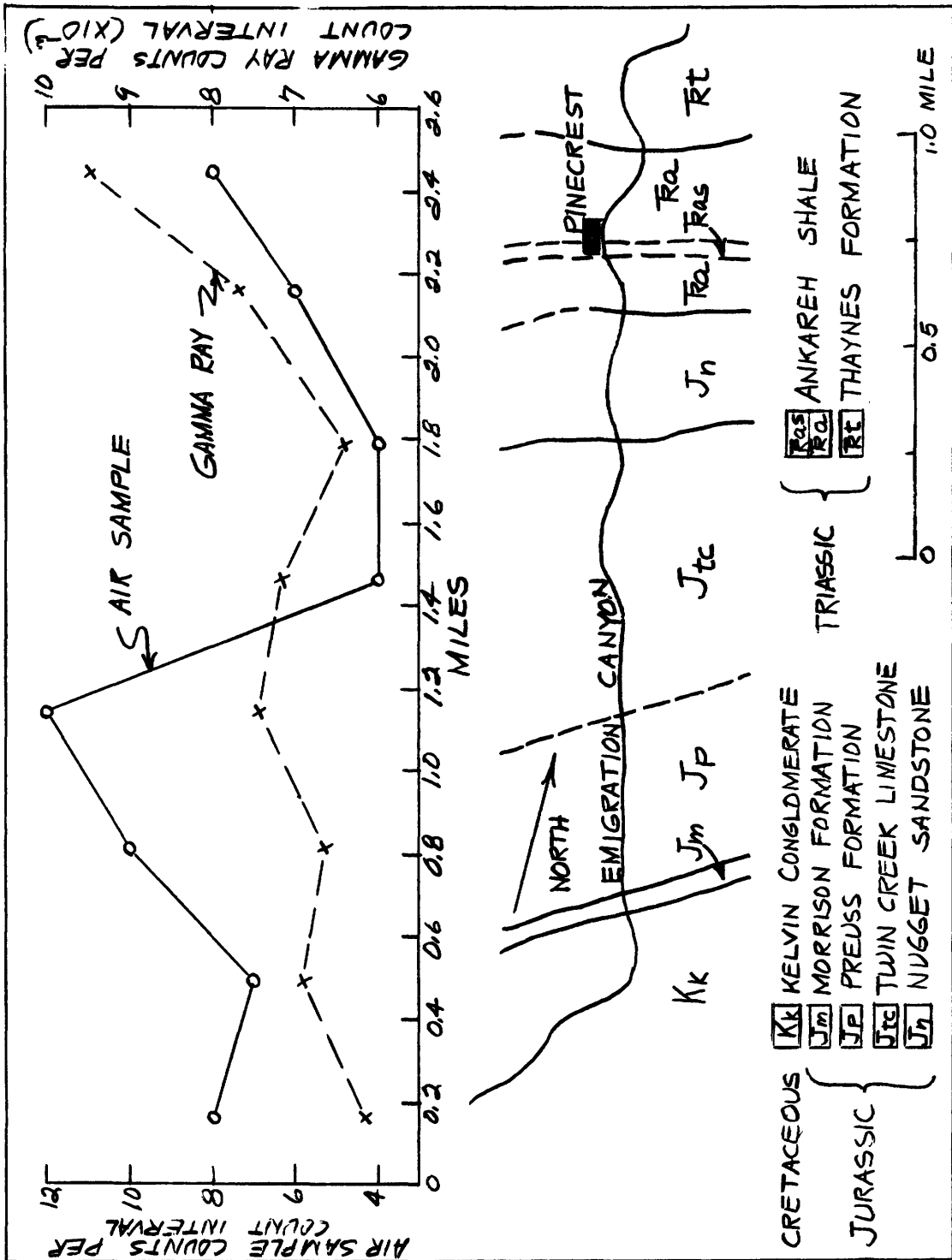


Fig. 29. Plan view of lithology traversed showing air sample and gamma-ray profiles along traverse line, Emigration Canyon.

Assuming that air samples represent the radon efflux from the lithologic units traversed, the relatively high air sample count obtained over the Ankareh shale would require radon escape through fractures in addition to normal diffusive losses. The existence of such fractures has not been confirmed.

The air sample traverse north of Park City, Utah crosses many of the same lithologic units found in Emigration Canyon, but the traverse line is in a broad, flat valley and provides a completely different sampling situation. An example of an air sample traverse at a speed of about 4 m.p.h. in this area is shown in fig. 30. Good correlation between gamma-ray and air sample highs suggests that the lithologic changes along the traverse line can be recognized by air sampling as well as by normal radiation surveys. Several traverses in this area support the assumption that the location of air sample highs is dependent not only on vehicle speed but also on the wind velocity and direction and on other meteorological conditions.

Limited air sampling was carried out over a near-surface uranium mine located about 50 miles northwest of Delta, Utah. High velocity winds and impassable terrain ruled out a thorough investigation of the vertical and horizontal migration of radon from the mine area, although the two short vehicle traverses completed further illustrate the close relation between gamma-ray anomalies and radon content of the air (fig. 31). No information concerning the extent of the uranium deposit or the geology of the area is available at this time.

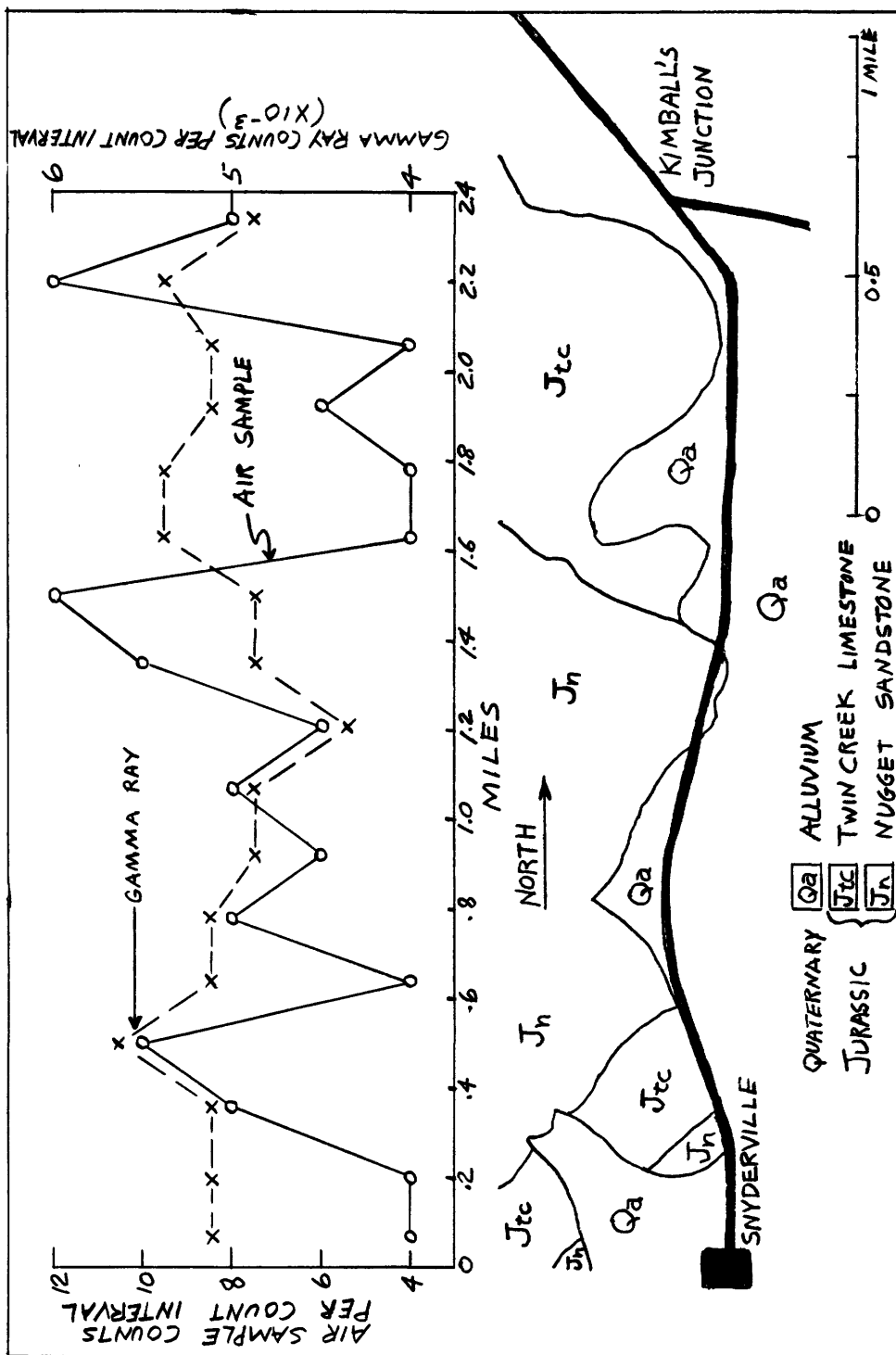


FIG. 30. Plan view of lithology traversed showing air sample and gamma-ray profiles along traverse line near Park City, Utah.

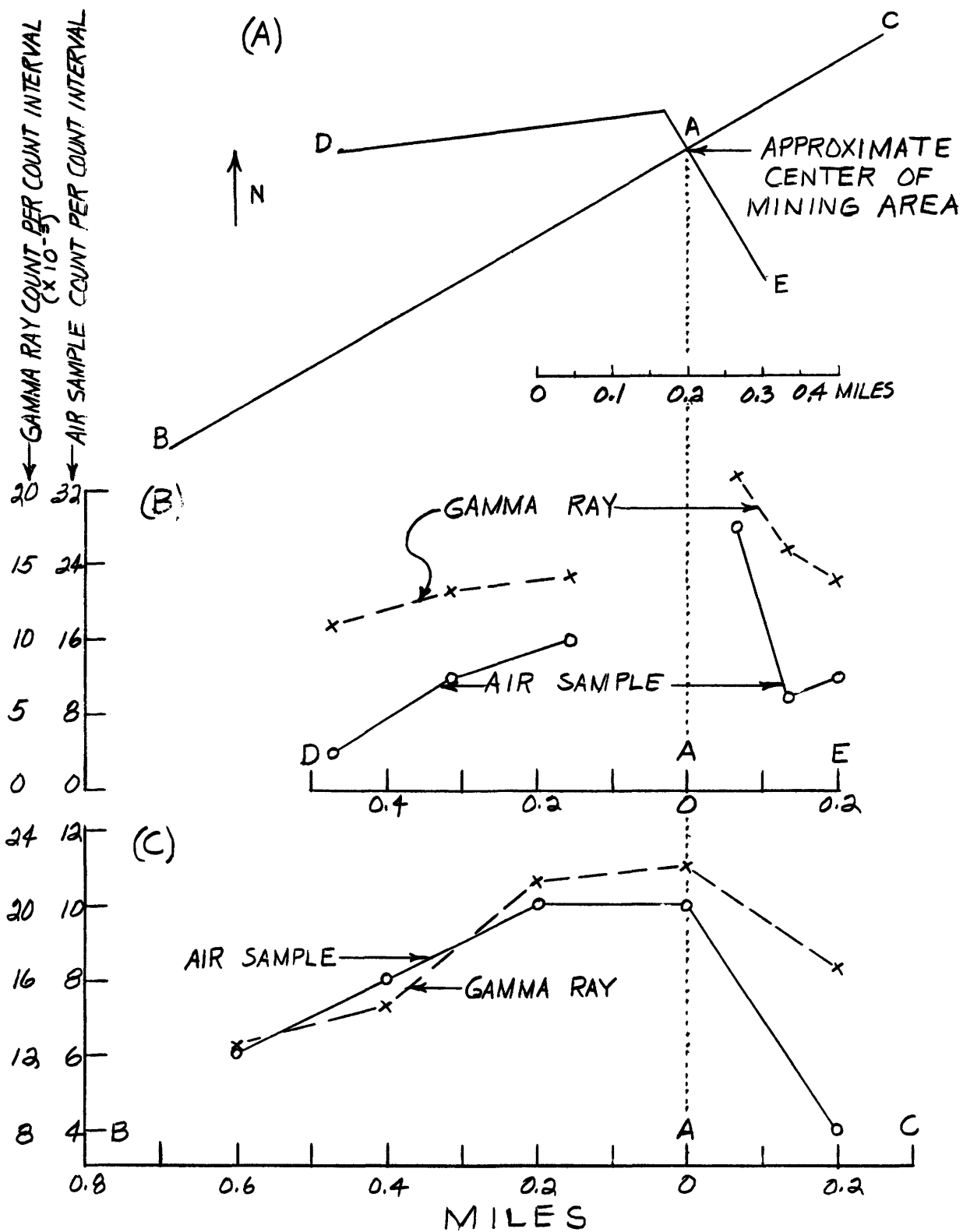


Fig. 31. Plan view of traverse lines across uranium mine (A) and gamma-ray count and air sample count for traverse DAE (B) and traverse BAC (C).

Air samples were also obtained over a hot spring drainage area, located about 50 miles north of Salt Lake City, Utah, where radium precipitating from the spring water results in a broad gamma-ray anomaly. An air-sample high near the hot spring is apparently due to the discharge of radon from the spring water into the air. However, analysis of these data is not complete.

A report on the radon content of the atmosphere over shallow uranium deposits in the Texas Coastal Plain has been completed as a section of a professional paper.

A report on the movement of radon through porous media is nearing completion.

Thermoluminescence

by

Frank E. Senftle

The first half of the report period was devoted to the construction of a magnetic balance and a device for measuring the thermoluminescent light yield of the specimens. This equipment has been finished and is operating satisfactorily.

It is generally believed that the thermoluminescent light is due to the energy released when a trapped electron drops into its normal low-level position. In the trapped position the electron spin is unpaired and hence will contribute to the magnetic susceptibility of the specimen. By measuring the change in susceptibility with the successive annealing of the thermoluminescent peaks, one could determine the number of traps in each peak. Preliminary measurements were made on calcite. The thermoluminescent glow curves were

determined for a number of specimens and portions of each specimen were heated so as to anneal out each peak. Magnetic susceptibility analyses on these same specimens did not show any large change in the magnetic susceptibility, when good clear white calcite was used. However, a 16 percent change was noted in the susceptibility when pink calcite was heated to 270° for 2 hours. As might be expected, the degree of purity of the specimen is important.

Further work is planned on other materials and in particular on zircon. In this case it is planned further to investigate the relationship between the magnetic susceptibility and the amount of radiation damage. Some measurements have already been made in this direction, but no interpretation has yet been made on the variations observed. The magnetic susceptibility of about 25 zircon⁴ samples from the Boulder Batholith have been measured. Another suite of zircons from various locations and with varying ages are also being measured.

Geology and Geochemistry of Thorium

Thorium determinations on rocks of the Boulder Creek batholith
by
George Phair and David Gottfried

Thorium determinations on 60 analyzed rocks from the Boulder Creek batholith, Colorado are nearly completed. Results generally run parallel to the earlier uranium values except that along the deformed margins of the batholith less thorium was lost from the rocks during metamorphism; hence Th/U ratios are higher (5-17) than in the less deformed interior (3-7). Thorium is here largely tied up in allanite, a fact which probably accounts for its solubility under standard laboratory leaching conditions (24 hours in 1+4 HCl).

Because the original thorium has been largely retained throughout a complex history the increase in thorium with increasing SiO_2 in the differentiation series as a whole is considerably more systematic than that of uranium, though still subject to wide variation. The total spread is about 2 fold between highest and lowest values for a fixed SiO_2 content.

Six of 8 rocks giving low zircon ages (less than 840 m.y.) have high Th/U ratios (greater than 6). The two remaining have Th/U ratios close to 5.0. All rocks giving high zircon ages (greater than 880 m.y.) have low Th/U ratios (less than 6). These data are compatible with the earlier interpretation that the low-age rocks together with the contained zircon had lost uranium during a younger deformation.

Modification of procedure for determining thorium
in the low parts per million range
by
F. S. Grimaldi and Lilly Jenkins

The procedure for the determination of thorium in the parts per million range in rocks (Levine and Grimaldi, 1958) was modified slightly to facilitate the preparation of the solution for analysis. The decomposition with HF-HNO_3 followed by repeated evaporation with HNO_3 to remove fluoride is retained. However, in the evaporation with HNO_3 , prolonged baking is avoided to minimize the precipitation of hydrous titanium dioxide. After the last evaporation the residue is taken up with 30 ml of (1+2) nitric acid and the solution is filtered and reserved. The residue is fused with $\text{K}_2\text{S}_2\text{O}_7$, dissolved in dilute nitric acid and any thorium in the solution recovered by KOH precipitation, sufficient excess being added to keep most of the aluminum in solution.

The KOH precipitate is dissolved off the paper in 10 ml or less of (1+1) HNO_3 and the solution obtained is added to the reserved solution. The combined solutions are evaporated until 2 to 4 ml remain, care being taken not to allow the solution to go completely to dryness. This technique prevents the formation of insoluble hydrolytic precipitates. Sufficient water is added to make 25 ml of solution. The solution is then ready for extraction and subsequent steps of the procedure are taken as previously described.

Reference

Levine, Harry and Grimaldi, F. S., 1958, Determination of thorium in the parts per million range in rocks: *Geochemica et Cosmochimica Acta*, v. 14, p. 93-97.

Investigations of thorium in veins,
Gunnison County, Colorado
by
J. C. Olson and D. C. Hedlund

In the course of geologic mapping of the Gateview and Cebolla $7\frac{1}{2}$ -minute quadrangles during the summer of 1958, 6 additional thorium deposits were examined in the Gateview quadrangle and 10 in the Cebolla. Of the 112 thorium deposits tested by scintillation counter thus far, the maximum radioactivity recorded on or adjacent to the exposure is in the range 0.05 to 0.1 mr per hour for 66 deposits, 0.1 to 0.2 for 29 deposits, 0.2 to 0.4 for 5 deposits, 0.4 to 0.7 for 6 deposits, 0.7 to 0.9 for 1 deposit, and 0.9 to 3.0 mr per hour for 5 deposits. Locally, higher readings can be obtained for selected material, but in all deposits the average radioactivity of the vein is lower than the figures given. The geologic mapping done thus far indicates

that thorium deposits in the Cebolla quadrangle are more sparsely distributed than those in the Gateview quadrangle, which have been described in TEI-690, p. 568-569; TEI-700, p. 280-282; and TEI-740, p. 311-313.

Geologic mapping of the southern half of the Cebolla quadrangle shows 8 small bodies of shonkinite and syenite in the Wolf Creek area of about 3 square miles. These potassium-rich intrusive bodies are elliptical in plan and range in size from 150 feet in diameter to 1,500 by 4,000 feet. Of the 10 thorium deposits found thus far in the Cebolla quadrangle, 6 are in the 3-square-mile area in which the shonkinite and syenite bodies occur.

Variations in the proportions of the rare-earth metals, yttrium, niobium, and thorium in different geologic environments are shown by semiquantitative spectrographic analyses of 3 groups of rocks: (1) thorium-bearing veins along shear zones in the Gateview quadrangle, 14 samples; (2) thorium-bearing veins along shear zones east of the Gateview quadrangle and about 2 to 4 miles northeast of Powderhorn, 6 samples; and (3) the Iron Hill carbonatite body and nearby carbonate veins in the Iron Hill complex of alkalic rocks, 10 samples. Although the data are still too fragmentary for a statistical study of these variations, some general trends can be pointed out at this time by a comparison of the thorium, niobium, yttrium, and lanthanum contents of the samples studied.

The samples of carbonate-rich rocks near Iron Hill show a low ratio of thorium to cerium-group rare earths (Th/La less than 0.6) and niobium (Th/Nb generally less than 1); La/Nb is generally between 1 and 10; Y/Nb is 0.1 to 1 in all but 1 of the samples; and Y/La is less than 0.1 with the exception of

a 1:1 ratio in two samples. Compared to the other two groups, the carbonate rocks near Iron Hill are relatively rich in Nb (0.X percent in 2 samples and 0.0X in 7) and La (0.X percent in 7 samples and 0.0X in the other 3). The Ce group of rare earths exceeds the Y group, shown by the Y content of only 0.0X in 4 samples and 0.00X in 6.

The thorium content of samples of the veins along shear zones in the Gateview quadrangle exceeds La, Y, and Nb. Nb in these 14 samples does not exceed 0.03 percent, which is appreciably lower than the other 2 groups of samples. Y and La are also relatively low, the maximum percentages being 0.07 and 0.15 respectively. La exceeds Y in 8 samples, equals it in 4 and Y exceeds La in 2.

Samples of the thorium-bearing shear zones in the area 2 to 4 miles northeast of Powderhorn are characterized by Th:Y and Th:La ratios generally greater than 2:1. The Nb content is generally less than that of carbonate rocks near Iron Hill, but 2 samples, contain as much as 0.X% Nb. Y/Nb ranges from 0.1 to 10 but in most samples is between 1 and 10. Unlike the other two groups of samples, Y exceeds La in 3 of the 6 samples (maximum 0.X%) and equals it in 2, as the La content is only 0.0X percent in 3 samples and 0.00X or less in the other 3.

Geologic Thermometry of Radioactive Materials

by

David B. Stewart

The temperature measurement and control of the heating stage for the X-ray diffractometer discussed in TEI-740 (p. 317) was calibrated against pure silver and sodium chloride. The stage performed well when properly aligned, and many

discussions show that it fills a need for other investigators. Some cooperative work on pyrrhotite has already been performed, and additional work on pyroxene and cordierite is planned.

The system $\text{CaCO}_3\text{-SrCO}_3$

Study of the system $\text{CaCO}_3\text{-SrCO}_3$ continued during the report period. The thermal expansion of orthorhombic SrCO_3 was determined with the heating stage for the diffractometer. The results from 20°C to 950°C are shown in figure 32. The composition $\text{Sr}_{.30}\text{Ca}_{.70}\text{CO}_3$ was studied to determine its symmetry at 650°C and above, but the weak diffraction pattern observed could not be interpreted unambiguously. Work with the heating stage was recessed until the newly designed mullite stage assembly is delivered from the fabricators. The present design, though capable of high quality results, requires too much operator time for specimen loading and alignment, and the new design is expected to eliminate this problem. A different design by Jamieson at the University of Chicago was tested but proved unsatisfactory.

Twenty-six runs involving $\text{CaCO}_3\text{-SrCO}_3$ were made at pressures of 2000 bars, many in the presence of water. These runs showed that the effect of pressure on the solvus in this system is quite small, and that water does not appreciably affect the rate of attaining equilibrium in the sub-solidus region. In addition, the introduction of water in some cases results in the formation of portlandite ($\text{Ca}(\text{OH})_2$) and introduces many problems in the determination of composition. However, water also causes melting at quite low temperatures and pressures. Paterson (1958) and Tuttle and Wyllie, (1958) have demonstrated

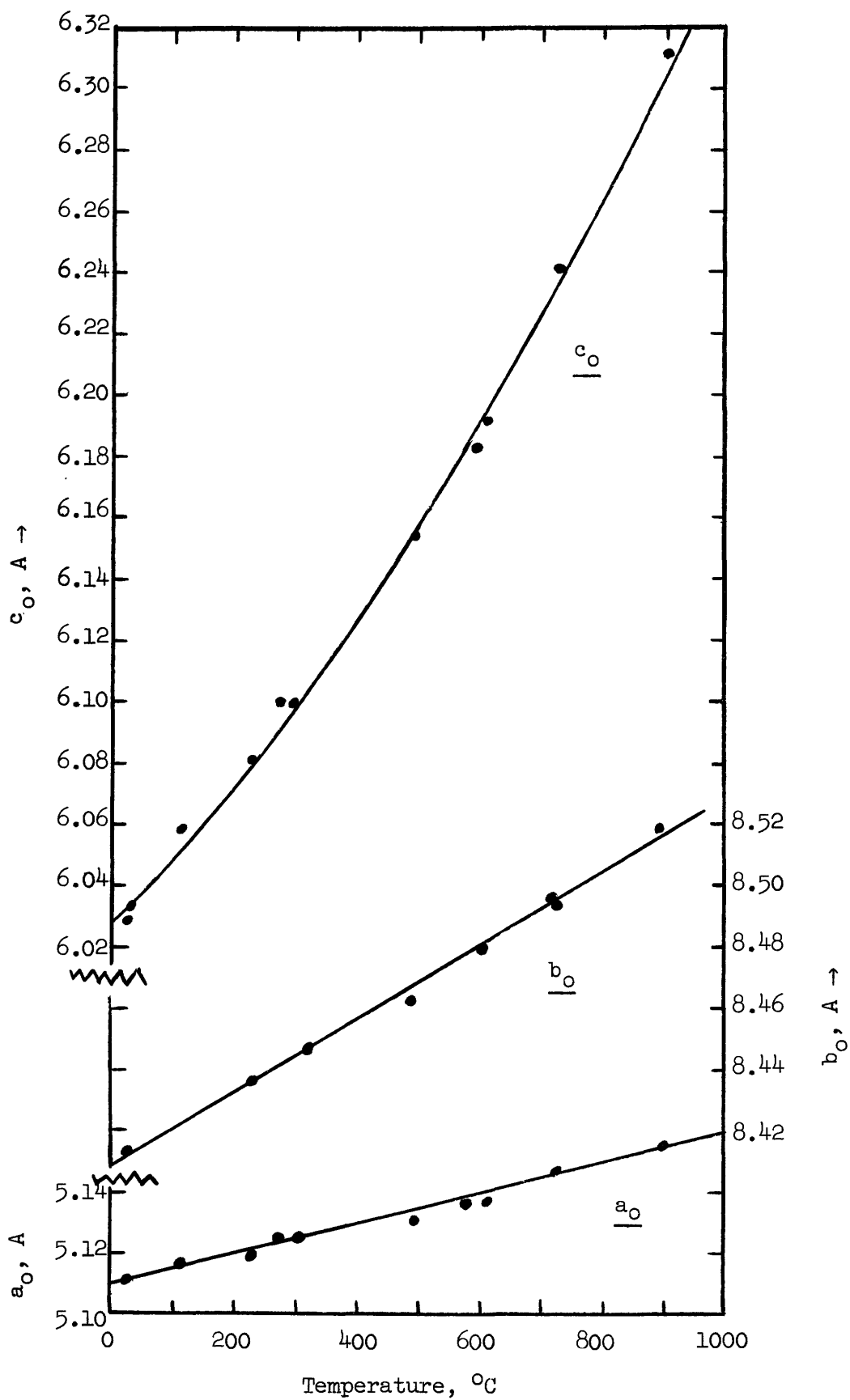


Figure 32.---Thermal expansion of SrCO₃.

that water affects melting in the system $H_2O-CaO-CO_2$ at temperatures as low as $660^{\circ}C$, and in the present work melting was observed for $Sr_{.30}Ca_{.70}CO_3-H_2O$ at $830^{\circ}C$ and 2,000 bars water pressure.

Work is now being directed toward the preparation and accurate measurement of the X-ray diffraction patterns of the orthorhombic strontium-calcium carbonates at room temperature, as well as sub-solidus equilibrium relations.

The system albite-silica-eucryptite-water

An investigation of the system albite-silica-eucryptite-water was started during the report period. This system contains the minerals spodumene, petalite and eucryptite, all of which are important sources of lithium. Spodumene-albite-quartz rock is an important assemblage in granitic pegmatites, and understanding of the origin of this assemblage will contribute to understanding the origin of pegmatites.

In addition to preparing the pure starting materials, nearly three hundred runs were performed to investigate the following problems:

1. The upper stability limit of bikitaite, $LiAlSi_2O_6 \cdot H_2O$ in the presence of excess water. It was found to be about $400^{\circ}C$ at pressures of 1,000 to 2,000 bars.

2. The stability of bikitaite at a water vapor pressure of 10.3 mm was determined. The water is zeolitic and is lost continuously between 160 and $360^{\circ}C$. The dehydration is rapid and reversible at a given temperature. It appears that the water occupies more than one structural site because two distinct breaks have been found in the dehydration curve. Accordingly a member of the X-ray group started a complete crystal structure determination of this substance.

3. The temperature of the transformation from α -to β -spodumene was found to be close to 495°C at 1 bar, 535°C at 2,000 bars, and less than 580°C at 4,000 bars. This suggests that the α -spodumene zones of pegmatites are formed at these temperatures or below. Curiously, β -spodumene has not been reported as being found in nature.

4. The melting point of β -spodumene in the presence of excess water was found to be 1090°C at 2,000 bars and below 900°C at 5,000 bars. The hydrous liquid formed contains about 6.5 weight percent H_2O at 2,000 bars and about 12 weight percent H_2O at 5,000 bars. Spodumene liquid contains as much, if not more, water than feldspar liquid at the same temperature and pressure. The gas that coexists with spodumene liquid is rich in silica; the gas leaches unmelted spodumene to β -eucryptite.

5. It was established that a complete solid solution series with high quartz structure (hexagonal trapezoidal) runs from SiO_2 to LiAlSiO_4 . The structure is metastable over much of this range, but forms readily during many runs and delays the attainment of true equilibrium.

The system ZnS-FeS-MnS-CdS

Studies in portions of the ZnS-FeS-MnS-CdS system are proceeding with much success. In the high temperature, or wurtzite, part of the system, reaction proceeds rapidly and large well-formed crystals are produced. Equilibrium appears to be established in about 40 hours at 900°C over much of the system, and in about 400 hours at 800°C .

Cooperative work by P. B. Barton, Jr., who is studying environments of ore deposition at the Survey laboratory, and Gunnar Kullerud of the Geophysical Laboratory, Carnegie Institution of Washington, has resulted in the resolution of the problem of the effect of FeS on the unit cell size of sphalerite. As originally measured by Kullerud (1953) the unit cell size of sphalerite has been related to the composition of sphalerite, and the composition in turn related to a solvus in the ZnS-FeS system. The latter relationship is the basis of an important geologic thermometer. Unfortunately, the original curve relating composition to cell size was found to be in error. New unit cell measurements of 30 synthetic sphalerite samples of different composition establish that a straight line function best fits the cell size out to 38 mol percent FeS, approximately the maximum solution of FeS in sphalerite. The equation best fitting the data is $a_0 = 5.4093 + 0.000456x$, where a_0 is the unit cell size of sphalerite containing x mol percent FeS. The difference between the new curve and the original curve is 0 at 0 mol percent FeS, and the new curve is 4.8 mol percent higher than the original curve at 30 mol percent FeS.

An error in Kullerud's original work is believed to be caused by partial oxidation of the FeS sample used in preparing sphalerites of "known" composition. Assuming that partial oxidation of the FeS did not seriously affect the position of the FeS-ZnS solvus, the original position of the solvus should be raised approximately 100°C at temperatures of 400 to 800°C . The solvus is now being remeasured by Kullerud and interpretations of temperature based

on the original solvus should be deferred until the new data are ready. Earlier work on the temperature of deposition of the sphalerite in the uranium ores from the Colorado Plateau will not be appreciably affected by these results.

The relation between cell size and composition in the system ZnS-FeS-MnS has been completed for both the wurtzite and sphalerite structures. Contrary to expectations, the effects of FeS and MnS on the unit cell size are not linearly additive. FeS causes a relatively greater increase of unit cell size in the presence of MnS than it does in MnS-free sphalerites. The same holds true for wurtzites. Analyzed natural sphalerites containing significant amounts of FeS and MnS are in good agreement with synthetic sphalerites. The immediate significance of this work is that it is incorrect to assume that the effects of FeS, MnS, and CdS on the cell size of sphalerite are linearly additive except where the individual component is present as less than 0.3 mol percent, in which case the error in the assumption is of the same order as the error of the measurement.

The cell size data in the ZnS-FeS-MnS system are now being used to determine the phase relations in the system. Work on the binary ZnS-MnS-system is finished down to 500°C. A wurtzite field lies between 25 mol percent MnS and 42 mol percent MnS at 500°C. By projection it appears that wurtzite may be a stable phase as low as 250°C at approximately 39 mol percent MnS. It is possible that some of the "high temperature" sphalerites containing large amounts of FeS and MnS actually formed as wurtzites and later inverted to sphalerites,

or else that these sphalerites are not indicative of "high temperature" at all. The ternary isothermal section at 800°C is completed.

Careful unit cell size work in "pure" sphalerites and wurtzites revealed that ZnS formed in the laboratory by precipitation from aqueous solution has a smaller cell size than that formed by direct reaction between Zn and S at high temperature. Thus sphalerite formed from Zn and S has a cell size of 5.4093 Å, but precipitated sphalerite from two different sources has a cell size of 5.4070 Å. This has been found to be due to ZnO in the ZnS lattice. The sphalerite with a cell size of 5.4070 Å contains approximately 0.7 weight percent ZnO. This was established by controlled oxidation of a known weight of Zn(S, O). By heating ZnS in the presence of a great excess of ZnO, 1.2 weight percent ZnO has been introduced into the wurtzite. Since ZnO has the wurtzite structure the interesting possibility arises that the very low temperature wurtzites found in some limestone nodules and ore deposits may in fact be stabilized by the presence of small amounts of ZnO in the structure, and that the ZnO component is required in the phase diagrams.

Other studies

Lead-bearing synthetic zircons and baddeleyite-lead silicate glass mixtures of zircon bulk composition were prepared from pure ZrO_2 , pure SiO_2 glass and a lead-bearing silicate glass. This work was done in cooperation with Harry Rose of the USGS laboratory spectrographic group. The synthetic zircon will be used in preparing standards for the spectrographic determination of lead in natural zircons that are analyzed in connection with geochronological studies. Eight grams of 85 percent zircon were prepared at 1450°C in sealed platinum capsules.

A series of studies was undertaken to determine the mineralogical changes that take place during ignition of a zircon sample in the carbon arc. Natural and synthetic zircon charges were studied after measured burning times; in addition during the burning the spectrum was photographed to determine when the lead was volatilized from the sample. Zircon charges burned with Na_2CO_3 , borax and lithium borate fluxes also were examined. The results can be interpreted by reference to the ZrO_2 - SiO_2 phase diagram; the process of lead removal appears identical in synthetic and natural zircon, and the lead is therefore probably in solid solution in the synthetic zircon.

The thermal stability of metamict minerals such as chevkinite and perrierite in air and in vacuum were studied.

The following abstracts were published during the report period:

Skinner, B. J., and Barton, B. B., Jr., 1958, Recent work on sphalerite: its bearing on the sphalerite geothermometer (abstract): Am. Assoc. Adv. Sci. Annual Meeting Program, Section E, Washington, p. 14.

Stewart, D. B., 1958, System $\text{CaAl}_2\text{Si}_2\text{O}_8$ - SiO_2 - H_2O : (abstract): Geol. Soc. America Annual Meeting Program, St. Louis, p. 144; Geol. Soc. America Bull., v. 69, no. 12, pt. 2.

References:

Kullerud, Gunnar, 1953, The FeS-ZnS System. A Geological Thermometer: Norsk. geol. tidsskr., v. 32, p. 61-147.

Paterson, M. S., 1958, The Melting of Calcite in the Presence of Water and Carbon Dioxide: Am. Mineralogist, v. 43, p. 603-606.

Tuttle, O. F., and Wyllie, P. J., 1958, Calcite-Water Join in the System CaO - CO_2 - H_2O (abstract): Geol. Soc. America Annual Meeting Program, St. Louis, p. 151-152; Geol. Soc. America Bull., v. 69, no. 12, pt. 2.

Crystallography of Uranium and Associated Minerals

by
Howard T. Evans

During the report period, new information was gained concerning the crystal chemistry of uranyl sulfate complexes. The following compounds were synthesized:

- | | |
|-----|--|
| I | $K_2UO_2(SO_4)_2 \cdot 2H_2O$, orthorhombic |
| II | $(NH_4)_2UO_2(SO_4)_2 \cdot 3H_2O$ |
| III | $Rb_2UO_2(SO_4)_2 \cdot 2H_2O$, orthorhombic |
| IV | $Cs_2UO_2(SO_4)_2 \cdot 4H_2O$ (?), orthorhombic |
| V | $Cs_2(UO_2)_2(SO_4)_3$, tetragonal |

All of these compounds appear to be noncentrosymmetric, thus making crystal structure analysis cumbersome. The heavy atoms were located in I and IV, but the nature of the $UO_2(SO_4)_2^{2-}$ complex has not yet been revealed. It is planned to extend these studies to the insoluble complexes of the zippeite group.

The crystal structure of the new compound, V, was worked out in detail. The symmetry is tetragonal, space groups $P4_2m$. A three-dimensional framework is formed by the uranyl and sulfate groups; each uranyl ion coordinates 5 oxygen atoms in its equatorial plane, each from a different sulfate group; and each sulfate group is attached to four uranyl groups. The pentagonal bipyramid coordination with oxygen for the uranyl ion was found also in carnotite, johannite and uranophane, and appears to be quite characteristic.

As in the past, the study of synthetic compounds such as these has proved of great value in connection with problems of mineral formation, for the following reasons, among others: (1) synthetic compounds which can be related chemically and structurally to mineral phases have structures more easily and

accurately solved than the minerals; (2) the synthetic compounds give valuable information about the dissolved ions in the solution from which the minerals are formed; and (3) the solution of synthetic structures adds to our information about the crystal chemical behavior of uranium and other elements, which is of great value in the solution and interpretation of the mineral structures themselves.

Structure studies on the mineral abernathyite, $KUO_2AsO_4 \cdot 4H_2O$ were begun. Electron density syntheses indicate that all the atoms in this structure can be unequivocally located. This will be the first detailed crystal structure analysis of a mineral in the autunite group. It is planned to extend the study to other members of the group which are crystallographically more complex.

Crystal structures of the following compounds and minerals are undergoing refinement by least squares analysis on the computer:

KVO_3	(completed)
NH_4VO_3	(completed)
Phase B	$(V_2O_3 \cdot 2V_2O_4 \cdot 5H_2O)$
Doloresite	$(3V_2O_4 \cdot 4H_2O)$
Haggite	$(V_2O_3 \cdot V_2O_4 \cdot 3H_2O)$
$K_3V_5O_{14}$	
$Cs_2(UO_2)_2V_2O_8$	(analog of carnotite)
$Cs_2(UO_2)_2(SO_4)_3$	(completed)

The continuation of these studies will keep the facilities of this project occupied for some time.

Infra-red And Ultra-violet Radiation Studies

by

R. M. Moxham

A study of infra-red and ultra-violet phenomena and their possible applications in geophysical exploration has been started. A review of classified documents pertaining to available airborne infra-red devices is being made.

Circuitry to be used in infra-red and ultra-violet luminescence studies is being designed. The circuit is intended to permit examination of discrete parts of the luminescence growth-decay curves where pulsed excitation is utilized. The results may indicate 1) the optimum timing between excitation and measurement and 2) optimum repetition rates.